UNIVERSITY OF CALIFORNIA, SAN DIEGO

MECHANISMS OF GROWTH OF ARTICULAR CARTILAGE: CELL ORGANIZATION AND FATES

A dissertation submitted in partial satisfaction of the

requirements for the degree Doctor of Philosophy

in

Bioengineering

by

Kyle D. Jadin

Committee in charge:

Professor Robert L. Sah, Chair
Professor Sangeeta N. Bhatia
Professor Sanjay K. Nigam
Professor Robert A. Pedowitz
Professor Jeffrey H. Price

2006

The dissertation of Kyle D. Jadin is approved, and it is acceptable in quality and form for publication on microfilm:

_____

_____

_____

_____

_____

_____

Chair

University of California, San Diego

2006

TABLE OF CONTENTS

LIST OF FIGURES AND TABLES

ACKNOWLEDGMENTS

I would like to thank all those who have made this thesis work possible through their support through the years. First, my adviser Dr. Robert Sah has been a source of continual guidance, motivation, and scientific expertise. I'd like to thank him for his tireless efforts in sculpting my scientific and communicative abilities, and in sharpening my publications and presentations, especially via emails at 3 AM.

I offer a special thanks to my thesis committee for their scientific guidance and for overseeing this project through the final stages: Dr. Jeff Price, Dr. Sangeeta Bhatia, Dr. Robert Pedowitz, and Dr. Sanjay Nigam.

I would like to acknowledge the Journal of Histochemistry and Cytochemistry for permission to reprint materials in Chapters 2. I would also like to acknowledge support by Arthritis Foundation, National Institute of Health, and the National Science Foundation.

This work has been supported by contributions of coauthors. Chapter 2 was published as "Depth-varying density and organization of chondrocyte in immature and mature bovine articular cartilage assessed by 3-D imaging and analysis". J Histochem Cytochem. 2005 Sep; 53(9):1109-19. For this article, thanks goes to Benjamin Wong, Drs. Won Bae, Kelvin Li, and Amanda Williamson, Barbara Schumacher, and Dr. Jeffrey Price.

Chapter 3 is in press in a special edition of *Biomaterials* as "Changes in cell organization in bovine articular cartilage during growth and maturation". Thanks to coauthors Won Bae and Barbara Schumacher.

Chapter 4 will be submitted to the *Journal of Orthopaedic Research* as "Depth-varying growth of articular cartilage explants revealed by biomechanical analysis of displacement of chondrocytes". I thank coauthors Anna Asanbaeva and Scott Tcheng for their help in preparing this article.

Finally, Chapter 5 will be submitted to the *Journal of Biomechanics and Mechanobiology* as "Cell proliferation in articular cartilage: contribution to dynamics of cellularity during growth". Thanks to coauthors Scott Tcheng and Barbara Schumacher for their contributions.

I extend a gracious thanks to the staff of the Bioengineering Department at UCSD. They have showed continued patience over the years, not only keeping me on track to receive my Ph.D., but in numerous other more administrative issues in which they have held my hand. I would especially like to thank Doug Gurevitch for his help in administration of the lab portion of a tissue engineering course for high school students that I instructed, and for his daily email updates on the status of the autoclave. Also, thanks to the staff for cheering me up on those rainy days in the lab, by always having a happy face.

I am especially gracious to those staff members in the lab, for always offering their support without hesitation. I'd like to thank previous staff members Carrie Wirt and Michael Voegtline for being supportive friends, and always putting a smile on my face. Also, Van Wong has shown unending patience in assisting me with all of my computer problems, and keeping the lab running smoothly through the various transitions. Barbara Schumacher was not only a valuable resource because of her extensive scientific knowledge, but a great friend. To all those other people who have helped behind the scenes over the years, Leo Schumacher, Theo Moy, Tae Kim, Augie Sage, and Kelly Fortune, I thank you.

My fellow graduate students over the years have enriched me scientifically, and overall made working in the lab an enjoyable experience. The students of CTE are unrivaled intellectually, and I look forward to seeing their immense impact to the scientific world of bioengineering in the future. They have also been exceptionally good spirited and fun people to be around, making even the most arduous of times tolerable. Former senior graduate students, Michael DiMicco, Kelvin Li, and Melissa Kurtis were a source of early inspiration, and continue to be friends. I was further enriched by the following generation of CTE graduate students, Won Bae, Travis Klein, Kevin McGowan, and Michele Temple. Won has contributed to a number of my projects, and is a model of professionalism, and Michele was a cheerful presence in the lab, and an excellent partner in executing the summer tissue engineering course for high school students. The current group of graduate students has been a pleasure to work with, and will always be friends. Tannin Schmidt has been around every step of the way, and has been a good buddy in and out of the lab, and I look forward to seeing him as the head of the bioengineering department of some prestigious (Canadian) university. Ken Gratz, Gayle Nugent, Kanika Chawla, and Anya Asanbaeva have always been fast on our heels with their spirited research, and have been fun and entertaining people to be around. Finally, it has been exciting watching the newest groups of graduate students, Megan Blewis, Nancy Hsieh, Ben Wong, Jen Antonacci, Jen Hwang, and Eun Hee Hon, start to put together the projects that will shape the future of cartilage tissue engineering research.

This dissertation would be only a shadow of what it has turned out to be without the direct help of a few up and coming students. Benjamin Wong was an early contributor to getting me started in the lab, and helping to publish my first paper. Also, I've had the pleasure of working with undergraduate Scott Tcheng over the past year, and

his contributions have been paramount to launching the final two chapters of this dissertation. Without him, I may have became the first 10th year graduate student.

Finally, I would like to thank the emotional support of my family and friends. My parents, Keith and Robbie Jadin, have supported my academic goals throughout my life, and my sister, Addi Jadin, has been a great source of stability over the years. It has been difficult being away from them while pursuing my PhD. in California, but my local friends have been like a second family to me. I'd especially like to thank Maril Sowell for always being a good friend, and like a second mother to me since I first arrived here.

VITA

2000	B.S., Chemical Engineering/Business Administration Michigan Technological University, Houghton, MI
2000-2006	Graduate Student Researcher Cartilage Tissue Engineering Laboratory University of California, San Diego, La Jolla, California
2001	M.S., Bioengineering University of California, San Diego, La Jolla, California
2006	Ph.D., Bioengineering University of California, San Diego, La Jolla, California

Book Chapter

Sah RL, Klein TJ, Schmidt TA, Albrecht DR, Bae WC, Nugent GE, McGowan KB, Temple MM, **Jadin KD**, Schumacher BL, Chen AC, Sandy JD: Articular cartilage repair, regeneration, and replacement. In: Arthritis and Allied Conditions: A Textbook of Rheumatology, 15th Ed., ed by WJ Koopman, Lippincott Williams & Wilkins, Philadelphia, 2004, pp 2277-301.

Journal Articles

Jadin KD, Wong BL, Bae WC, Li KW, Williamson AK, Schumacher BL, Price JH, Sah RL. Depth-varying density and organization of chondrocyte in immature and mature bovine articular cartilage assessed by 3-D imaging and analysis. *J Histochem Cytochem*. 2005 Sep; 53(9):1109-19.

Li J, **Jadin K**, Masuda K, Sah R, Muehleman C: Characterization of lesions of the talus and description of tram-track lesions. Foot Ankle Int. 2006, 27:344-55.

Jadin KD, Schumacher BL, Bae, WC, Sah RL. 3-D Imaging of chondrocytes in articular cartilage: Growth-associated changes in cell organization. Submitted to special edition of *Biomaterials* (by invitation) May, 2006.

Selected Abstracts

Jadin KD, Wong BL, Li KW, Bae WC, Williamson AK, Schumacher BL, Price JH, Sah RL: Depth-associated variation in chondrocyte density in bovine articular cartilage during growth and maturation. *Trans Orthop Res Soc* 28:469, 2003.

Chawla K, Klein TJ, Schumacher BL, **Jadin KD**, Schmidt TA, Voegtline MS, Thonar EJ-MA, Masuda K, Sah RL: Tracking donor chondrocytes in stratified tissue-engineered cartilage after implantation *in vivo*. *Trans Orthop Res Soc* 29:306, 2004.

Jadin KD, Schumacher BL, Price JH, Sah RL: Chondrocyte organization of bovine articular cartilage in the superficial zone during growth and maturation. *Trans Orthop Res Soc* 29:550, 2004.

Temple MM, **Jadin KD**, Bissar O, Bae WC, Chen MQ, Price JH, Sah RL: Changes in chondrocyte content and organization in human articular cartilage with early degeneration. *Trans Orthop Res Soc* 29:943, 2004.

Jadin KD, Schumacher BL, Price JH, Sah RL: 3-D analysis of chondrocyte organization in articular cartilage during growth. *Int Cart Repair Soc* 5, 2004.

Temple M, Bae W, **Jadin K**, Bissar O, Chen M, Price J, Sah R: Decreased cellularity in the superficial zone of human articular cartilage in early degeneration. *Int Cart Repair Soc* 5, 2004.

Chawla K, Klein TJ, Schumacher BL, **Jadin KD**, Schmidt TA, Chen AC, Wong V, Nakagawa K, Thonar EJ-MA, Masuda K, Sah RL: Enhanced formation of stratified tissue-engineered porcine cartilage from chondrocyte subpopulations with bone morphogenetic protein-7 (BMP-7). *Trans Orthop Res Soc* 30:294, 2005.

Lewis CW, **Jadin KD**, Wheeler JM, Bae WC, Sah, RL: 3D morphology of adult human calcified cartilage. *Trans Orthop Res Soc* 30:1466, 2005.

Jadin KD, Schumacher BL, Bae, WC, Sah RL. Changes in cell organization in bovine articular cartilage during growth and maturation. *Trans Orthop Res Soc* 30:47, 2006.

Jadin KD, Schumacher BL, Sah RL. Proliferation of chondrocytes within articular cartilage. *Trans Orthop Res Soc* 30:1357, 2006.

Jadin KD, Tcheng SW, Sah RL. Depth-varying growth of articular cartilage explants revealed by biomechanical analysis of displacement of chondrocytes. *Trans Orthop Res Soc* 30:1495, 2006.

ABSTRACT OF THE DISSERTATION

MECHANISMS OF GROWTH OF
ARTICULAR CARTILAGE:
CELL ORGANIZATION AND FATES

by

Kyle D. Jadin

Doctor of Philosophy in Bioengineering
University of California, San Diego, 2006
Professor Robert L. Sah, Chair

Articular cartilage is a connective tissue covering the ends of long bones and responsible for facilitating normal joint motion. When adult tissue is damaged or diseased, it does not heal adequately, and further breakdown ensues so that replacement tissue or enhanced repair is needed. Strategies for generating engineered tissue or instigating a repair response might be achieved using a biomimetic approach, where the normal *in vivo* mechanisms of growth and maturation are recapitulated. The objective of this dissertation was to further the understanding of how the chondrocytes within articular cartilage are positioned to contribute to growth and homeostasis, by attaining and maintaining a distinct cell organization and undergoing proliferation.

The organization and fates of chondrocytes in cartilage vary with depth from the articular surface and are consistent with an anabolic growth phenotype in immature tissue and a more stable state of homeostasis in mature tissue. From 3-D imaging and analysis of cartilage, the cells in the adult stage are sparse, while cell density is high in growing tissue, especially near the surface, and cells are spread out evenly to maintain a close proximity to the rapidly growing and remodeling tissue. The spatially-varying growth of immature articular cartilage *in vitro* was analyzed by the displacement of cell nuclei at a surface, revealing that cartilage explants are predisposed to growth occurring primarily near the articular surface. Finally, by analyzing tissue for proliferating cells, it was found that the cell population can be expanded by proliferation during *in vivo* growth, with the highest capacity for proliferation (*in vitro*) near the articular surface. The experimental data from these studies combined with a theoretical model describing the dynamics of cartilage cellularity underscores the contribution of cell proliferation to maintenance of high cell density, especially near the articular surface, during cartilage growth.

This dissertation highlighted the ability of the cell population to maintain an organization with cells positioned to elicit a highly anabolic state in immature articular cartilage and a more efficient state of homeostasis in adult tissue. The results described herein may allow tissue engineering or repair strategies that more closely mimic *in vivo* mechanisms, in which growth, maturation, and repair are guided by a population of cells with specific organization and proliferative activity.

CHAPTER 1

INTRODUCTION

1.1 General Introduction to the Dissertation

During development, the chondrocytes in articular cartilage are responsible for guiding the growth and maturation of the tissue towards functioning as a load-bearing, wear-resistant, low-friction surface for joint articulation. In an effort to engineer cartilage for repair of damaged joint surfaces, the most successful strategy may be to fabricate tissue resembling that at an immature stage, and coaxing it to grow and mature appropriately with biochemical and biomechanical signals. The cells within such a construct, as in immature tissue, may require distinct depth-varying phenotypes and organization to respond to external signals to achieve both growth to cover the expanding joint surface and maturation to achieve proper functionality. The precise way in which the organization and fates of cells in immature articular cartilage might contribute to growth and maturation, is not clear.

The overall motivation of this dissertation was to contribute to an understanding of the role of cell organization and fates in mediating the growth of articular cartilage through matrix accretion and cell proliferation. Specifically, the objectives of this work were: (1) develop image acquisition and processing routines to localize chondrocyte

nuclei in 3-D (Chapter 2), (2) compare cell density and organization in specific sites of the bovine stifle joint of fetal, calf, and adult animals (Chapter 3), (3) determine the spatially-varying growth of immature tissue *in vitro* (Chapter 4), and (4) develop and test a cellular model of tissue growth, after assessing the extent of cell proliferation as a function of depth in tissue cultured *in vitro,* and proliferative events in the superficial zone of both tissue cultured *in vitro*, and freshly harvested tissue representing the *in vivo* condition (Chapter 5).

Chapter 1 begins with a general description of the composition and function of mature articular cartilage. This is followed by a definition of growth and an overview of the structural, functional, and compositional changes that occur during *in vivo* growth and maturation. Next, the role of cell proliferation in growth will be discussed, and the distinct mechanisms of growth that may occur in articular cartilage will be introduced. Finally, an overview of techniques that have been used to investigate cell organization and proliferation within tissue will be presented.

Chapter 2, which has been published in the *Journal of Histochemistry and Cytochemistry*, describes validated and semi-automated 3-D imaging and imaging processing methods for localizing cell nuclei in articular cartilage. This method is applied to bovine articular cartilage at different stages of growth to assess the depth-varying cell density and distance of each point in the tissue to the nearest neighboring cell, a measure of both cell density and cell organization (clustering). The methods described here provided an accurate (>95% sensitivity and specificity) approach for localizing cells in 3-D, relative to manual identification. Also, the cell density results were consistent with previous studies, decreasing with depth and growth. Finally, whereas in immature tissue

there is a small distance of tissue to the nearest cell (<10 μm), this distance is relatively high (>20 μm) in the majority of adult tissue.

Chapter 3, submitted to a special edition of *Biomaterials* entitled "Cellular and Molecular Techniques for Evaluation of Biological Materials", applies the methods described in Chapter 2 to a number of animals. In this study, similar imaging and image processing methods were applied, with addition of a 3-D Mexican hat filter to enhance nuclei relative to background and improve the consistency of nuclei localization across multiple samples. This paper also further extends the description of cell organization by calculation of the nearest neighbor vector, from which the distance and angle (relative to the articular surface) between neighboring cells were calculated. The 3-D metric of angle to the nearest neighboring cell highlights the characteristic organization of cells in adult tissue, with horizontal clusters of cells in the superficial zone, and vertical columns in the deep. This is in contrast to immature fetal and calf tissue, where orientation of cells is nearly isotropic (32°) at all depths. The distance to nearest cell did not change appreciably, however, suggesting the presence of closely situated cell groups in articular cartilage at all growth stages and depths.

Chapter 4 investigates the spatially-varying growth of immature articular cartilage explants *in vitro*, with enzymatic and chemical modulation of the extracellular matrix. Articular cartilage explants from an immature calf were grown in culture after depletion of GAG with chondroitinase ABC (C-ABC) or with inhibition of collagen crosslinks with β-aminopropionitrile (BAPN). Cell nuclei on the edges of these explants were tracked at different time points during *in vitro* growth, and their displacements used to describe the strain (ε_{rr}, ε_{rz}, ε_{zz}) due to tissue growth as a function of depth from the articular surface

(z=0) and from the disk center (r=0). Axial growth (ε_{zz}) exceeded radial growth (ε_{rr}) and shear (ε_{rz}) by a factor of 20, and was highest near the articular surface and at the disk center. Tissue growth was dependent on the state of the extracellular matrix, as C-ABC treated samples did not grow over the culture duration, and BAPN treated samples exhibited accelerated growth.

Chapter 5 investigates the contribution of cell proliferation in growing and mature articular cartilage by developing and evaluating a cellular model describing tissue growth. A conservation equation was derived to describe the change in the cellularity in a small volume of tissue due to both tissue growth and cell fates. Cartilage from fetal, calf, and adult bovine animals was cultured in the presence of bromodeoxyuridine (BrdU), which is incorporated into the DNA of cells passing through the S-phase of the cell cycle, and probed with fluorescent antibodies as an indicator of proliferative activity from the surface to ~0.8 mm in depth. Cultured tissue, and freshly harvested explants, were stained and imaged to identify cells in mitosis by cytoskeleton and nucleus morphology. Dividing cells were present in cultured tissue, indicating the capacity of cells to divide *in vitro*, and were concentrated near the articular surface. In freshly harvested tissue, dividing cells were seen near the surface of immature but not in mature cartilage, suggesting a role of proliferation in *in vivo* growth but not homeostasis. This cell proliferation data, along with data from previous chapters, was incorporated into the cellular model of growth, and highlighted that during *in vitro* growth, the accelerated matrix expansion leads to a large decrease in cellularity. On the contrary, a simulation of

in vivo growth resulted in cellularity that was maintained by cell proliferation over 60 days of growth.

Chapter 6 summarizes the major findings of this study, and their implications for future articular cartilage research.

1.2 Structure, Composition, and Function of Mature Articular Cartilage

Mature articular cartilage has distinct physical and chemical properties given rise to by its constituent cells and extracellular matrix molecules which impart the ability to provide a low-friction, wear-resistant, load-bearing surface for joint articulation. These properties vary significantly with depth from the articular surface, which has led to the description of superficial, middle, and deep zones [5, 6], each with a distinct role in the overall function of the articular cartilage layer.

1.2.1 Extracellular matrix content and arrangement

The primary molecules of cartilage are collagen type II and proteoglycans in the extracellular matrix [35, 37]. The relative content, structure, and organization of these varies with depth from the articular surface, with key features in each of the distinct zones. In the superficial zone, the collagen fibrils are thin and dense, running parallel to the articular surface, and the proteoglycan content is at its lowest [42]. In the middle zone, the collagen fibers are larger and more randomly organized, and the proteoglycan

content is higher. Finally, in the deep zone, the collagen fiber diameter is largest, although the concentration of these molecules is lower, whereas the proteoglycan concentration is highest.

The properties of the extracellular matrix also vary with distance from the cell, possibly to alleviate mechanical discontinuities between the stiff extracellular matrix and the softer cell cytoplasm. Chondrocytes are surrounded by a thin layer of matrix known as the *pericellular* region, which has a more amorphous character and is virtually devoid of collagen fibrils. Outside of this is the *territorial* region which makes up the majority of the articular cartilage, especially in the superficial and middle zones. In the deep zone, an *interterritorial* region is seen far away from cells, characterized by larger proteoglycan aggregates [42].

1.2.2 Chondrocyte organization

Mature articular cartilage is a hypocellular tissue with chondrocytes making up only a small proportion of the tissue volume (1-2%), but assuming a very depth-dependent density and organization [21]. In the superficial zone of articular cartilage, cell density is relatively high and cells are flattened vertically and arranged in clusters parallel to the surface [45, 49]. In contrast, in the deep zone, cells are present at a lower density, spheroidal in shape, and are organized into columns [21, 22, 49]. These arrangements appear to be consistent with the local extracellular matrix, particularly the collagen fibers [11]. This may suggest an active role of cells in maintenance of the heterogenous matrix, or a passive response as cells interdigitate with the surrounding collagen superstructures.

1.2.3. Mechanical properties

Articular cartilage is a biphasic material with mechanical properties that highlight its roles in joint articulation. Compressive stiffness, a key feature of articular cartilage for resisting load, is related to the density of collagen and glycosaminoglycan (GAG), the latter having a strong affinity to water due to the positively charged side chains, and the former providing a fiber network [17, 35]. Tensile strength, also important in bearing loads and resisting wear, is attributed primarily to the integrity of this collagen network. The low friction properties of the articular cartilage surface appear to be due, at least in part, to the lubricating molecule proteoglycan-4, present at the articular surface and synthesized by cells of the superficial zone [44]. Finally, the hydraulic permeability may be a critical regulator of biochemical concentrations within the tissue.

The mechanical properties of articular cartilage vary with depth, allowing it to distribute load effectively from the surface to the underlying bone, permit sliding of opposed cartilage surfaces, and control the local concentration of cytokines. The compressive strength is low near the articular surface, increasing the contact area between joint surfaces, and this increases with depth, being maximal near the bone [43]. Also, the permeability is lowest near the surface, allowing for transport of nutrients and waste in and out of the deeper layers of tissue [29]. Finally, in the superficial zone, the tensile strength is higher, so that the shear and tensile forces created by joint contact and sliding are resisted [53].

1.3 Articular Cartilage Growth and Maturation: Structure-Function Relationships

During *in vivo* development and growth, the size of the knee joint increases and the articular cartilage grows to cover the expanding joint surface, and matures to achieve the mechanical properties described above. Also, the underlying bone advances by calcification toward the articular surface, successively diminishing the thickness of the articular cartilage layer. This process is guided by a combination of intrinsic and extrinsic signals that dictate cell fates and matrix metabolism, and structural organization leading to changes in tissue function (Figure 1.1). Recapitulating this process *in vitro* is one approach for forming tissue engineered cartilage with the desired functional properties. Understanding the relationships between structure and function will elicit more effective approaches to modulating engineered or donor tissue to match the desired implant properties.

1.3.1 Definition of growth

During normal *in vivo* development, biological tissues undergo different dynamic processes such as growth, remodeling, and maturation. Growth is defined as an increase in size due to accretion of material similar to that already present. This increase in size is often accompanied by remodeling, so that when new material is added, the structure of the original tissue is altered to create a new equilibrium state [27]. In turn, tissue remodeling may occur with or without growth, to ultimately lead to a new state of

maturation. Tissue maturation can consist of increased heterogeneity and anisotropy, as well as more complex structure, but ultimately is hallmarked by a heightened functional state. This dissertation focuses mainly on tissue expansion due to growth, which occurs *in vivo* in conjunction with remodeling and maturation, which may or may not be the case during different conditions of *in vitro* growth.

1.3.2 *In vivo* variations with growth stage

The mechanical properties of articular cartilage evolve during development and post-natal growth related to changes in the structure and composition (maturation) of the extracellular matrix. The compressive and tensile strength increase from fetal to adult tissue [54, 55]. These changes are accompanied by increases in collagen and collagen cross-link concentration. During post natal growth, the organization of collagen fibers also change, specifically increasing their vertical arrangement in the deeper zones of tissue [11].

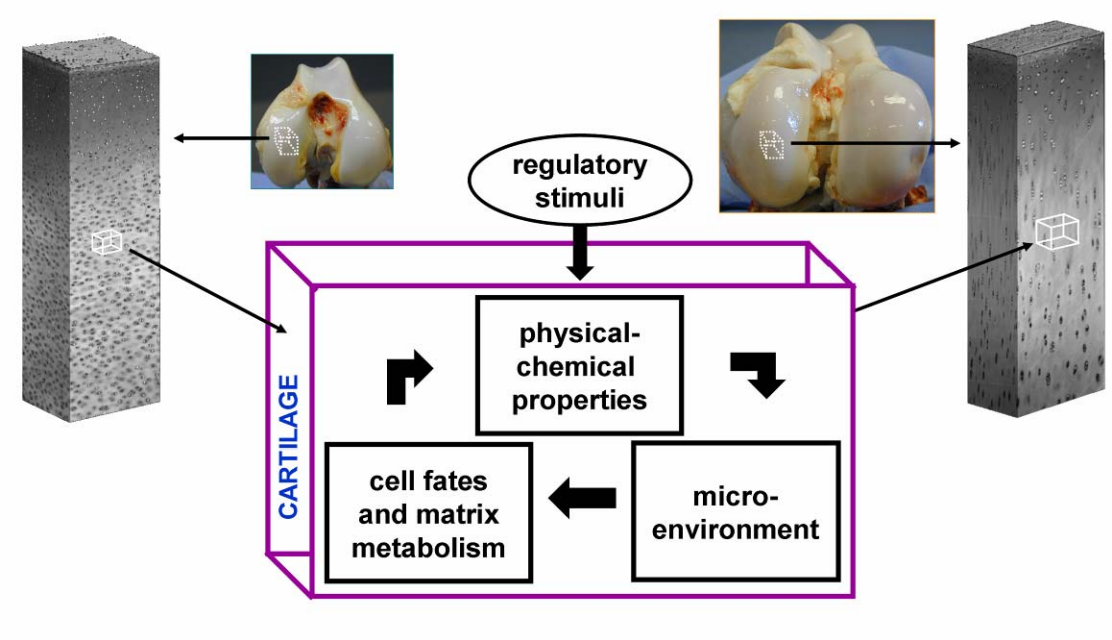

Figure 1.1. Structure-function relationships that guide the growth of articular cartilage. Adapted from [23].

1.3.3 *In vitro* modulation of growth

Alterations to the extracellular matrix composition by culture with specific growth factors and cytokines can elicit specific growth and maturation phenotypes, by disrupting the balance between the swelling pressure of the GAG with the restraining function of the crosslinked collagen network. These relationships were suggested first by Maroudas, and highlight the direct role that the ECM structure and composition play in function [36].

The growth of cartilage *in vitro* may be directly affected by alteration of extracellular matrix components by enzymatic and chemical treatments. One such treatment, enzymatic digestion with Chondroitinase ABC (C-ABC), can deplete the GAG within articular cartilage explants by breaking down the large proteoglycan molecules. This treatment has been shown to inhibit growth of articular cartilage disks in culture [4]. Another agent, B-aminopropionitrile (BAPN), effectively blocks formation of new lysyl oxidase mediated collagen crosslinks [24], thus attenuating the restraining force of the collagen network. In this case, the swelling pressure of the negatively charged proteoglycans exceeds the restraining force, and the articular cartilage shows expansive growth greater than untreated tissue [4]. The growth of articular cartilage can be directly modulated *in vitro* by application of chemical agents that disrupt the balance between the restraining force of the collagen network and the swelling pressure of sGAG molecules.

1.4 Cell Organization and Fates in Growing Articular Cartilage

Cells in immature articular cartilage are responsible for guiding the growth, remodeling, and maturation of the tissue. The organization of the population of cells at advancing stages of development and growth provides insight into their role in mediating growth, while incidences of cell fate processes such as cell division can indicate specific sites of concentrated growth by expansion of the cell population.

1.4.1. Variations in cell organization with growth

From the time of joint cavitation to eventual functional maturation, the cells in articular cartilage undergo a substantial change in organization, from an initial homogeneous mass of cells to a sparse and distinctly organized cell population within a dense extracellular matrix. The density of cells decreases throughout development and post-natal growth as the tissue expands [23, 25] (Figure 1.2). These changes suggest a decreasing anabolic rate, as the volume of the metabolic domain under the control of each cell increases [21]. Further, this decrease in cell density is consistent with a mechanism of growth by which the cells are pushed apart by accretion of new tissue and remodeling of the existing extracellular matrix.

Cells in immature articular cartilage are organized into densely packed horizontal clusters in the superficial-most tissue, but lack a characteristic deep zone [39]. This evenly-spaced arrangement enhances the proximity of cells to tissue to allow active remodeling. In the later stages of growth and maturation, cells become sparse and

organization of cells begins to mirror the heterogeneous orientation and arrangement of extracellular matrix molecules, as the phenotype shifts from growth to homeostasis.

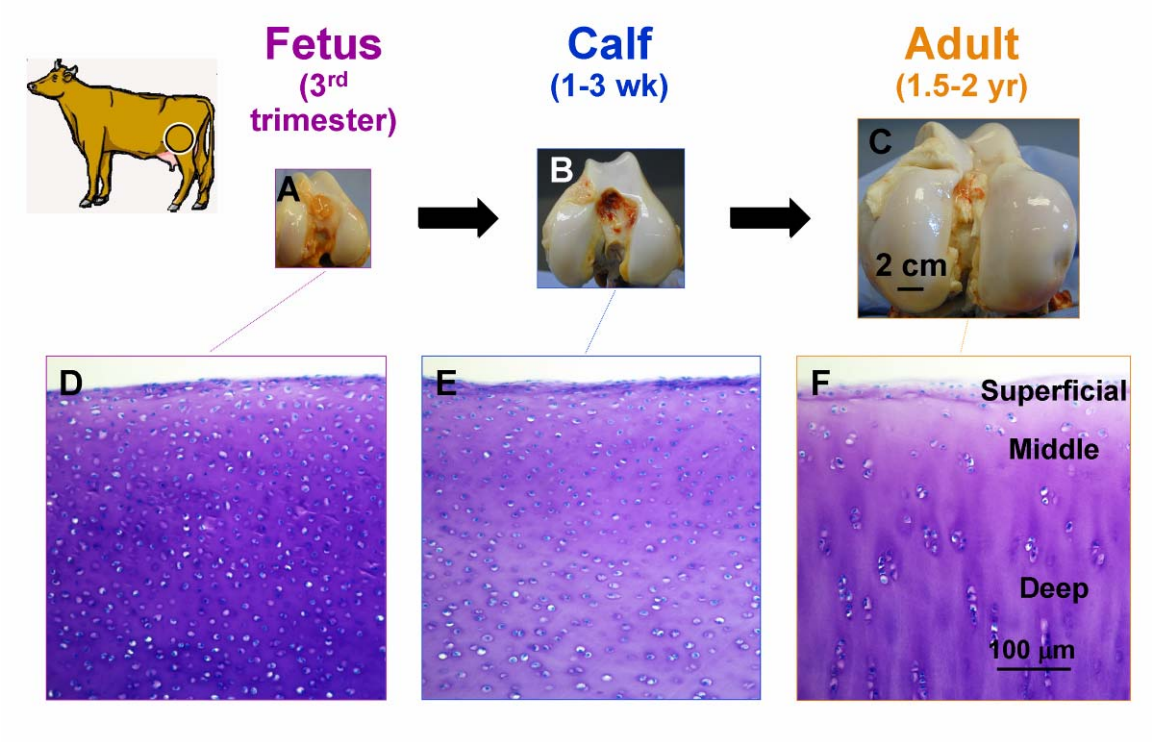

Figure 1.2. Toloudine blue staining illustrates cell organization changes in articular cartilage during growth, leading to formation of superficial, middle, and deep zones of mature articular cartilage. (A-C unpublished from Amanda K. Williamson, D-F unpublished from Barbara L. Schumacher)

1.4.2. Cell fates in tissue growth

The localization of cell fate events in biological tissues during development can reflect the pattern and mechanisms of growth. Mankin [31-34] described 2 bands of proliferating chondrocytes in the immature rabbit articular cartilage, at the surface and near the subchondral bone. More recently, proliferating cells have been identified near the articular surface [19, 25], but not near the subchondral bone. Further, the superficial zone has been implicated as a source of cells with a progenitor-like subpopulation of cells [2, 12, 16, 51]. Cell death has been implicated as one possible fate of cells approaching or enveloped by the calcified cartilage in the endochondral ossification process [25]. Other authors have suggested that cells near the advancing subchondral bone redifferentiate into osteoblasts or osteoclasts. Tracking the fate of cells in a volume of tissue during development may allow for an understanding of depth-specific growth mechanisms (See Section 1.5).

Although cell fate events such as division and death may occur at a low frequency, their contribution to tissue dynamics may be substantial. For example, during tissue growth from the fetal to calf stage, the superficial most layer of cartilage may expand in volume by ~10 times (determined by the change in the diameter of the condyle of ~2 times) while the cell density may only drop by 50% [55]. Thus the number of cells must increase by 5 times. To achieve such an expansion over ~1 month duration requires only ~5% of the cells to divide each day. Detectability of mitotic events may be difficult, because the duration of the mitosis may be ~1 hour, so that only 0.2% of cells are dividing at any time. This proportion may be even lower as the animal reaches maturity, and thus detecting these events may be exceedingly difficult. Clearly, techniques are

needed to label divisions over a longer duration, or to rapidly screen a large number of cells, and these methods are discussed in Section 1.6.

1.5 Mechanisms of Growth of Articular Cartilage

Biological tissues can grow by a combination of different mechanisms, mediated by cells and the extracellular matrix they deposit and remodel (Figure 1.3). Two such mechanisms of growth of soft tissues are appositional and interstitial growth. The relative extents of these may vary in different tissues and organs, and this balance may be critical to achieve expansionary growth concomitant with maturation and functionality for the developing animal. Understanding the synergy between these two types of growth may be critical not only to developmental biologists, but to tissue engineers seeking to use a biomimetic approach to forming tissues and organs.

1.5.1. Appositional growth

In general, appositional growth is defined as that occurring at a surface by formation of new cells and tissue, and such a definition can be extended to articular cartilage [48]. Appositional growth is best illustrated in growth of rigid tissues, where volume changes are associated with successive addition of layers of material on the surface of existing tissue. Such is the case in the growth of long bones, where the growth plate cartilage present on the end of the bone is successively calcified to elongate the

bone. In general, appositional growth occurs at a tissue surface, without altering the original tissue composition or structure by remodeling.

Findings of proliferative cells in the superficial zone of articular cartilage have been interpreted as evidence of appositional growth [19]. In this instance, the articular cartilage grows primarily in a specific location near the surface, such that the majority of the original deeper tissue is unaltered in the process of expansionary growth. Thus, it can be said that this deeper region is growing by apposition, by addition of new material at its surface, or the interface between the stagnant deep and growing surface tissue. Such a definition is consistent with appositional growth of long bones described above, although requires the delineation of the expansionary surface region from the more fixed deeper region.

1.5.2. Interstitial growth

Interstitial growth is defined as that due to expansion in volume by formation of new cells and tissue within the existing tissue mass [48]. Such growth is accompanied by both an increase in mass, and remodeling of the surrounding tissue to incorporate the new material and increase the volume. This type of growth can only occur within soft tissues that deform when stressed by introduction of new material, and remodel to reach a new equilibrium net stress-free state. Building on the previous example, interstitial growth occurs within the growth plate cartilage that is present at the end of long bones, providing it with an expanding source of new material for appositional growth. Here the different zones contribute to expansion of the tissue by generation of new cells by proliferation,

accretion of extracellular matrix, and hypertrophy of cells [57], and this model may have similarities in articular cartilage [21].

The extent of interstitial mechanisms of growth in articular cartilage are not known, although it is likely to contribute at varying degrees in the different depth zones of the tissue (Figure 1.3). The expansion of tissue during growth is accompanied by a decrease in the density of cells [30, 54, 55]. Such a phenomenon may occur in the presence of cell death or through expansion of the tissue due to accretion of newly synthesized extracellular matrix molecules. Apoptotic cell death is not widespread in adult articular cartilage [1] and may only occur in immature tissue near the subchondral bone [25]. These observations suggest that rather than sporadic removal via apoptosis, cells are pushed apart during growth by addition of new extracellular matrix mass and remodeling of the existing tissue, leading to a decrease in cell density. Characterizing cell population organization and cell death at different growth stages suggests that cartilage growth may occur predominantly by matrix accretion in some regions, especially where proliferation is limited or absent.

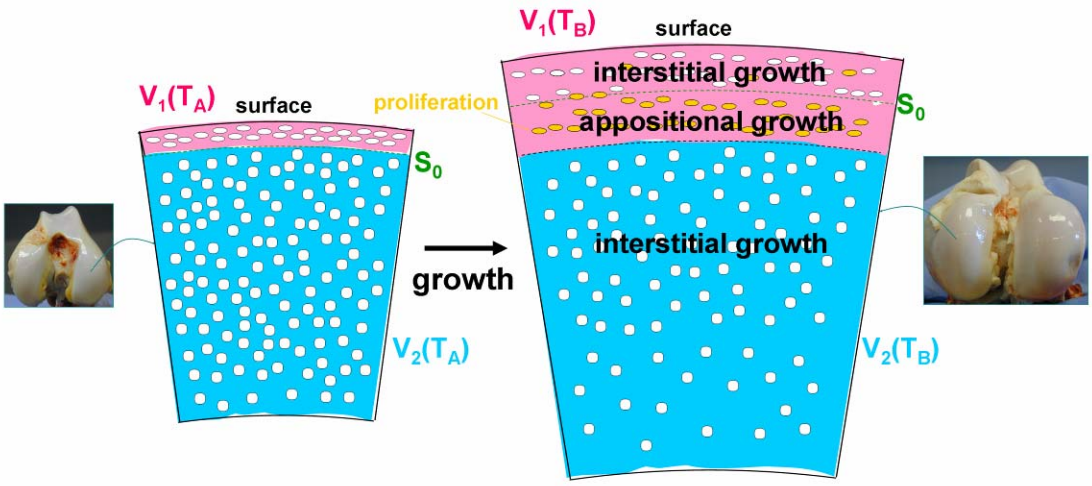

Figure 1.3. Hypothesized mechanisms of growth of articular cartilage, both by formation of new cells and tissue appositionally, and expansion of the existing tissue by matrix accretion interstitially.

1.5.3. Biomechanical Models of Tissue Growth

Growth of a 3-D body can be described by displacement of the points that make it up, both within the volume or at the surface (Figure 1.4). Cell proliferation and death, as well as matrix accumulation around cells, occurring within the tissue (interstitially) are considered a *volume* distribution of mass sources or sinks in space-time. These same processes at a surface are considered a *surface* distribution of mass sources or sinks (appositional). In the former case, the uniform growth of a region $R_1(t=T_A)$, i.e., layer 1 of tissue at time T_A, to a region $R_1(t=T_B)$ can be described by the relative motion of constitutive points, such that if the equations governing the displacement of a sample of these points are known, then all other points displace accordingly to satisfy these equations. In the case of appositional growth at a surface, S_0, a new region, R_1', arises from the original region R_1 at S_0. The displacement of points in $R_1(t=T_A)$ do not satisfy the same displacement equations as $R_1(t=T_B)$ except at the interface S_0 [47] (Figure 2). This description of growth within the volume of a body (interstitially) and at the surface of a body (appositionally) provides a mathematical framework for the quantitative analysis of growth.

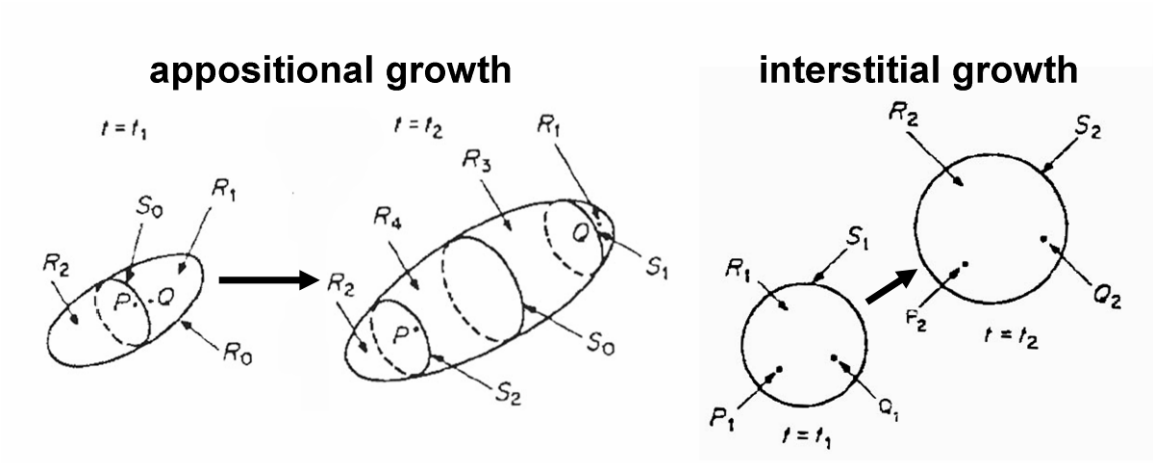

Figure 1.4. Displacement of points within growing bodies in appositional and interstitial growth. from [47]

The deformation of articular cartilage due to growth may be modeled by a sample of points within the tissue that can be generalized to describe all points. This approach has been utilized to assess tissue strain due to osmotic loading by tracking dye applied to a cut surface [38] or due to compression by tracking cells by their stained nuclei at a cut surface [26, 43]. In the case of cells, these approaches can be also applied in 3-D, in conjunction with 3-D imaging and image processing methods. These methods may also be generalized, so that rather than assessing tissue deformations by motion of known points, they are determined by the relative spacing of groups of cells. Such is the approach in development of the aforementioned hypothesis above, that the tissue is growing interstitially and pushing cells apart, upon demonstrating that the density of cells is decreasing with growth. This approach may also be extended to include cell fates, if the kinetics of these processes over the growth duration is known. Thus it is feasible to fully describe the spatially-varying deformation due to growth of articular cartilage, only by taking into account changes in cell organization and cell fates.

1.6 Characterization of Cell Organization and Fates

The characterization of cell organization and fates in articular cartilage in the context of growth would be a step toward understanding the role of such features in governing growth dynamics at the tissue level. In previous studies, biochemical and histological techniques have been used to quantify the number of cells per tissue volume [13, 22, 41, 50, 54, 55, 58] in tissues. At the next level of organization, the local arrangement of cells and cell groups have been qualitatively described by observing tissue sections from vertical and en face views [21, 22, 45, 49]. Finally, studies aimed at

assessing kinetics of cells within tissues have led to spatial localization of dividing cells during in vivo growth and repair [19, 25, 31, 32, 34]. Clearly, articular cartilage is characterized by a population of cells that are heterogeneous in both space and time, and effective techniques to characterize these changes would be useful in understanding the role of cells in tissue dynamics. 3-D imaging and image processing provides a means to assess the changes in the organization of large populations of cells, and to detect infrequent events such as division and death, while clever labeling techniques extend the duration over which dividing cells can be identified.

1.6.1. 3-D Imaging

True 3-D imaging of cells within tissues allows direct assessment of the overall global organization of cells, as well as the local arrangements of cell groups, without physically altering the tissue. Several techniques have been used for a variety of applications, with a range of attributes depending on the mechanisms of detecting light interactions with the objects of interest (cells). Laser scanning confocal microscopy uses pinhole apertures to focus excitation and collection of light to a single z plane within a tissue [9], and has been used to measure the morphology of individual chondrocytes in articular cartilage [14, 18, 28]. More recently, two-photon confocal microscopy has been developed with the goal of increasing depth of penetration, and decreasing the level of energy needed to generate contrast [10], and has allowed imaging of live cells in tissues [8]. Optical Coherence Tomography (OCT) uses the interference of a scanning light beam passing through a specimen, relative to a reference mirror at different distances, to generate a 3-D image depicting cells because of their contrasting interference [20]. Finally, Optical Projection Tomography (OPT) generates a 3-D image by reconstructing views of a specimen from several different angles, similar to micro-computed

tomography, and has the potential to resolve groups of molecules on the cellular level [46].

In another approach, a series of images are taken in conjunction with physical sectioning, and then reconstructed to form a 3-D image. Digital Volumetric Imaging (DVI) is one such technique, and has been used to form high resolution 3-D images of several different tissues [15]. This method involves embedding a fluorescently stained tissue volume in a hard opaque polymer, sequential imaging and cutting of the tissue at the surface of the block, followed by reconstruction to form a 3-D image dataset. Using a similar approach, brain tissue was imaged at similarly high resolution [52] by a combination of two-photon confocal microscopy and laser ablation to penetrate into successive deeper layers of tissue.

1.6.2. Detection of Cell Proliferation

Cell proliferation events occurring within tissues can be effectively labeled over a long duration by incorporating thymidine analogs into the DNA of cells passing through the S phase just prior to cell division. In early studies, tritiated thymidine was introduced into animals, taken up by cells, and added to replicating DNA in place of the native thymidine nucleic acid [31, 32, 34]. Radiolabeled molecules such as tritiated thymidine can be detected by radiography, so that cells that have divided can be distinguished from those cells that have remained in $G_{0,}$ or the resting phase of the cell cycle. More recently, a similar analog bromodeoxyuridine (BrdU) was developed, and allows detection using chemical antibodies specific to the BrdU molecule, rather than radiography [3]. This strategy has been used extensively in a variety of studies, and in one particularly elegant approach, BrdU was introduced into animals at various times up until sacrifice to determine the kinetics of cell division within growth plate cartilage [56]. Introduction of

thymidine analogs into living tissues is an effective technique to unequivocally ascertain if a cell has divided during a particular period of time.

Another method of detecting cell proliferation is to target specific nuclear antigens that are present or elevated during the cell cycle, such as proliferating cell nuclear antigen (PCNA) and Ki-67 nuclear antigen. PCNA is a nuclear protein primarily found during the S phase of the cell cycle, and it can be detected via immunohistochemistry. However, the PCNA protein has been found in non-dividing cells that are capable of division, and the results may be affected by fixation [25].

The extent to which individual cells have proliferated over a period can be assessed by analyzing the decay in fluorescence after labeling due to the successive halving of cell contents during division. Cells labeled using fluorescent dyes such as for cell cytoplasm [40] and the cell membrane [7] will lose half of their fluorescence during cell division, as the content of fluorescent molecules is halved. Thus, the generation number (# of divisions undergone) by each cell can be assessed by summing each cell's fluorescence intensity. This may require carefully controlled and calibrated imaging and analysis techniques, which are exceedingly difficult to accomplish in 3-D tissue explants.

Cells undergoing division assume a distinctive morphology, which can be identified using appropriate dyes. This introduces a more direct approach to identifying dividing cells at any time point by their morphological appearance. Early attempts were made in articular cartilage by Mankin [34], in which dividing cells were identified by a nucleus with condensed chromosomes, in contrast to resting nuclei that have a more rounded shape. These occurrences may be exceedingly rare, especially in more mature tissue, because of the short duration of mitosis, so the chemical agent colchicine was applied over a period of time to arrest cells entering into metaphase, thus integrating the number of cells that can be identified by condensed nuclei and mitotic spindle. Efforts to

identify dividing cells have been aided in recent years by the development of fluorescent labels for both nuclei and cytoskeleton, and 3-D imaging techniques to capture a large number of cells within tissue.

1.7 References

1. Aigner T, Hemmel M, Neureiter D, Gebhard PM, Zeiler G, Kirchner T, McKenna L: Apoptotic cell death is not a widespread phenomenon in normal aging and osteoarthritic human articular knee cartilage. *Arthritis Rhuem* 44:1304-12, 2001.

2. Alsalameh S, Amin R, Gemba T, Lotz M: Identification of mesenchymal progenitor cells in normal and osteoarthritic human articular cartilage. *Arthritis Rheum* 50:1522-32, 2004.

3. Apte SS: Validation of bromodeoxyuridine immunohistochemistry for localization of S-phase cells in decalcified tissues. A comparative study with tritiated thymidine autoradiography. *Histochem J* 22:401-8, 1990.

4. Asanbaeva A, McGowan KB, Masuda K, Klisch SM, Thonar EJ-MA, Sah RL: Mechanisms of cartilage growth: alteration and function and composition in vitro by deposition of collagen and proteoglycan matrix components. *Trans Orthop Res Soc* 29:554, 2004.

5. Aydelotte MB, Greenhill RR, Kuettner KE: Differences between sub-populations of cultured bovine articular chondrocytes. II. Proteoglycan metabolism. *Connect Tissue Res* 18:223-34, 1988.

6. Aydelotte MB, Kuettner KE: Differences between sub-populations of cultured bovine articular chondrocytes. I. morphology and cartilage matrix production. *Connect Tissue Res* 18:205-22, 1988.

7. Boutonnat J, Muirhead KA, Barbier M, Mousseau M, Ronot X, Seigneurin D: PKH26 probe in the study of the proliferation of chemoresistant leukemic sublines. *Anticancer Res* 18:4243-51, 1998.

8. Brakenhoff GJ, Squier J, Norris T, Bliton AC, Wade MH, Athey B: Real-time two-photon confocal microscopy using a femtosecond, amplified Ti:sapphire system. *J Microsc* 181 (Pt 3):253-9, 1996.

9. Brakenhoff GvS, EA. van der Voort, HTM. Naninga, N.: Three-dimensional confocal fluorescence microscopy. *Methods in Cell Biology* 30:379-98, 1989.

10. Centonze VW, JG.: Multiphoton Excitation Provides Optical Sections from Deeper within Scattering Specimens than Confocal Imaging. *Biophysical Journal* 75:2015-24, 1998.

11. Clark JM, Norman A, Notzli H: Postnatal development of the collagen matrix in rabbit tibial plateau articular cartilage. *J Anat* 191:215-21, 1997.

12. Dowthwaite GP, Bishop JC, Redman SN, Khan IM, Rooney P, Evans DJ, Haughton L, Bayram Z, Boyer S, Thompson B, Wolfe MS, Archer CW: The surface of articular cartilage contains a progenitor cell population. *J Cell Sci* 117:889-997, 2004.

13. Eggli PS, Hunziker EB, Schenk RK: Quantitation of structural features characterizing weight- and less-weight-bearing regions in articular cartilage: a stereological analysis of medial femoral condyles in young adult rabbits. *Anat Rec* 222:217-27, 1988.

14. Errington RJ, Fricker MD, Wood JL, Hall AC, White NS: Four-dimensional imaging of living chondrocytes in cartilage using confocal microscopy: a pragmatic approach. *Am J Physiol* 272:C1040-51, 1997.

15. Ewald AJ, McBride H, Reddington M, Fraser SE, Kerschmann R: Surface imaging microscopy, an automated method for visualizing whole embryo samples in three dimensions at high resolution. *Dev Dyn* 225:369-75, 2002.

16. Fickert SF, J. Brenner, RE.: Identification of subpopulations with characterisitics of mesenchymal progenitor cells from human osteoarthritic cartilage using triple staining for cell surface markers. *Arthritis Research and Therapy* 6:R422-R32, 2004.

17. Grodzinsky AJ: Electromechanical and physicochemical properties of connective tissue. *CRC Crit Rev Bioeng* 9:133-99, 1983.

18. Guilak F, Ratcliffe A, Mow VC: Chondrocyte deformation and local tissue strain in articular cartilage: a confocal microscopy study. *J Orthop Res* 13:410-21, 1995.

19. Hayes AJ, MacPherson S, Morrison H, Dowthwaite G, Archer CW: The development of articular cartilage: evidence for an appositional growth mechanism. *Anat Embryol (Berl)* 203:469-79, 2001.

20. Huang DS, EA. Lin, CP. Schuman, JS. Stinson, WG. Chang, W. Hee, MR. Flotte, T. Gregory, K. Puliafato, CA.: Optical coherence tomography. *Science* 254:1178-81, 1991.

21. Hunziker EB: Articular cartilage structure in humans and experimental animals. In: *Articular Cartilage and Osteoarthritis,* ed. by KE Kuettner, Schleyerbach R, Peyron JG, Hascall VC, Raven Press, New York, 1992, 183-99.

22. Hunziker EB, Quinn TM, Hauselmann HJ: Quantitative structural organization of normal adult human articular cartilage. *Osteoarthritis Cartilage* 10:564-72, 2002.

23. Jadin KD, Wong BL, Bae WC, Li KW, Williamson AK, Schumacher BL, Price JH, Sah RL: Depth-varying density and organization of chondrocyte in immature and mature bovine articular cartilage assessed by 3-D imaging and analysis. *J Histochem Cytochem* 53:1109-19, 2005.

24. Kagan HM, Sullivan KA: Lysyl oxidase: preparation and role in elastin biosynthesis. *Methods Enzymol* 82:637-49, 1982.

25. Kavanagh E: Division and death of cells in developing synovial joints and long bones. *Cell Biology International* 26:679-88, 2002.

26. Klein TJ, Chaudhry M, Bae WC, Sah RL: Depth-dependent biomechanical and biochemical properties of fetal, newborn, and tissue-engineered articular cartilage. *J Biomech*, 2005.

27. Klisch SM, Chen SS, Sah RL, Hoger A: A growth mixture theory for cartilage with applications to growth-related experiments on cartilage explants. *J Biomech Eng* 125:169-79, 2003.

28. Knight MM, Ross JM, Sherwin AF, Lee DA, Bader DL, Poole CA: Chondrocyte deformation within mechanically and enzymatically extracted chondrons compressed in agarose. *Biochim Biophys Acta* 1526:141-6, 2001.

29. Leddy H: Site-specific molecular diffusion in articular cartilage measured using fluorescence recovery after photobleaching. *Annals of Biomedical Engineering* 31:753-60, 2003.

30. Li KW, Williamson AK, Wang AS, Sah RL: Growth responses of cartilage to static and dynamic compression. *Clin Orthop Relat Res* 391S:34-48, 2001.

31. Mankin HJ: Localization of tritiated thymidine in articular cartilage of rabbits. I. growth in immature cartilage. *J Bone Joint Surg Am* 44-A:682-98, 1962.

32. Mankin HJ: Localization of tritiated thymidine in articular cartilage of rabbits. II. repair in immature cartilage. *J Bone Joint Surg Am* 44-A:688-98, 1962.

33. Mankin HJ: Localization of tritiated thymidine in articular cartilage of rabbits. III. mature articular cartilage. *J Bone Joint Surg Am* 45-A:529-40, 1963.

34. Mankin HJ: Mitosis in articular cartilage of immature rabbits. A histologic, stathmokinetic (colchicine) and autoradiographic study. *Clin Orthop Rel Res* 34:170-83, 1964.

35. Maroudas A: Physico-chemical properties of articular cartilage. In: *Adult Articular Cartilage,* ed. by MAR Freeman, Pitman Medical, Tunbridge Wells, England, 1979, 215-90.

36. Maroudas A, Venn M: Chemical composition and swelling of normal and osteoarthrotic femoral head cartilage. II. Swelling. *Ann Rheum Dis* 36:399-406, 1977.

37. Mow VC, Ratcliffe A, Poole AR: Cartilage and diarthrodial joints as paradigms for hierarchical materials and structures. *Biomaterials* 13:67-97, 1992.

38. Narmoneva DA, Wang JY, Setton LA: Nonuniform swelling-induced residual strains in articular cartilage. *J Biomech* 32:401-8, 1999.

39. Oreja MR, MQ., Abelleira, AC. Garcia, MAG. Garcia, MAS. Barreiro, FJJ.: Variation in Articular Cartilage in Rabbits Between Weeks Six and Eight. *The Anatomical Record* 241:34-8, 1995.

40. Parish CR: Fluorescent dyes for lymphocyte migration and proliferation studies. *Immunol Cell Biol* 77:499-508, 1999.

41. Paukkonen K, Selkainaho K, Jurvelin J, Helminen HJ: Morphometry of articular cartilage: a stereological method using light microscopy. *Anat Rec* 210:675-82, 1984.

42. Poole AR, Kojima T, Yasuda T, Mwale F, Kobayashi M, Laverty S: Composition and structure of articular cartilage: a template for tissue repair. *Clin Orthop Rel Res*:S26-33., 2001.

43. Schinagl RM, Gurskis D, Chen AC, Sah RL: Depth-dependent confined compression modulus of full-thickness bovine articular cartilage. *J Orthop Res* 15:499-506, 1997.

44. Schumacher BL, Block JA, Schmid TM, Aydelotte MB, Kuettner KE: A novel proteoglycan synthesized and secreted by chondrocytes of the superficial zone of articular cartilage. *Arch Biochem Biophys* 311:144-52, 1994.

45. Schumacher BL, Su J-L, Lindley KM, Kuettner KE, Cole AA: Horizontally oriented clusters of multiple chondrons in the superficial zone of ankle, but not knee articular cartilage. *Anat Rec* 266:241-8, 2002.

46. Sharpe J, Ahlgren, U. Perry, P. Hill, B. Ross, A. Hecksher-Sorensen, J. Baldock, R. Davidson, D.: Optical Projection Tomography as a Tool for 3D Microscopy and Gene Expression Studies. *Science* 296:541-5, 2002.

47. Skalak R, Gasgupta G, Moss M, Otten E, Dullemeijer P, Vilmann H: Analytical description of growth. *J Theor Biol* 94:555-77, 1982.

48. Stockwell RA. Biology of Cartilage Cells. New York: Cambridge University Press; 1979.

49. Stockwell RA, Meachim G: The chondrocytes. In: *Adult Articular Cartilage,* ed. by MAR Freeman, Pitman Medical, Tunbridge Wells, England, 1979, 69-144.

50. Temple MM, Masuda K, Pietryla DW, Thonar EJ-MA, Sah RL: Age- and site-associated weakening of human articular cartilage: relationship to collagen denaturation. *Trans Orthop Res Soc* 28:707, 2003.

51. Thornemo MT, T. Sjogren Jansson, E. Larsson, A. Lovstedt, K. Nannmark, U. Brittberg, M. Lindahl, A.: Clonal Populations of Chondrocytes with Progenitor Properties Identified within Human Articular Cartilage. *Cells Tissues Organs* 180:141-50, 2005.

52. Tsai PF, B. Ifarraguerri, AI. Thompson, BD. Lev-Ram, V. Schaffer, CB. Xiong, Q. Tsien, RY. Squier, JA. Kleinfeld, D.: All-Optical Histology Using Ultrashort Laser Pulses. *Neurotechnique* 39:27-41, 2003.

53. Verteramo A, Seedhom BB: Zonal and directional variations in tensile properties of bovine articular cartilage with special reference to strain rate variation. *Biorheology* 41:203-13, 2004.

54. Williamson AK, Chen AC, Masuda K, Thonar EJ-MA, Sah RL: Tensile mechanical properties of bovine articular cartilage: variations with growth and relationships to collagen network components. *J Orthop Res* 21:872-80, 2003.

55. Williamson AK, Chen AC, Sah RL: Compressive properties and function-composition relationships of developing bovine articular cartilage. *J Orthop Res* 19:1113-21, 2001.

56. Wilsman NJ, Farnum CE, Green EM, Lieferman EM, Clayton MK: Cell cycle analysis of proliferative zone chondrocytes in growth plates elongating at different rates. *J Orthop Res* 14:562-72, 1996.

57. Wilsman NJ, Farnum CE, Leiferman EM, Fry M, Barreto C: Differential growth by growth plates as a function of multiple parameters of chondrocytic kinetics. *J Orthop Res* 14:927-36, 1996.

58. Wong M, Wuethrich P, Eggli P, Hunziker E: Zone-specific cell biosynthetic activity in mature bovine articular cartilage: a new method using confocal microscopic stereology and quantitative autoradiography. *J Orthop Res* 14:424-32, 1996.

CHAPTER 2

DEPTH-VARYING DENSITY AND ORGANIZATION OF CHONDROCYTES IN IMMATURE AND MATURE BOVINE ARTICULAR CARTILAGE ASSESSED BY 3-D IMAGING AND ANALYSIS

2.1 Abstract

Articular cartilage is a heterogeneous tissue, varying with depth, as well as with maturation, in mechanical properties, matrix composition and orientation, and cell density and organization. The objective of the present study was to establish an automated method for localizing individual cells in three-dimensional (3-D) images of cartilage and to use this method to quantify the depth-associated variation in cellularity and cell organization at different stages of tissue growth. Three-dimensional images of fetal, calf, and adult cartilage were obtained by digital volumetric imaging, and then processed to identify cell nuclei. Accuracy of nucleus localization by the automated method was high, with 99% sensitivity relative to manual localization. Using nuclei localized as centroid positions, cellularity decreased from 290, 310, and 150 million cells per cm^3 near the articular surface in fetal, calf, and adult samples, respectively, to 120, 110, and 50 million cells per cm^3 at a depth of 1.0 mm. Cell organization, determined

from the Euclidean Distance Transform, gave an average vector to the nearest cell nucleus with amplitude (distance) of 7.9, 7.1, and 9.1 μm near the articular surface of fetal, calf, and adult samples, increasing to 11.6, 12.0, and 19.2 μm at a depth of 0.7 mm. The angle of this vector (with respect to the transverse plane) was 30-31° throughout the full depth of fetal and calf cartilage and decreased from 31° near the surface of adult tissue, to 25° at a depth of 0.7 mm. The methodologies described here may be applied to characterize and assess the role of 3-D cellular organization during the dynamic processes of cartilage growth and maturation, as well as in aging, degeneration, and regeneration.

2.2 Introduction

Mature articular cartilage is a hypocellular tissue with cell density and organization that vary with depth from the articular surface. The importance of the cell population characteristics of the chondrocytes in cartilage for growth, healing and maintenance of a wear-resistant, frictionless, load-bearing surface for joint articulation, however, remains to be fully elucidated. The depth-associated variation in cell and extracellular matrix properties in mature articular cartilage has led to description of superficial (0-10% depth from the articular surface), middle (10-40%), and deep (40-100%) zones in cartilage as having distinct compositions, structures, and functions [7]. In the superficial zone, cell density is relatively high and cells are arranged in clusters parallel to the surface [22, 23]. In contrast, in the deep zone, cells are present at a lower density and are organized into columns [7, 9, 23]. Within each zone, individual chondrocytes, as well as groups of chondrocytes comprising chondrons, are positioned to have a certain pericellular domain over which they actively metabolize matrix components [7]. With increasing distance from cells, regions of tissue undergo decreasing matrix metabolism [19] and in mature tissue, where cells are relatively sparse and clustered in groups, distant interterritorial regions may be susceptible to functional deterioration. Thus, the density and arrangement of chondrocytes in mature articular cartilage may be critical for maintaining normal joint homeostasis.

During growth and maturation, the density and organization of chondrocytes are also likely to be important, and, in particular, underlie the changes in cell fate processes and matrix metabolism that result in expansion of cartilage tissue. The high density of

cells in immature cartilage tissue, especially in the superficial zone, may contribute to a net anabolic state, leading to tissue growth. Cell organization in immature cartilage is relatively homogeneous [7, 26, 27], without a region with the structural characteristics of the deep zone of mature cartilage. The characterization of cell density and organization in articular cartilage in the context of growth would be a step toward understanding the role of such features in governing growth dynamics at the tissue level.

Determination of cell density provides a first level of characterization of cell populations within tissue. One approach to estimating cell number in a given volume of tissue is to biochemically analyze DNA content [10]. This method has been used to determine the cellularity in small volumes of tissue sections, such as from the superficial, middle and deep zones of mature articular cartilage [25], and across maturational stage (fetal, calf, and adult) [26, 27]. Another approach is to use stereological methods to analyze 2-D sections, which allows for unbiased estimation of cell number per tissue volume [2, 9, 18, 29]. On the other hand, with both biochemical and histological methods, it is difficult to evaluate higher levels of cell organization. Biochemical methods may not have sufficient sensitivity to characterize increasingly small tissue volumes, while analysis of 2-D histological sections requires sufficient sampling to obtain information about 3-D structures.

A next level of characterization of cell populations is by assessment of spatial organization. This has usually been done qualitatively, with 2-D microscopy of vertical sections of cartilage. Examination of histological sections by light microscopy, or by fluorescence microscopy after labeling with fluorescent (e.g., DNA binding) dyes, depicts arrangement of cells or cell nuclei in cross sections. Vertical sections providing

side profile views have revealed the columnar organization of cells of the deep zone [7, 9, 23] of articular cartilage. En face sections, providing tangential views, have revealed horizontal clusters in the superficial zone [22, 23]. The distinct arrangement of chondrocytes in the various regions of cartilage, obtained with views at various planes, suggests a need to examine cellular organization in 3-D.

3-D imaging and image processing of articular cartilage allows for direct assessment of cell organization in tissue volumes of various sizes and geometries (Figure 2.1). With confocal microscopy, successive thin z-sections are obtained by axial motion of the sample stage, allowing for capture of registered serial sections. However, even with laser-based multi-photon systems, imaging depth into the tissue is limited by diffusion and scattering of light, typically ~100 μm in cartilage (Fig. 2.1A) [28]. A relatively new technique, digital volumetric imaging (DVI), overcomes this limitation via surface imaging microscopy, wherein volumes are obtained by physical sectioning and imaging the surface of fluorescently stained tissue embedded in an opaque polymer [4]. With this method, a large tissue volume, with depths effectively unlimited and practically up to several mm, can be imaged at high resolution (Fig. 2.1B). With 3-D data from such methods, 3-D image processing methods could be used to identify tissue features (e.g., cells) and quantify their organization. Automation and standardization of such methods would be useful to analyze samples quickly and repeatably.

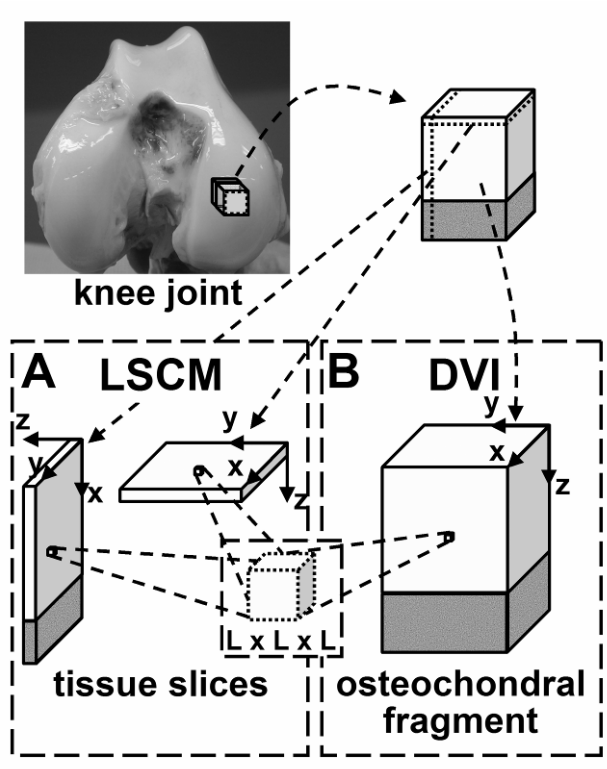

Figure 2.1: Difference in volume of osteochondral tissue acquired by (A) laser scanning confocal microscopy (LSCM) and (B) digital volumetric imaging (DVI). Size of image voxel, LxLxL, acquired in LSCM and DVI images, is shown schematically.

Thus, the overall objective of this study was to develop and validate a new method of quantifying cellularity and cell organization in fetal, calf, and adult bovine articular cartilage, by using DVI to obtain tissue images and by testing semi-automated image processing routines to localize cell nuclei.

2.3 Materials and Methods

Osteochondral blocks were harvested from bovine stifle joints at three stages of growth, fluorescently stained, and imaged in 3-D. A total of three 1 cm^3 blocks were used, one each from the patellofemoral groove of fetal (3^{rd} trimester), calf (1-3 weeks), and adult (1 year) animals. Samples were fixed in 4% paraformaldehyde in PBS at pH 7.4 and 4ºC for 3 days. The cartilage was then rinsed 3 times in PBS. The blocks were cut on a sledge microtome to form histological sample blocks with an area of ~0.5 mm x 3.5 mm (x-y) including the intact articular surface, and a depth (z) extending to ~1.5 mm (partial thickness) for the fetal and calf samples, and ~1.2 mm to bone (full thickness) for the adult sample. The x and z dimensions were measured using a contact sensing micrometer. Samples were sent to Resolution Sciences Corporation, Inc. (Corte Madera, CA) where they were processed as described [4] by staining with Resolution Standard Stain (Acridine Orange and Eosin Y), except with articular cartilage blocks as samples instead of whole chick embryos. Samples were dehydrated using step-wise treatments with ethanol, embedded in Spur resin with Sudan Black opacifier for 10X magnification, and imaged with a Nikon E600 fluorescence microscope with a 10X Plan Apochromat objective (NA 0.45). 3-D image data sets made up of dual color channel voxels were

visualized using RESView™ 3.0 software (Resolution Sciences Corporation). Cell nuclei were stained red and matrix components appeared green, while cell cytoplasm was dark (unstained). Measurements of tissue dimensions in images at high resolution (10 μm) before and after fixation, staining, and dyhydration confirmed a slight shrinkage, with the original cut dimensions being decreased both parallel and perpendicular to the articular surface (-1.4±0.8% and -2.2±0.1%, respectively, mean±SD, n=3) and the volume being decreased (-5.0 ±1.5%). Since these changes were small, dimensions are presented without any corrections for shrinkage. 3-D renderings and 2-D cross sections of image data were exported as high resolution bitmaps for qualitative viewing, and 3-D image subsets were exported for processing with Matlab® 6.1 software (The Mathworks, Inc., Natick, MA).

Because the color intensities of cell nuclei and matrix varied with depth and across samples, the red intensity data was normalized to allow for standardization of the subsequent image processing step of image segmentation by intensity thresholding (Figure 2.2). For 3-D image subsets of 0.2 mm x 0.2 mm x 1.0 mm (113 x 113 x 600 voxels), the 3-D 8-bit red channel intensities were reconstructed in Matlab® 6.1. Line profiles, through cell nuclei and extracellular matrix, in 2-D x-y cross sections were taken at various z locations to obtain measures of the heterogeneity in image intensity. Using data from successive 2-D sections through the depth (z-direction) of tissue, the raw sample depth-varying intensity was tabulated for nuclei and extracellular matrix. The characteristic matrix value at each depth was estimated as the location of the peak in the voxel intensity histogram for each depth. The value for nuclei was approximated as the

upper percentile in the histogram corresponding to half of the estimated nuclei volume fraction in cartilage from previous work, or ~1% [18]. Profiles of depth-varying intensity for nuclei and for matrix were then computed using a piecewise linear fit (8 pieces of sizes of 5%, 5%, 10%, 10%, 10%, 20%, 20%, 20% of the total depth). The data were then shifted and scaled linearly, so that fits (as a function of depth) of nuclei and matrix had values of 160 and 80, respectively, well within the 0-255 values of 8-bit data.

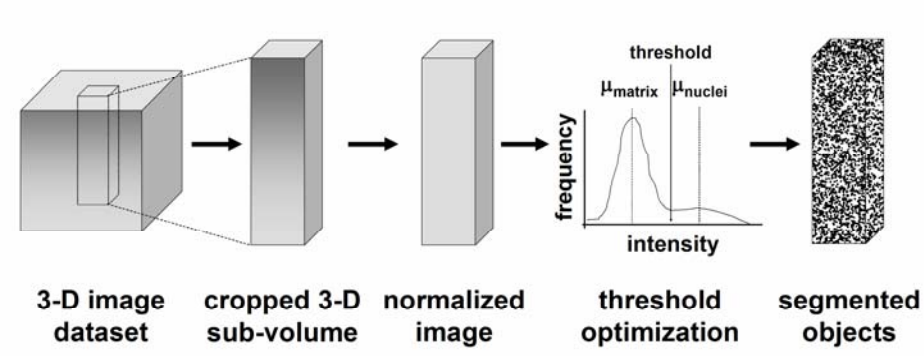

Figure 2.2: Flow diagram summarizing the image processing routine for localizing cell nuclei as segmented objects from a 3-D image data set.

An estimate for optimal threshold level to segment the normalized data sets was then determined and applied. The threshold value was based on calculations assuming two Gaussian intensity distributions, one for matrix voxels and another for nuclei voxels. A red intensity histogram of the constituent voxels for each subset was constructed to show the distributions of matrix and nuclei voxels, as well as those sampling the transition between these regions. Normalized red channel histograms revealed a large matrix peak at an intensity of 80. The peak at 80 was fit with a Gaussian distribution and subtracted, leaving nuclei and intermediate voxels. Intermediate voxels were then successively removed by best-fit Gaussian curves of remaining transition and nuclei voxels, until the percentage of voxels remaining in the nuclei population out of the total data set size was approximately equal to the expected volume percentage of nuclei (1%) based on previous studies [18]. An optimal threshold value for each data set was calculated in order to minimize error due to nuclei characterized inappropriately as matrix (false negative) and matrix characterized inappropriately as nuclei (false positive). Using this analysis, for all data sets, the minimum total error coincided with a threshold of 130.

Next, image data were processed to make null the regions of high intensity matrix staining. To do so, the green color channel data was segmented into cytoplasm (low intensity), matrix (medium to high intensity), and nuclei (high intensity). A ‘seed’ was then planted in the medium to high intensity matrix region, and all voxels connected to the propagating seed group in the matrix intensity range were removed. Cell nuclei were not removed using this routine because of the low green intensity (unstained) cell

cytoplasm that isolated nuclei from the extracted matrix (no connectivity to propagating seed).

In the final image processing step, images were segmented based on intensity in order to isolate cell nuclei and then determine nuclei locations. The theoretical intensity threshold calculated above was applied to separate background from nuclei voxels. Interconnected voxels were then grouped to identify individual cell nuclei objects, and the 3-D centroid positions were determined as each object's center of intensity.

The validity of the automated image processing was assessed as sensitivity and specificity measures in distinct depth regions using manual methods of cell identification as a gold standard. Nuclei centroid positions were determined manually in parts of image subsets for comparison with the image processing results. Cell nuclei 3-D positions were estimated by manual inspection of a stack of 2-D images. Small volumes (35 μm in the y direction and 100-250 μm in each of the x and z directions) of the superficial, middle and deep regions of mature articular cartilage, and corresponding depth (z) regions in fetal and calf tissue, were cropped in each of the sample growth stages of surface area sufficient to count 50-100 cell nuclei. Objects were identified in these samples using the approach of the dissector method. Once identified, cell nuclei centroids were estimated in 3-D as the 2-D centroid of the nucleus in the mid-section of the stack containing the nucleus.

Cell nuclei localization by automated and manual methods were compared to determine the dependence of the results on intensity threshold value. Cell nuclei positions found using the two methods were overlaid, showing inconsistencies (greater than 2

voxels away in x, y, and z directions) in localization by the automated routine. Results were tabulated as follows:

True positive: cell nuclei locations identified manually and automatically

False positive: cell nuclei locations identified automatically only

False negative: cell nuclei locations identified manually only

The overall sensitivity of the automated method was assessed as the number of correctly identified objects divided by the number of actual objects identified manually. The specificity was determined as the number of correctly identified objects divided by the total number of identified objects.

The image processing routine was then applied to assess the depth-associated variation in cell density. Object centroids in the RESView 3.0 coordinate system (x, y, z) were transformed to a new coordinate system (X,Y,Z) to indicate depth from the articular surface plane (Z=0). The surface plane was determined by first defining the centroids of four surface nuclei as being the most superficial in four corners (50 x 50 μm^2 cross sectional areas). The surface normal to the plane was then found (as the cross product of two vectors formed from the most superficial point to the two adjacent points). Object centroids were counted in 0.1 mm deep (Z) sections and 0.2 mm x 0.2 mm cross-sectional area (X,Y), excluding 5 μm at each X-Y surface to eliminate edge effects. Voxels that were devoid of cartilage tissue, for example, due to blood vessels, were also omitted from the depth bin when cell number per tissue volume was calculated. The automated process was repeated for four distinct sub-volumes, at locations ~600 μm apart within each of the samples. These repeated measures were averaged and compared across growth stage with depth to provide a measure of variability within 3-D data sets.

Cell nuclei locations in small regions of the superficial, middle, and deep depth regions were analyzed to quantify tissue proximity and angle to cell nuclei in a particular region. Coordinate locations in volumes 50 μm deep starting at the articular surface, and at 0.25 mm and 1 mm in depth were isolated. The 3-D Euclidean Distance Transform [20] was then tabulated, giving the position of the nearest cell nucleus centroid. From this, the proximity and magnitude of angle to the nearest centroid in the Z-direction with respect to the X-Y plane were calculated, discarding data within 5 μm of the centroid (representing mostly intracellular locations). The cumulative distribution function of

distance values was plotted at 5, 10, 15, and 20 μm proximities, and the average angle to the nearest object was calculated, for each depth region and growth stage. Again, each data point was expressed as the mean±standard deviation of four repeated measures.

2.4 Results

Three-dimensional renders of image data portrayed qualitative differences in the density and organization of chondrocytes at different stages of growth, from immature tissue to mature articular cartilage (Figures 2.3, 2.4). Chondrocytes of the superficial region appeared flattened from a side profile view (Fig. 2.3A-C) and discoid from an en face view in all growth stages (Fig. 2.3D-F), and the nucleus of each cell had a similar shape, being smaller in size and located in the center of the cell cytoplasm region. Cells with such characteristics were present from the articular surface down to a depth of ~50 μm in adult tissue, and localized more near the surface in fetal and calf cartilage. Below this region (Fig. 2.3G-I), cells appeared rounded, with some cell nuclei arranged in pairs, especially in immature tissue. Cells of the deeper region (Fig. 2.3J-L) of mature cartilage were in the form of columns, while those of immature cartilage did not exhibit such an organization and did not appear different from cells in the middle region to the depth surveyed in this study.

A high contrast in red intensity was present between cell nuclei and the surrounding cytoplasm and matrix background. The variation in color intensity with depth within a sample and between samples of different ages was observed in the full 3-D depth views as well as in the regional 2-D cross sections (Figure 2.3). The intensity of the

nuclei increased from the superficial region to the middle and deep regions and then diminished in the deep region of the adult sample. Upon normalization, 2-D cross sections exhibited approximately uniform intensity, with line profiles of normalized data confirming that baseline matrix and nuclei intensity peaks were similar for all regions and samples (Figure 2.5). Representative color values of matrix and nuclei further confirmed the uniform color scheme of the data sets and the achieved target intensities of 80 and 160 for matrix and nuclei, respectively (Figure 2.6).

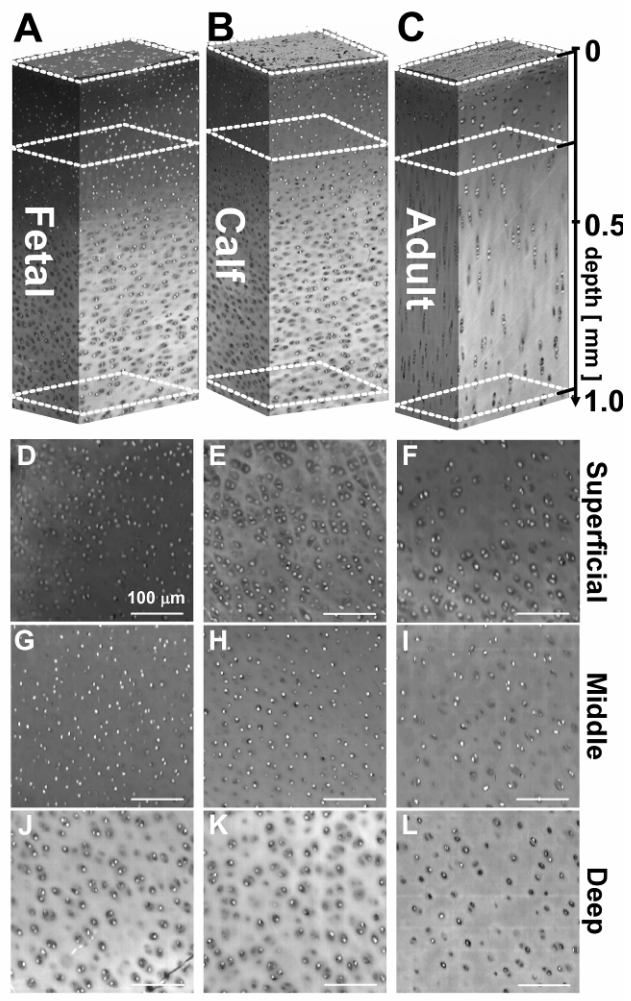

Figure 2.3. Depth-varying cell organization of bovine articular cartilage at different stages of growth. 3-D render of fetal (A), calf (B) and adult (C) tissue. Depth from the articular surface is indicated. Dashed boxes indicate locations where 2-D en face views are presented for superficial (DEF), middle (GHI), and deep (JKL) regions.

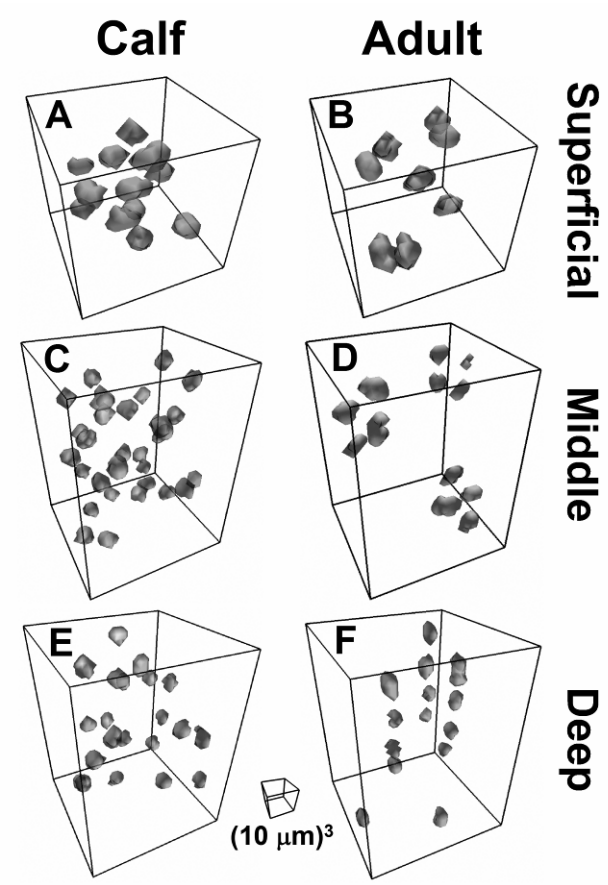

Figure 2.4. Organization of cell nuclei in 3-D in small sub-sections of calf and adult tissue in portions of three classical depth zones are shown (50 x 50 x 50 μm^3 for superficial, 50 x 50 x 70 μm^3 for middle and deep). Image datasets were color segmented, and rendered in 3-D with a perspective view. Box indicates 10 x 10 x 10 μm^3 image scale.

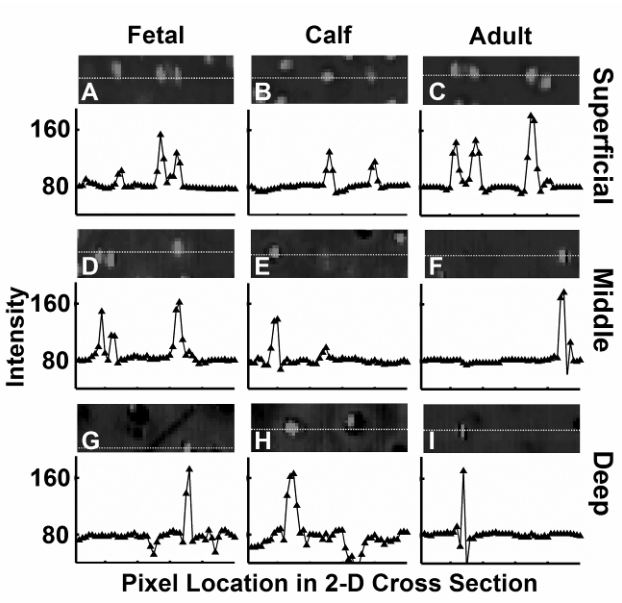

Figure 2.5. Characteristic difference in intensity between cell nuclei and extracellular matrix in normalized data sets. Profile of intensity along lines through nuclei from superficial (ABC), middle (DEF), and deep (GHI) regions of fetal, calf, and adult samples. Target intensities of matrix and nuclei were 80 and 160, respectively.

Analysis of the location of cell nuclei using the automated image processing routine had a high accuracy, relative to the manually-determined location of cells. The threshold level for image segmentation had a relatively small effect on the fidelity of cell nucleus identification. Total errors reached minima in each of the subsets at a threshold level that was in between the intensities of matrix and nuclei values (Figure 2.7), and typically near the threshold intensity value (130) obtained theoretically from analysis of intensity distribution. Using a threshold of 130, errors in each of the superficial, middle, and deep regions were determined (Table 2.1). Along with 610 true positive cells, a total of 7 false negatives and 10 false positive errors were noted, yielding an overall sensitivity (true positives relative to true positives and false negatives) of 99%, and a specificity of 98%. Sources of false negative error included low intensity nuclei and non-delineated nuclei due to nuclei arranged in clusters. The sole source of false positive error was high intensity matrix staining. Error of each type (false negative and false positive) did not exceed 4% in each region. Because the accuracy was high, automatically determined cell nuclei locations were used (without corrections) for subsequent analysis.

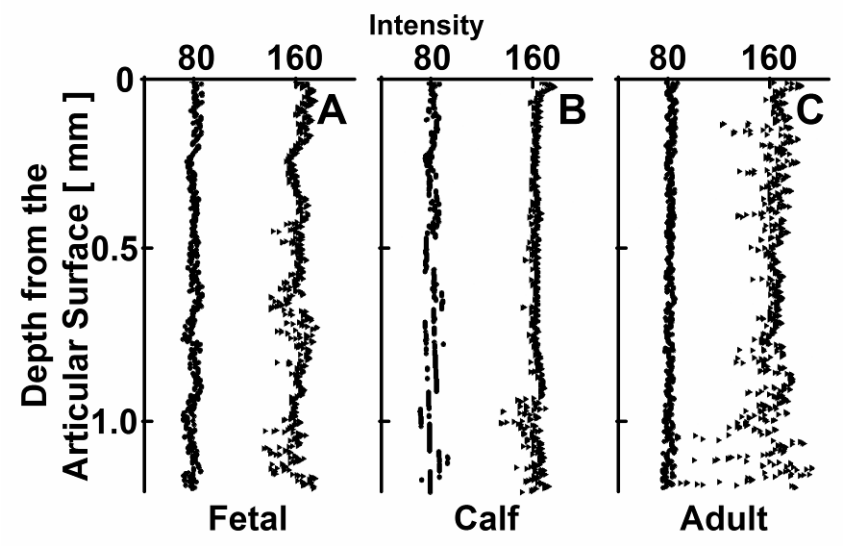

Figure 2.6. Characteristic depth-associated variation in intensity, after normalization, of nuclei (▲) and extracellular matrix (●) for fetal (A), calf (B), and adult (C) data sets.

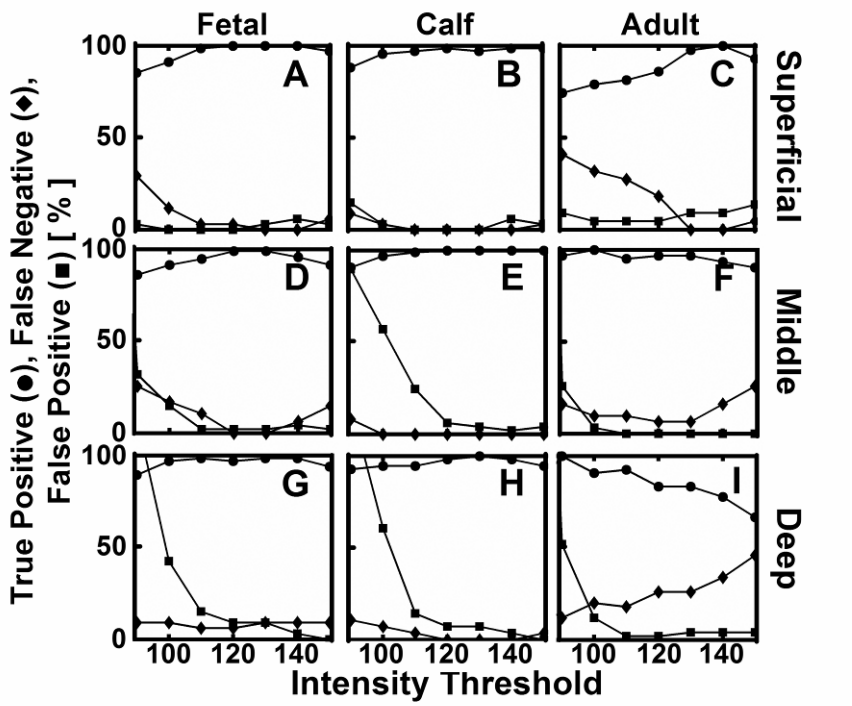

Figure 2.7. Effect of threshold intensity level on accuracy of automated routine to identify and localize nuclei. Automatically localized nuclei were compared to those from manual inspection of fetal, calf, and adult sub-samples with ~40-100 cell nuclei in superficial (ABC), middle (DEF), and deep (GHI) regions. The intensity level of 130 (dashed lines) was chosen for subsequent analyses.

Table 2.1. Error analysis of automated image processing routine for cell nuclei. Numbers of true positives (tp), false negatives (fn) and false positives (fp) were determined for a threshold intensity level of 130 in fetal, calf and adult sub-samples in the superficial, middle and deep regions of tissue.

	Fetal			Calf			Adult		
	tp	fn	fp	tp	fn	fp	tp	fn	fp
Superficial	64	0	1	64	0	0	41	0	2
Middle	91	0	1	98	0	2	60	2	0
Deep	62	2	2	55	0	2	75	3	0

Overall, cellularity decreased with maturation and with depth from the articular surface, down to a depth of 1.0 mm, in the samples analyzed. Cellularity dropped with depth from the articular surface, decreasing from 290 to 120, 310 to 110, and 150 to 50 million cells per cm^3 for fetal, calf, and adult samples (Figure 2.8). Most of the depth-associated decrease in cellularity was in the superficial ~500 μm of tissue in immature samples, and ~100 μm of tissue in mature samples, respectively. At each depth, articular cartilage exhibited cellularity that was lower (30% to 50%) in adult cartilage than immature cartilage samples. However, data from samples from different animals would be needed to generalize this conclusion for populations of bovine animals.Between the subvolumes analyzed from each samples' 3-D image dataset, there was relatively little variation. Estimation of cellularity from the automated method within the tissue samples at each growth stage yielded a coefficient of variation of 7%, 6%, and 7% for fetal, calf and adult samples among the four 0.2 mm x 0.2 mm x 1.0 mm locations spaced 600 μm apart in the x direction. The corresponding average standard deviation of cellularity was 8, 8, and 3 million cells per cm^3 through the full depth for fetal, calf and adult samples, respectively.

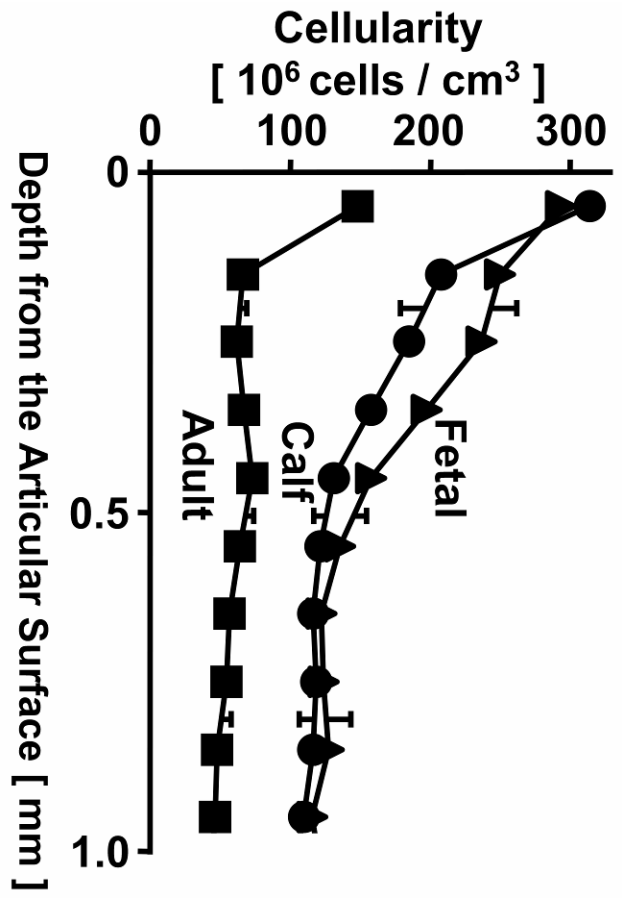

Figure 2.8. Variation in cellularity with depth in fetal (▲), calf (●), and adult (■) samples. Cellularity presented in 0.1 mm depth bins, from the articular surface to 1.2 mm in depth. Data are expressed as mean ±SD of repeated measures at four equally spaced volumes, each with a cross sectional area of 200x200 μm^2.

The distance from voxels to the nearest cell increased with depth from the articular surface and with increasing stage of maturation (Figure 2.9). In immature fetal and calf tissue, much of the tissue is in close proximity to a cell centroid location, as indicated by a high percentage of low intensity pixels in the distance transform maps of tissue cross sections at depths of Z=0, 200, and 700 μm. In mature adult tissue, a high percentage (30-50%) of pixels in the maps were of high intensity, representing tissue that was not associated closely with (within 20 μm of) a cell, especially in the middle and deep regions. In contrast, in immature tissue, the majority of the tissue volume (~60%) was within 10 μm (Figure 2.10). Further, in the superficial and middle regions of immature tissue, only small volumes (<5%) of tissue were outside of 15 μm from a cell nucleus centroid.

The angle at which tissue was situated relative to the nearest cell changed with depth from the articular surface in mature tissue, but not in immature cartilage (Figure 2.11). The average magnitude of the angle from tissue voxels to the nearest cell nucleus centroid, measured relative to the X/Y plane, was 30-31° for immature fetal and calf tissue and in the superficial region of adult cartilage. In mature cartilage, this angle decreased to 25° in the deep region, reflecting cell organization in this region.

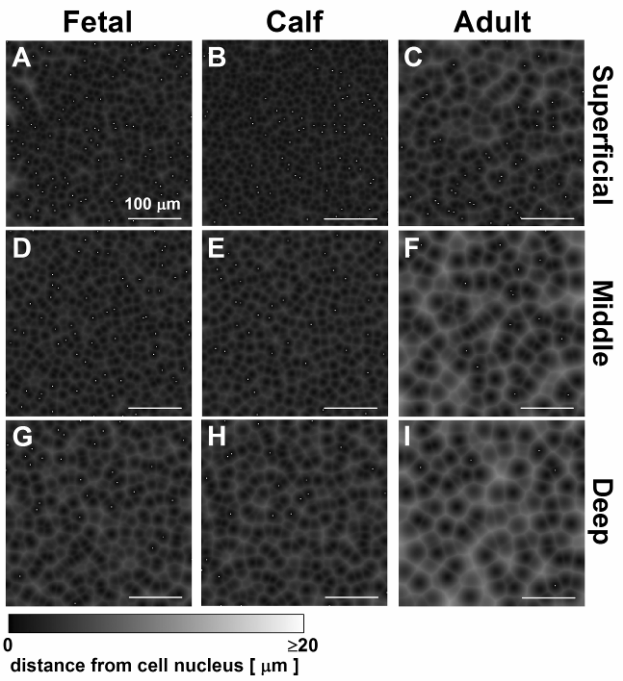

Figure 2.9. Proximity maps illustrating distance from each location to the nearest cell nucleus. Image data of Figure 3 were analyzed by distance transforms of superficial (ABC), middle (DEF), and deep (GHI) regions of articular cartilage corresponding to fetal, calf and adult stages of development (compare to Fig. 3, DEF, GHI, JKL). Gray scale intensity indicates 3-D distance as shown (0-20μm). Cell nuclei centroids within 0.5 μm of the cross section plane are indicated as white dots.

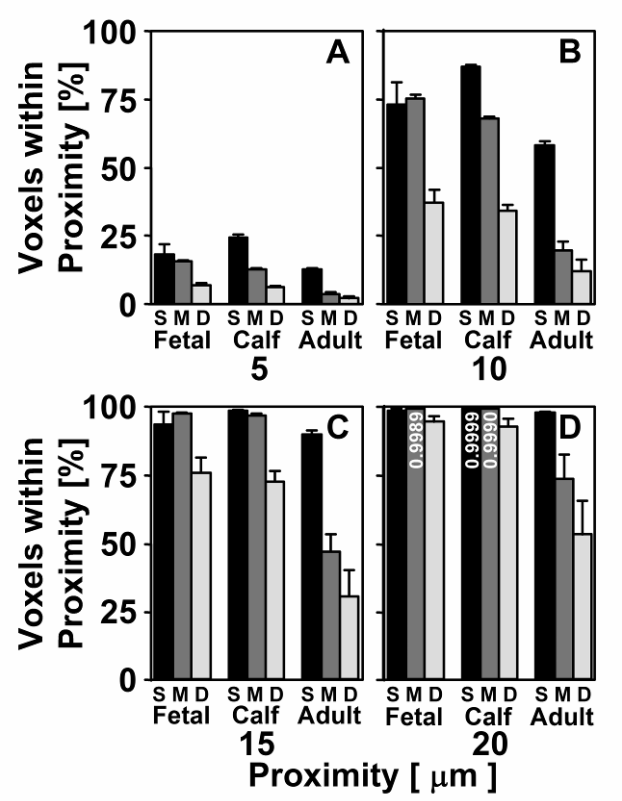

Figure 2.10. Depth- and growth-associated variation in tissue proximity to chondrocytes in articular cartilage. The percentage of voxels within the indicated proximity of the nearest cell nucleus centroid was computed for 50 μm thick sections in the superficial, middle, and deep (S,M,D) regions of fetal, calf , and adult bovine articular cartilage. Mean±SD of repeated measures at four locations per sample.

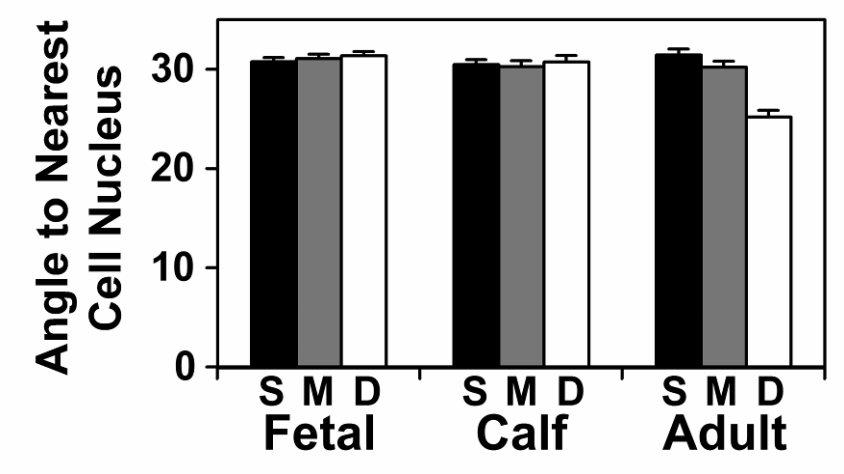

Figure 2.11. Depth- and growth-associated variation in tissue angle to chondrocytes in articular cartilage. The angle of each tissue voxel to the nearest cell nucleus centroid in the Z direction versus the X-Y plane was found for 50 μm thick sections in the superficial, middle, and deep (S,M,D) regions of fetal, calf, and adult bovine articular cartilage. Mean±SD of repeated measures at four locations per sample.

2.5 Discussion

This study developed a methodology to characterize cell density and 3-D cell organization in articular cartilage at different stages of growth. Surface imaging microscopy was applied to obtain 3-D images of articular cartilage through superficial, middle and deep zones of mature bovine articular cartilage and corresponding depths in fetal and calf tissue (Figure 2.3). Using a semi-automated method for determining the 3-D location of cells in cartilage samples, cellularity (Figure 2.8) and tissue proximity to the nearest cell nucleus (Figures 2.9 and 2.10) decreased with depth from the articular surface, as well as during growth and maturation. Renders of groups of individual cell nuclei illustrated the tight packing of cells in calf tissue (Fig. 2.4A,C,E) relative to adult tissue (Fig. 2.4B,D,F). Further, the views of adult tissue confirmed the presence of horizontal pairs of cells in the superficial region (Fig. 2.4A), columns of cells in the deep region (Fig. 2.4C), as well as oblique clusters of cells in the middle region (Fig. 2.4B) that were not evident in 2-D sections. Application of this methodology may provide the information needed to assess how the 3-D organization of populations of cells in articular cartilage contributes to the structural evolution of cartilage during growth.

Samples were prepared in such a way to preserve in situ bulk geometry and local cell organization. Large (1 cm^3) blocks of tissue were fixed fresh after harvest to prevent the swelling that occurs when bovine calf and adult tissue is cut into smaller portions [16, 21]. Preservation of in situ bulk geometry with little shrinkage through the imaging procedure (fixation, staining, and dehydration) was verified by comparing bulk tissue dimensions of the sample at these various stages using high resolution microscopy.

Fixation was done at 4°C to minimize enzyme-mediated degradative changes that might alter cellular morphology and spatial organization, and also cell fate processes such as division and death. Other studies have utilized sample preparation methods to minimize macroscopic sample shrinkage. These studies have maintained cartilage attached to underlying bone, used chemical fixation for long periods of time, and stored samples in 70% ethanol at 4°C [9]. Other studies have imaged samples while maintained in isotonic buffer solutions without fixation [3, 5].

While overall dimensions were affected only slightly by sample preparation, it is also possible that more subtle features of the tissue were affected [6]. The estimation of the position of each cell, based on the centroid location of each nucleus, may be affected by the relative location of the nucleus within a cell, as well as effects of fixation. The fixation method used here may have resulted in a slight change in the microstructure of the tissue. Other studies [8, 24] have utilized alternative sample preparation methods to minimize fixation effects on cell and extracellular matrix structure and the cell-matrix interface. On the other hand, at the resolution of images obtained here, there was no gap evident between the cell membrane and the pericellular matrix, a hallmark of shrinkage that occurs with traditional fixation and paraffin embedding. Thus, the chemical fixation and use of plastic embedding appears to have minimized distortion. It is possible that methodologies may be further refined, in conjunction with appropriate cellular stains, to assess other features, such as the volume fraction of cells or nuclei. In addition, views of 2-D surfaces of cartilage samples, both in vertical and tangential (en face) images, were consistent with previous studies. For example, images of the superficial zone showed a

cell organization similar to that described for human tissue [22], with cells at a high density and in a clustered arrangement.

The image processing method involved segmenting and identifying cell nuclei. While cells were generally identified with a high sensitivity and specificity, some inaccuracies were apparent. These resulted from variability in fluorescence from nuclei, and inaccurate boundary delineation between cells. Several additions to the procedure used may improve the accuracy of cell nuclei localization. These include imaging at a resolution giving a voxel length less than 1.77 μm, and application of additional image analysis methods and algorithms.

Although the resolution of the voxels were $(1.77um)^3$, the determination of cell nucleus position as the calculated centroid location is likely to yield an estimate of the position of the nucleus with sub-voxel precision. Typically, the calculation of centroid position, involving spatial variation in grey-scale levels, gives a 10-fold [12] enhancement of resolution, relative to the voxel resolution, for high S/N ratio images. This concept also applies to object boundaries, which can be interpolated from grayscale pixel data to yield sub-pixel resolution [20], from which object shapes and volumes can be accurately estimated.

Normalization of datasets with respect to nuclei and background allowed automated intensity segmentation of datasets at a threshold determined from histogram analysis. The optimal threshold found from this analysis was consistent in the different depth regions and growth stages, suggesting that the normalization routine was independent of absolute sample intensity and cell content. Whether the threshold found

here is valid in additional samples, however, may be scrutinized in future studies, since only one sample of fetal, calf, and adult tissue was processed and analyzed here.

The time required for analyzing samples with the current methodology is highly dependent on the time of sample preparation, and to a lesser extent on analysis of images; thus, the overall analysis time is highly dependent on the statistical design and requirements of a particular experiment. The duration of the sample preparation period is ~14 days. The image acquisition method requires ~6 hours for making and imaging 1000 slices at 1024x1024, ~2 hours for fully-automated pre-processing of data, and another ~1 hour for the data reduction to obtain the metrics described herein. If the sample volume is relatively large to the overall specimen, the metrics obtained from the overall image, or portions therein, may be representative of the specimen, and thus effectively minimize manual preparation of multiple sections from a specimen. On the other hand, if the sample volume is small to that of the specimen, then multiple DVI samples would be needed.

Estimates of the trends in cellularity in bovine articular cartilage obtained using the 3-D imaging methodology were in general agreement with those found previously. Similar to the results of the present study, cellularity was found to decrease with depth from the articular surface and with normal growth, using biochemical quantification of DNA content [26, 27]. Absolute estimates using these biochemical assays on the first 1 mm in depth from the articular surface in fetal, calf, and adult tissue [14] are in general agreement with those obtained using the current 3-D imaging methodology. Depth-varying bovine articular cartilage cellularity determined using DVI and automated image processing also is consistent with cell density trends previously determined for other

experimental animals using stereological methods of image processing [2, 9, 18, 29]. The rapid drop in cell density with depth past the superficial zone (first ~10% of tissue depth) observed in this study was not observed in mature rabbit articular cartilage [2, 18], but is present in larger mammals, such as in the adult bovine animal [29] and adult human [9]. Previous estimates of cell density in bovine animals using stereological estimates yielded a lower number of cells per unit tissue volume [29]. However, this study analyzed cartilage from the humeral head, so that differences are likely to reflect differences between that site and the less weight-bearing patellofemoral groove in the current work. The cellularity of weight-bearing regions has been found to be significantly lower than that of less weight-bearing regions in adult rabbits, on the order of up to one-half [2]. To compare precisely the absolute values found using the technique developed here with those found with other methods, analysis of more samples will need to be analyzed.

Previous studies have quantified morphology of cell nuclei in articular cartilage, using both 2-D and 3-D image acquisition and analysis methods [2, 5, 9, 18]. In the current study, images were acquired at a somewhat lower resolution than in those previous studies in order to sample large image volumes; thus, image resolution was not sufficient to precisely localize the boundaries of cell nuclei. Also, cell boundaries were not assessed in the current study, as the stains used were not optimized to provide contrast at this region. Thus, it was not possible to compare the current findings with those analyses of cell volume fraction in cartilage. Other stains, higher resolution imaging, and further image processing methods to delineate cell and nuclei boundaries may allow such a comparison in the future.

Acquisition of large 3-D structural bioinformatics data sets for articular cartilage at different stages of growth illustrates the potential for examining the organization of large groups of cells in growing tissues. The complex arrangements (columns, pairs, clusters; Figure 2.3, 2.4) of chondrocytes may reflect their physiological roles during growth and ultimately homeostasis, and also functional interactions throughout the tissue depth. A means for quantitative assessment of the 3-D spatial arrangement of cell populations is a significant step toward understand the roles of such cell organization in tissue dynamics.

The high proximity to the nearest cell nucleus observed in immature cartilage compared to mature cartilage may help explain this tissue's ability to effectively heal partial or full-thickness defects [17], and the general lack of successful repair in adult cartilage. Diffusion of molecules in cartilage matrix is typically hindered, especially as molecular size increases [15]. Pulse-chase labeling of proteoglycans has revealed that much of the deposition and turnover of these molecules in bovine cartilage occurs within 8 μm of the cell membrane [19], or approximately 13 μm from the cell center for a cell with 10 μm diameter. Because a majority of the tissue space in mature bovine cartilage is outside of this proximity to the cell (Figure 2.10), effective healing may be impaired by insufficient matrix turnover. In contrast, in immature tissue, ~85% of the tissue volume in the superficial and middle zones is included in this region of high matrix turnover.

The average angle at which tissue is situated with respect to the nearest cell describes one feature of the higher order 3-D arrangement of cells in the tissue (Figure 2.11). By comparison, for 2-D sheets of cells, this angle approaches 90° (relative to the

X-Y plane) where the closest cell to any point in the tissue is almost purely in the Z-direction. For cell columns, on the other hand, the average angle is near zero, with most of the tissue positioned in the transverse direction from cells. Intermediate average angles are typical for cells in an organization in between these extremes; for example, for cells arranged in an isotropic cubic lattice structure, the average angle is 33°. The results from the current study showing little difference in angle with depth in immature tissue reflect the lack of the classical organization of cells that is apparent in adult cartilage. In mature tissue, however, the columnar arrangement of cells in the deep zone is evident and consistent with a decrease in an average angle of tissue to the nearest cell to 25°. The appearance of groups of sheet-like horizontal clusters in the superficial zone did not result in an angle approaching that of the ideal case, likely because of the tight vertical packing of these cell groups made possible by their flattened shape.

The image processing methods used here could also be applied to 3-D images of cartilage obtained by other methods, such as confocal microscopy of cartilage or chondrocyte-laden materials with fluorescently-labeled cell nuclei [1, 5, 9, 11, 13].

The methods developed in this study may be applicable to a variety of tissues, in which cell organization over the length scale of ~1 mm are of interest. In addition, although the fluorescence signal from the tissue in the present study was derived by staining with exogenous dyes, it may also be possible to analyze fluorescent signals intrinsic to, or genetically engineered, into cells and tissues.

2.6 Acknowledgments

This chapter, in full, was published as "Depth-varying density and organization of chondrocyte in immature and mature bovine articular cartilage assessed by 3-D imaging and analysis". J Histochem Cytochem. 2005 Sep; 53(9):1109-19. The dissertation author is the primary investigator and thanks co-authors, Barbara Schumacher, graduate student Benjamin Wong, and Drs. Won Bae, Kelvin Li, Amanda Williamson, and Jeff Price for their contribution. This work was supported by the National Institute of Health, National Science Foundation, and National Aeronautics and Space Administration.

2.7 References

1. Durrant LA, Archer CW, Benjamin M, Ralphs JR: Organisation of the chondrocyte cytoskeleton and its response to changing mechanical conditions in organ culture. *J Anat* 194:343-53, 1999.

2. Eggli PS, Hunziker EB, Schenk RK: Quantitation of structural features characterizing weight- and less-weight-bearing regions in articular cartilage: a stereological analysis of medial femoral condyles in young adult rabbits. *Anat Rec* 222:217-27, 1988.

3. Errington RJ, Fricker MD, Wood JL, Hall AC, White NS: Four-dimensional imaging of living chondrocytes in cartilage using confocal microscopy: a pragmatic approach. *Am J Physiol* 272:C1040-51, 1997.

4. Ewald AJ, McBride H, Reddington M, Fraser SE, Kerschmann R: Surface imaging microscopy, an automated method for visualizing whole embryo samples in three dimensions at high resolution. *Dev Dyn* 225:369-75, 2002.

5. Guilak F, Ratcliffe A, Mow VC: Chondrocyte deformation and local tissue strain in articular cartilage: a confocal microscopy study. *J Orthop Res* 13:410-21, 1995.

6. Hunziker EB: Tissue sampling and preservation. In: *Methods in Cartilage Research,* ed. by KE Keuttner, Maroudas A, Harcourt Brace Jovanovich Ltd., London, 1990, 19-25.

7. Hunziker EB: Articular cartilage structure in humans and experimental animals. In: *Articular Cartilage and Osteoarthritis,* ed. by KE Kuettner, Schleyerbach R, Peyron JG, Hascall VC, Raven Press, New York, 1992, 183-99.

8. Hunziker EB, Hermann W, Schenk RK, Mueller M, Moor H: Cartilage ultrastructure after high pressure freezing, freeze substitution, and low temperature embedding. I. chondrocyte ultrastructure - implications for the theories of mineralization and vascular invasion. *J Cell Biol* 98:267-76, 1984.

9. Hunziker EB, Quinn TM, Hauselmann HJ: Quantitative structural organization of normal adult human articular cartilage. *Osteoarthritis Cartilage* 10:564-72, 2002.

10. Kim YJ, Sah RLY, Doong JYH, Grodzinsky AJ: Fluorometric assay of DNA in cartilage explants using Hoechst 33258. *Anal Biochem* 174:168-76, 1988.

11. Knight MM, van de Breevaart Bravenboer J, Lee DA, van Osch GJ, Weinans H, Bader DL: Cell and nucleus deformation in compressed chondrocyte-alginate constructs: temporal changes and calculation of cell modulus. *Biochim Biophys Acta* 1570:1-8, 2002.

12. Kubitscheck U, Kuckmann O, Kues T, Peters R: Imaging and tracking of single GFP molecules in solution. *Biophys J* 78:2170-9, 2000.

13. Lee DA, Knight MM, Bolton JF, Idowu BD, Kayser MV, Bader DL: Chondrocyte deformation within compressed agarose constructs at the cellular and sub-cellular levels. *J Biomech* 33:81-95, 2000.

14. Li KW, Williamson AK, Wang AS, Sah RL: Growth responses of cartilage to static and dynamic compression. *Clin Orthop Relat Res* 391S:34-48, 2001.

15. Maroudas A: Physico-chemical properties of articular cartilage. In: *Adult Articular Cartilage,* ed. by MAR Freeman, Pitman Medical, Tunbridge Wells, England, 1979, 215-90.

16. Myers ER, Lai WM, Mow VC: A continuum theory and an experiment for the ion-induced swelling behavior of articular cartilage. *J Biomech Eng* 106:151-8, 1984.

17. Namba RS, Meuli M, Sullivan KM, Le A, Adzick NS: Spontaneous repair of superficial defects in articular cartilage in a fetal lamb model. *J Bone Joint Surg Am* 80-A:4-10, 1998.

18. Paukkonen K, Selkainaho K, Jurvelin J, Helminen HJ: Morphometry of articular cartilage: a stereological method using light microscopy. *Anat Rec* 210:675-82, 1984.

19. Quinn TM, Maung AA, Grodzinsky AJ, Hunziker EB, Sandy JD: Physical and biological regulation of proteoglycan turnover around chondrocytes in cartilage explants. Implications for tissue degradation and repair. *Ann NY Acad Sci* 878:420-41, 1999.

20. Russ C. The Image Processing Handbook. 3rd ed. Boca Raton: CRC; 1999.

21. Sah RL, Grodzinsky AJ: Biosynthetic response to mechanical and electrical forces: calf articular cartilage in organ culture. In: *The Biology of Tooth Movement,* ed. by LA Norton, Burstone CJ, CRC Press, Boca Raton, FL, 1989, 335-47.

22. Schumacher BL, Su J-L, Lindley KM, Kuettner KE, Cole AA: Horizontally oriented clusters of multiple chondrons in the superficial zone of ankle, but not knee articular cartilage. *Anat Rec* 266:241-8, 2002.

23. Stockwell RA, Meachim G: The chondrocytes. In: *Adult Articular Cartilage,* ed. by MAR Freeman, Pitman Medical, Tunbridge Wells, England, 1979, 69-144.

24. Studer D, Michel M, Wohlwend M, Hunziker EB, Buschmann MD: Vitrification of articular cartilage by high-pressure freezing. *J Microsc* 179:321-32, 1995.

25. Temple MM, Masuda K, Pietryla DW, Thonar EJ-MA, Sah RL: Age- and site-associated weakening of human articular cartilage: relationship to collagen denaturation. *Trans Orthop Res Soc* 28:707, 2003.

26. Williamson AK, Chen AC, Masuda K, Thonar EJ-MA, Sah RL: Tensile mechanical properties of bovine articular cartilage: variations with growth and relationships to collagen network components. *J Orthop Res* 21:872-80, 2003.

27. Williamson AK, Chen AC, Sah RL: Compressive properties and function-composition relationships of developing bovine articular cartilage. *J Orthop Res* 19:1113-21, 2001.

28. Wong B, Wallace V, Coleno M, Benton H, Tromberg B: Two-Photon Excitation Laser Scanning Microscopy of Human, Porcine, and Rabbit Nasal Septal Cartilage. *Tissue Engineering* 7:599-606, 2001.

29. Wong M, Wuethrich P, Eggli P, Hunziker E: Zone-specific cell biosynthetic activity in mature bovine articular cartilage: a new method using confocal microscopic stereology and quantitative autoradiography. *J Orthop Res* 14:424-32, 1996.

CHAPTER 3

3-D IMAGING OF CHONDROCYTES IN ARTICULAR CARTILAGE: GROWTH-ASSOCIATED CHANGES IN CELL ORGANIZATION

3.1 Abstract

3-D imaging and analysis techniques can be used to assess the organization of cells in biological tissues, providing key insights into the role of cell arrangement in growth, homeostasis, and degeneration. The objective of the present study was to use such methods to assess the growth-related changes in cell organization of articular cartilage from different sites in the bovine knee. Three-dimensional images of fetal, calf, and adult cartilage were obtained and processed to identify cell nuclei. The density of cells was lower with growth and with increasing depth from the articular surface. The cell organization, assessed by the angle to the nearest neighboring cell, also varied with growth, and reflected the classical organization of cells in adult tissue, with neighboring cells arranged horizontally in the superficial zone (average angle of 20°) and vertically in the deep zone (60°). In all other regions and growth stages of cartilage, the angle was

~32°, indicative of an isotropic organization. On the contrary, the nearest neighbor distance did not vary significantly with growth or depth. Together, these results indicate that cartilage growth is associated with distinctive 3-D arrangements of groups of chondrocytes.

3.2 Introduction

Biomedical imaging techniques are used frequently to characterize the changing microstructure of biological tissues at various stages of development, growth, aging, injury, and disease. Often, the constituent cells are of interest because of their role in mediating tissue formation, repair and degeneration. The changing function of a population of cells may be reflected by the changes in their organization. Thus, delineation of cell organization may lead to a tissue-scale understanding of cell-guided formation, responses to injury, and degradation. This paper provides a brief review of imaging techniques used to examine cells within tissues, and then describes an investigation of changes in cell organization in the context of articular cartilage development and growth by analysis of fetal, calf, and adult tissue.

Imaging of Cell Populations within Tissues

The traditional method of assessing the organization of groups of cells in tissue has been by analysis of thin sections with 2-D light microscopy. Using such 2-D images, stereological analysis has evolved to allow for unbiased estimation of cell morphology and number per volume [7, 13, 24, 34]. In the case of quantifying cell number per volume, new cells are counted in sequential image sections and the number divided by the total volume of tissue inspected. These procedures have proven useful in tabulating depth-varying cellularity in articular cartilage [7, 13]. However, evaluation of higher levels of cell organization is difficult because cells are not spatially localized in these

procedures and sample thickness may not be large enough to identify entire clusters of cells.

Three-dimensional imaging and image processing modalities have been used to directly analyze cell organization within tissues. Laser-scanning confocal microscopy allows for capture of 3-D tissue features stained with specific fluorescent probes by using pinhole apertures to exclude the excitation beam and collect fluorescence from a thin (in the z direction) optical section [4]. More recently, two photon excitation laser scanning confocal microscopy has been employed on a variety of tissues, and can detect endogenous fluorophores excited by absorption of two-photons of twice the wavelength (half the energy) that is normally needed for excitation [5]. Using this technique, cellular components can be visualized to a depth of up to several hundred microns. Another technique, Optical Coherence Tomography, uses a different strategy to collect a series of z data at a single x-y point in combination with scanning in the x-y plane to form a 3-D image [11]. In this technique, broadband light is split and passed into the tissue sample and an adjustable path length reference mirror, and the magnitude of the interference between the light reflected from these two targets represents the image intensity. This technique is in contrast to a newer approach, Optical Projection Tomography, in which a series of images are collected from different angles, either of transmitted brightfield light, or by emitted fluorescence signal from excited molecules [27]. Using this method, a 3-D image is formed by mathematical reconstruction of the series of views from 0 to 360 degrees, with algorithms similar to those used in micro-computed tomography. This method has the potential to resolve groups of stained molecules (either fluorescent or colorimetric) on the cellular level, up to a depth of 1 cm.

Finally, methods have been developed to obtain a 3-D image by reconstruction of serial images acquired using sequential imaging and physical sectioning. In one such technique, brain tissue was imaged at a surface using two-photon laser scanning confocal microscopy, and then laser-ablated to expose the next deeper layer [31]. This process was repeated to form a 3-D image with high resolution achieved by two-photon confocal microscopy, and size sufficient to visualize 3-D structures on the millimeter length scale. In another commercial procedure, called digital volumetric imaging (DVI), 2-D images of a tissue surface are captured using conventional fluorescence microscopy, and thin sections are sequentially removed by a diamond knife microtome [16]. This procedure involves (A) fluorescence staining and fixation of tissue and embedding with an opacified polymer, (B) automated serial sectioning and imaging through a 3-D tissue block, and (C) post-processing for viewing the image data and extracting image features. In the plane (x-y) of sectioning, resolution and field of view are determined by the objective lens and imaging camera. In the depth (z-axis) direction, resolution is determined by section thickness (with opacity of the polymer matched to achieve a surface measure), and the number of z-sections is effectively unlimited. This technique was originally developed using specific fluorescent markers for cell nuclei (Acridine Orange) and extracellular matrix (Eosin-Y), although its capability may be extended to identifying cell subpopulations with distinct phenotypes by incorporation of more specific fluorescent markers such as tagged antibodies. Recent studies have demonstrated the accuracy of DVI imaging (versus confocal imaging) [8], and the efficacy in quantifying the depth-varying organization of cells in conjunction with validated image processing routines, with high sensitivity and specificity, in bovine articular cartilage at

different stages of growth [14]. The current study uses these DVI methods to localize cells in a series of samples from animals at distinct growth stages, and to analyze cell organization by computing novel metrics of distance and angle from each cell to neighboring cells.

Cell Organization Changes in Articular Cartilage during Growth

Articular cartilage undergoes substantial growth and functional maturation between the time of joint cavitation and attainment of skeletal maturity [33]. The organization of chondrocytes in cartilage reflects, and may contribute to, articular cartilage dynamics during fetal development and post-natal growth, and at skeletal maturity [29]. In particular, the decrease in cell density during growth through the full tissue volume results from cells' separation during accretion of extracellular matrix molecules. The relatively high density of evenly-spaced chondrocytes in immature tissue are arranged favorably to actively deposit and remodel nearby extracellular matrix, essential to tissue growth and maturation. The higher density of cells, and tight vertical packing of horizontally oriented clusters of cells, near the articular surface [26], may enhance growth in this region. On the other hand, in mature articular cartilage, the low density of cells together with their clustering leads to regions of tissue relatively far from the nearest cells. This structure may predispose tissue to ineffective remodeling and repair and make it highly susceptible to structural and functional deterioration. This effect may be exacerbated in the deeper tissue regions, where cells are in sparse groups arranged in vertical columns [12]. Analysis of the depth-variation in cell organization at

different stages of growth and maturation allows further understanding of the role of the indwelling cells in articular cartilage growth and homeostasis.

In immature articular cartilage, the population of cells is situated to contribute to a highly anabolic state of tissue growth. From previous 3D analysis of cell locations in immature tissue, a large proportion of the tissue is within ~10 μm of the nearest cell [14], within the distance over which a cell can actively metabolize proteoglycan molecules [25]. This proximity to tissue results from both the high density of chondrocytes, as well as their arrangement. Near the articular surface, horizontal clusters of tightly packed, flattened chondrocytes are observed, whereas deeper in the tissue, cells are less dense but have a more homogeneous arrangement [12]. The way in which the cells reach this arrangement is not known; however, the increase in the distance between cells with growth suggests that accretion of extracellular matrix may be pushing cells apart, while the closely situated and horizontally-oriented cell groups at the articular surface may be being generated by cell proliferation. Recently, proliferating chondrocytes have been identified near the articular surface of immature tissue [10, 15, 18-20], as have progenitor or stem cells [1, 6, 9, 30]. The organization of cells in immature tissue is likely to facilitate a high rate of tissue growth, and the position of cells relative to one another may provide insight into key features of growth, such as matrix accretion and cell proliferation.

Upon maturation, the cartilage attains a classical cell organization that is associated with maintenance of tissue homeostasis [12]. In particular, cell density decreases with depth from the articular surface [13, 21, 28], and cells are arranged into characteristic groups ranging from horizontal clusters at the surface to vertical columns in

the deep regions [12, 13, 26]. Previous studies have also found that the cell density varies across the joint surface, and may depend on the magnitude of load which it bears [2, 7]. Thus, the intrinsic and extrinsic cellular cues may be different across a joint surface and lead to variable growth and evolution of distinct cell groups. The progression of articular cartilage cell organization to the final heterogeneous state may be better understood by quantifying the local organization of cells and cell groups as a function of depth and joint site at a sequence of developmental stages.

We recently described a 3-D histological method for determining the location of chondrocytes in cartilage in conjunction with DVI [14]. Although the study focused on determining cellularity in 3-D image datasets, these methodologies could be extended to other higher order metrics of chondrocyte organization, particularly the relative arrangements of small groups of cells. 3-D imaging and image processing could be applied to quantify features of cell organization, and assess the variation with growth.

The objective of the present study was to use DVI imaging and 3-D image processing methods in order to quantify the cellularity and local organization of cells in bovine articular cartilage, as a function of depth from the surface, at different stages of growth, both for the weight-bearing femoral condyle (FC) and the intermittently-loaded patellofemoral groove (PFG).

3.3 Materials and Methods

Sample Preparation

Articular cartilage was harvested from two sites of the bovine distal femur at different growth stages and prepared for 3-D histology. A total of 18 osteochondral blocks, 1 cm^3 in volume, were harvested from the lateral femoral condyle and patellofemoral groove of 3 fetal (2^{nd} trimester, 229±11 days gestation) [23], 3 calf (1-3 wk), and 3 adult (1-2 yr) bovine stifle joints, obtained from an abattoir. Samples were fixed in 4% paraformaldehyde in PBS at pH 7.4 and 4ºC for 3 days, and then trimmed to pieces ~1.5 mm x ~3 mm in surface area and to a depth of ~1.5 mm from the articular surface.

3-D Histology

Articular cartilage pieces were stained and imaged to localize cell nuclei within the 3-D cartilage block using DVI as described previously [8, 14]. Briefly, samples were stained using Eosin Y and Acridine Orange, sequentially dehydrated in graded alcohol, and held in xylene until processing. Samples were then embedded in Spurr resin with 50% opacity, and imaged using DVI (MicroSciences Corp., Corte Madera, CA) at a voxel resolution of $(1.77\ \mu m)^3$.

3-D Image Processing

The cell organization in image datasets was analyzed qualitatively and quantitatively using Matlab® 7.1 software (The Mathworks, Inc., Natick, MA). Image subsets with a surface area of $(0.2\ mm)^2$ and a depth of ~1.0 mm were exported as a stack of 2-D images from RESView 3.1™ (MicroSciences Corp.). Image stacks were imported into Matlab® 7.1 to form a 3-D image matrix. Three-dimensional images were

transformed so that the articular surface plane was parallel to the x-y plane and depth from the articular surface aligned with the z axis using a two step process. First, images were rotated in 3-D until the surface was approximately parallel to the x-y plane by inspection. Second, the articular surface was approximated by the best-fit plane through 9 reference surface points in a 3 by 3 grid, and the dataset transformed to a coordinate system where this best-fit plane was Z=0 everywhere [14].

Image datasets were processed to localize cell nuclei by their 3-D centroid location as described previously [14] with additional enhancement by 3-D spatial filtering. Briefly, the intensity was normalized as a function of depth, so that the average background intensity was 80 and the average nuclei intensity was 160. Next, image contrast of cell nuclei were enhanced relative to the background by 3-D convolution with a 5 x 5 x 5 Mexican Hat filter with σ equal to 1. In this way, objects of similar size and shape to the cell nuclei with a high intensity were enhanced, and high intensity, high frequency noise or low frequency background was attenuated. Images were again intensity normalized as a function of depth, as differently shaped nuclei through the tissue depth were enhanced to different degrees. Images were intensity segmented at a threshold of 130, determined by analysis of pixel histograms [14], into object and background voxels, and connected object voxels were grouped to form individual objects (cell nuclei). Accurate segmentation was confirmed by overlaying the segmented image on the original grayscale image, and estimating false positive and false negative objects relative to true positive results in different depth regions. Accuracy was found to be high (>95%) in a subset of 200 μm x 200 μm x 100 μm regions at varying depths in each of the samples analyzed, similar to that reported quantitatively previously [14]. Centroid

locations were translated in the *Z* direction so that the most superficial cell nucleus was at *Z*=0.

A number of features of cell organization were assessed. Cellularity was computed as a function of *Z* in successive 100 μm thick layers to a depth of 800 μm, excluding 5 μm at each x and y edge to eliminate bias from nuclei touching the image dataset boundary. For each cell nucleus centroid, the nearest neighbor was identified as the closest cell nucleus centroid, and the distance and angle (relative to the x-y plane) to it were calculated, with an angle of 0° indicating a horizontal orientation and 90° indicating vertical. To eliminate edge effects, cells that were closer to the edge of the region of interest than to their nearest neighboring cell were not included. The average distance and angle was calculated as a function of depth in 100 μm thick layers to a depth of 800 μm. For objects positioned randomly in a 3-D image region of the same size as the 3-D bins analyzed here, simulations demonstrated the average nearest neighbor angle to be 32°, independent of the density of objects. Finally, mutual neighbors were identified as those cells that were themselves the nearest neighbor of *their* nearest neighbor to quantify the distinct pairing of cells. The proportion of cells that were mutual neighbors was computed as a function of depth from the articular surface. The average proportion of nearest neighbors that were mutual for objects positioned randomly in a 3-D image region of the same size as the 3-D bins analyzed here was 59%, again determined by simulations and independent of the density of objects in the volume.

Statistics

Data are presented as mean ± SEM. ANOVA was performed for the measures of cellularity, nearest neighbor distance, nearest neighbor angle, and mutual neighbor proportion, with growth stage as the main factor, and depth and joint site as the repeated measures. For the measures of cellularity and nearest neighbor distance, post-hoc pairwise comparisons were made between growth stages. For the measures of nearest neighbor angle and mutual neighbor proportion, the values from each growth stage were compared against those from computer simulations of randomly distributed cells, using a planned comparison with a Bonferroni adjustment of the p-value (×3). Where applicable, p values are presented after correction.

3.4 Results

Qualitatively, the 3-D images clearly demonstrated cells and their nuclei, allowing for automated localization of cell nuclei (Figure 3.1A-C). The methods described for spatially normalizing nuclei and background intensities resulted in images that were accurately segmented using a consistent intensity threshold of 130. The sensitivity and specificity of cell nucleus localization was high (~95-100%) for all growth stages and tissue depths as assessed by inspection of raw image stacks overlaid with segmented images.

The density of cells in a given tissue volume depended on the growth stage and the depth from the articular surface (Figures 3.1, 3.2A). The cellularity of articular cartilage decreased markedly with maturation ($p<0.001$), with reductions of 30% (fetal to calf) and 60% (calf to adult) in the tissue volume analyzed. The cellularity also decreased

with depth from the articular surface ($p<0.001$). This depth-variation in cellularity was more marked for more immature tissue (depth-growth stage interaction, $p<0.001$), decreasing from 420±50 million cells/cm^3 at 0-100 μm to 200±30 at 700-800 μm in fetal tissue, and 260±20 to 150±5 in calf, and 100±6 to 70±4 in adult. The depth-associated variation in cellularity was also distinct in the PFG and FC ($p<0.001$), especially relative to the superficial (0-100 μm) region.

Cell organization also varied with growth and tissue depth (Figures 3.1, 3.2B-D). Adult cartilage demonstrated horizontal clusters in the superficial zone, and oblique and vertical columns in the middle and deep zones, respectively (Figure 3.1). Quantitatively, the 3-D metric of angle to the nearest neighbor was sensitive to such organization, being significantly different across growth stages ($p<0.001$) and through the depth of the tissue ($p<0.001$) with an interactive effect ($p<0.001$, Figure 3.2C). In mature tissue, this angle increased from 20° in the superficial zone (0-100 μm) to 60° in the deep zone (>500 μm), while in fetal and calf tissue the angle was ~32° except in certain regions (100-600 μm, especially in the FC), where the angle was intermediate to that in adult deep tissue (~40°). In contrast, the distance to nearest neighbor (Figure 3.2B) did not vary with age ($p=0.60$) or site ($p=0.21$), and showed only a slight tendency to vary with depth ($p=0.06$) with all average distances only varying from 8-13 μm. The proportion of neighbors that were mutual also did not change significantly with growth stage, from 68±3% in fetal, 66±3% in calf, and 72±3% in adult, but did vary with depth ($p<0.001$). The proportion was higher than the average of ~59% calculated for a 3-D volume with randomly

distributed objects (Figure 3.2D), achieving significance ($p<0.01$) at all depths of adult tissue, and most depths of the immature fetal and calf ($p<0.05$).

Scatter plots and averages of angle versus distance to the 1st, 2nd, and 4th nearest neighboring cells further highlighted the distinct populations of cells with preferentially oriented neighbors in adult tissue and the isotropic organization in fetal and calf (Figures 3.3, 3.4). In the superficial zone, the angles to the nearest neighboring cells were distributed from 0 to 90° in fetal and calf, but showed a high concentration near 0° in the superficial zone of adult tissue, and near 90° in the deep zone.

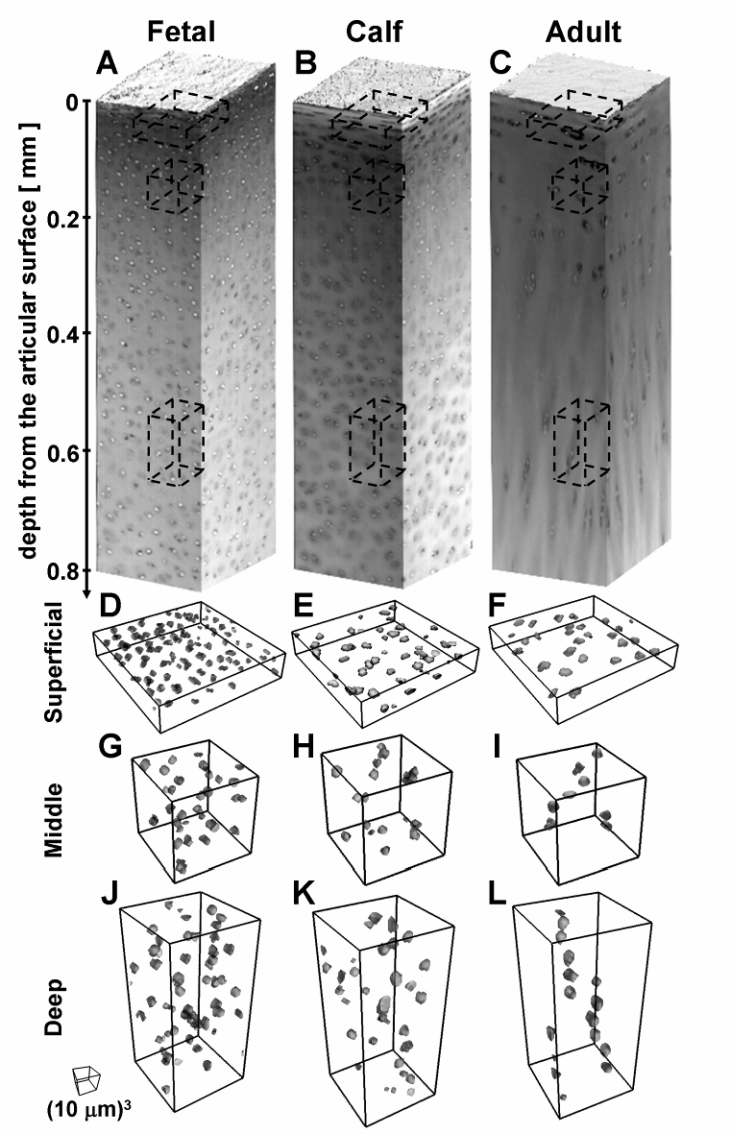

Figure 3.1. The depth-varying organization of cells depicted by 3-D image renders of bovine articular cartilage at different growth stages. Raw images of fetal (A), calf (B), and adult (C) tissue. Dashed boxes indicate sub-regions with segmented cell nuclei for superficial (D-F), middle (G-I), and deep (J-L) tissue regions.

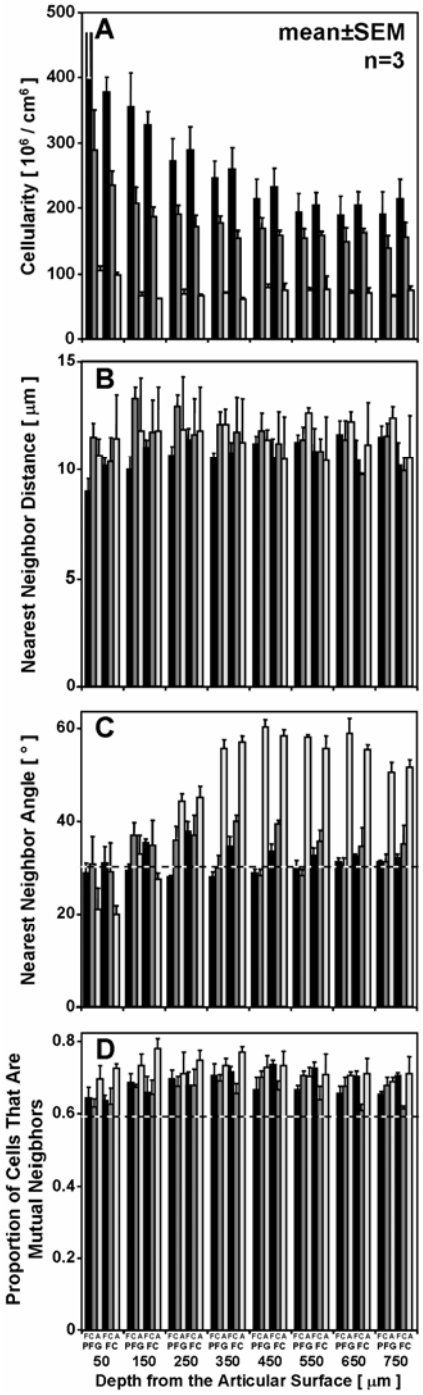

Figure 3.2. Variation in cell organization with depth in fetal (■), calf (■), and adult (□) bovine articular cartilage. Cell density (A), nearest neighbor distance (B), nearest neighbor angle (C), and proportion of mutual neighbors (D) shown for the patellofemoral groove (PFG) and femoral condyle (FC) from the articular surface to 800 μm in depth. Dashed lines (C, D) indicate values determined from simulations with cells arranged randomly.

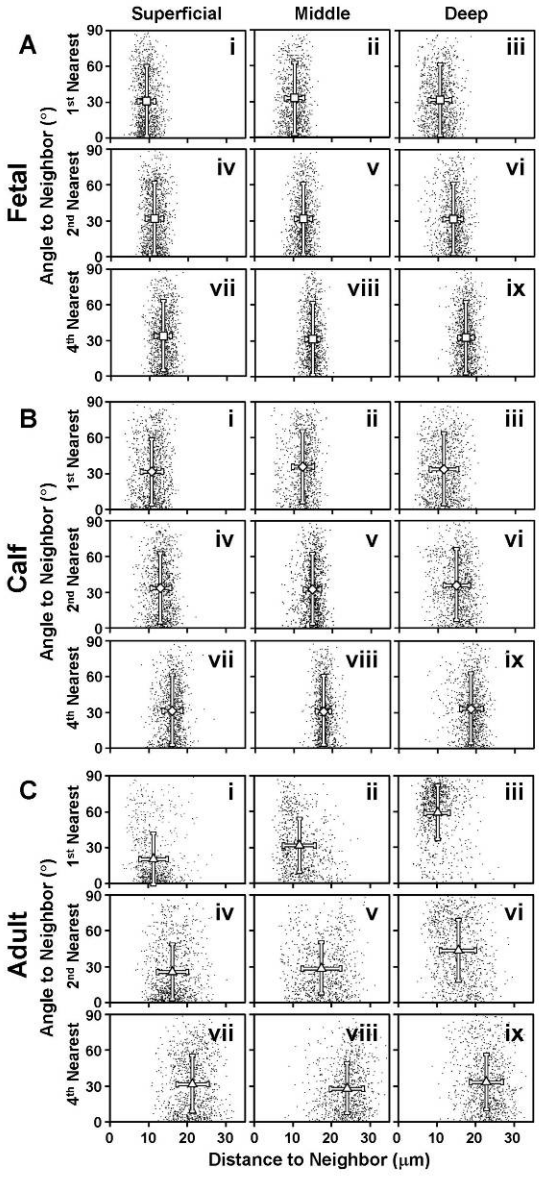

Figure 3.3. Depth- and growth-associated variation in vectors to neighboring cells. The angle and distance to the A) 1st , B) 2nd, and C) 4th nearest neighboring cell nuclei are plotted for 1000 cell nuclei along with the mean±SD in the superficial (0-100 μm), middle (100-200 μm), and deep (400-600 μm) regions of fetal (□), calf (◇), and adult (△) tissue.

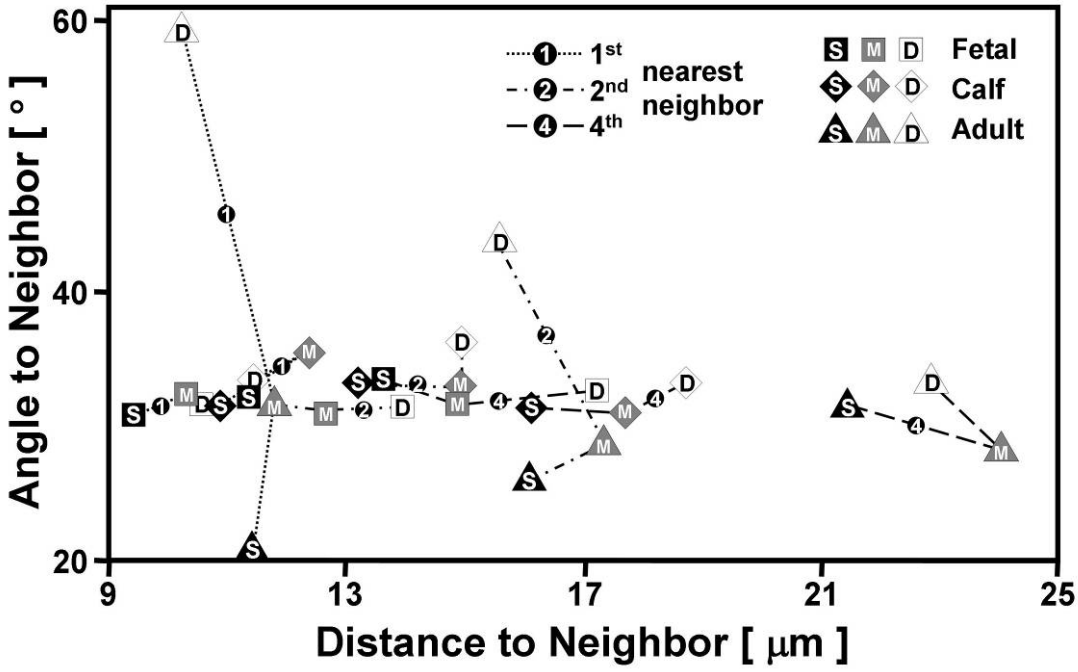

Figure 3.4. Depth-and growth-associated variation in average vector to neighboring cells. The average angle and distance to the 1st, 2nd, and 4th nearest neighboring cell nuclei are plotted for the superficial (S), middle (M) and deep (D) regions of fetal (□), calf (◇), and adult (△) tissue.

3-D renders of cell nuclei with the vectors to the nearest neighboring cell nuclei (Figure 3.5) further illustrate the horizontal orientation of neighboring cells in the superficial zone and the vertical orientation in the deep zone in the adult, and the isotropic arrangement in fetal tissue. These trends continued for the 2nd nearest cell where the average angle was 26° in the superficial and 43° in the deep, and a smaller proportion of the cells had horizontal (in the superficial) or vertical (in the deep) orientations. By the 4th neighbor, the average angle approached that for isotropic tissue (~32°) in all growth stages and depths. The scatter plots also illustrate the consistent distance of nearest neighboring cells across depth and growth stage, despite substantial changes in cellularity. On the other hand, the trends become more consistent with cellularity in the 2nd and 4th nearest neighbors, where distances increased with decreasing cellularity, and the distance to the 4th neighbor varied from ~15 μm in the middle zone of fetal tissue, to 18 μm in calf, and 24 μm in adult (Figure 3.4).

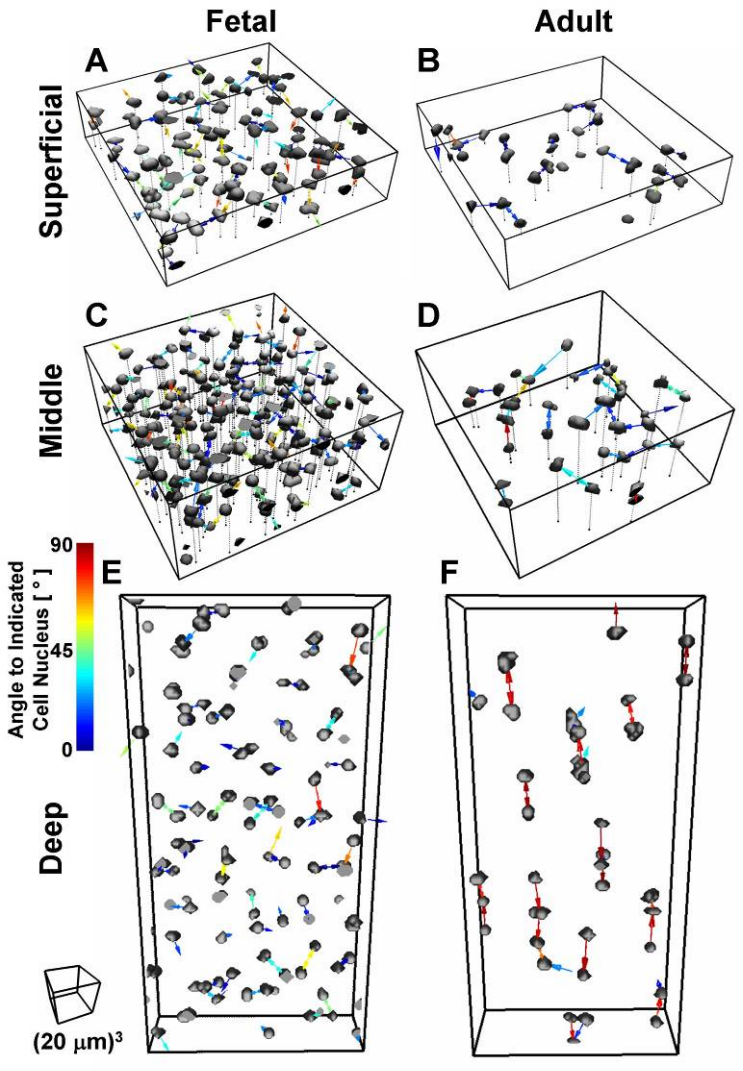

Figure 3.5. Depth-associated cell organization highlighted by nearest neighbor vectors. The angle of vector in the z direction relative to the x/y plane is indicated by the color legend from 0-90°. Data presented for fetal and adult tissue in subsets of the superficial (0-100 μm), middle (100-200 μm) and deep (400-600 μm) tissue regions.

3.5 Discussion

This study investigated the variations in the organization of cells in the superficial-most 800 μm of articular cartilage on the lateral patellofemoral groove and femoral condyle in three stages of growth in bovine stifle joints. Using previously described 3-D imaging and analysis methods, and novel metrics of the distance and angle to neighboring cells, the organization of cells was characterized in the various tissue regions. The cell density decreased monotonically with growth from the fetal to calf to adult stage, and with depth from the articular surface in a way that varied with joint site (Figures 3.1, 3.2A). Despite the variations in cell density, the distance to the nearest neighboring cell did not vary significantly (Figure 3.2B). On the contrary, the angle to the nearest neighboring cell was sensitive to changes in cell organization by the adult stage of growth, being particularly low (20°) in the superficial zone and high (60°) in the deep zone (Figure 3.2C, 3.3, 3.4 and 3.5). Further, cells tended to associate as small groups, with a higher incidence of mutual neighbors (68% for fetal, 66% for calf, 72% for adult) than expected by chance (59%) (Figures 3.2D, 3.3A, 3.3B, 3.3C, 3.4 and 3.5). The growth-associated changes in cell organization highlighted in this study may offer further insight into the role of populations of cells in articular cartilage growth, and the evolution of characteristic groupings of cells witnessed in mature tissue.

The study focused on a region of articular cartilage at the articular surface. This region, of ~1 mm thickness, extends through only a small proportion of the total thickness of fetal and calf tissue (>1 cm). However, this region appears representative of full-thickness articular cartilage at those growth stages, and extends through most of the

thickness of mature tissue. In immature tissue, trends of cellularity with depth (Figure 3.2A) stabilize beyond 500 μm from the surface. Also, much of the cartilage present in the immature joint is destined for calcification by expansion of the underlying secondary center of ossification, whereas the most superficial tissue gives rise to the articular cartilage layer of the mature joint. Other studies investigating the full thickness of tissue in immature animals describe a homogeneous distribution of cells in the deep regions, with no characteristic deep zone organization [22]. The organization of adult cartilage may also be specialized at and near the calcified cartilage region, but was not investigated in this study.

The 3-D image datasets generated using digital volumetric imaging were analyzed using similar methods to the previous study, but improved by application of 3-D spatial filtering. The image datasets showed staining consistent with the previous study [14], with intense bright nuclei and non-specific staining of background extracellular matrix. In some sample regions, the intensity of this background staining exceeded that of nuclei. This would have led to classification of matrix inappropriately as cells, i.e. false positive error (>20%). To prevent such errors, 3-D convolution using a Mexican Hat filter was employed prior to segmentation in all images to enhance the cell nuclei and attenuate the background. The robustness of the previously developed methods in conjunction with 3-D spatial filtering was demonstrated by its efficacy in the heterogeneous fetal, calf, and adult tissue, from the articular surface to a depth of 800 μm.

The cellularity quantified here from 3-D imaging shows variation with age, depth, and joint site consistent with other biochemical and histological studies. From biochemical analysis of DNA content in developing and growing bovine tissue, the

cellularity decreased with growth stage [32, 33] and depth from the articular surface [17], as in the current study. The reduction in cell density with depth from the articular surface of adult articular cartilage has been identified in numerous 2-D and 3-D histological studies in a variety of animals [7, 13, 21, 24, 28, 34]. The effect of joint site on cell density seen in other studies [2, 7] was apparent at certain depths from the articular surface, but not when overall tissue thickness was considered. The more subtle differences observed in the current work could be due to the location of the source tissue. In this study, joint sites with very different loading regimes, such as the weight-bearing region (central femoral condyle) and non weight-bearing region (central patellofemoral groove) were examined, as opposed to the medial vs. lateral [2] or central vs. peripheral [7] femoral condyle. Absolute estimates of cell density were consistent with other studies [14, 17]. The cell density in the fetal tissue was high in the present study compared to our previous study (~450 compared to 290 million cells per cm^3 in the superficial zone) [14], likely due to sampling at an earlier stage of growth (2^{nd} trimester compared to 3^{rd} trimester).

The analysis of cell organization revealed a relatively constant distance to the nearest neighboring cell, despite the substantial decrease in cellularity with depth and growth stage. These results suggest that small groups of 2-3 cells are closely situated, whereas the gap between these groups increases from fetal to calf to adult as illustrated by an increase in the 4^{th} nearest neighbor with growth. Further, nearest neighboring cells were often mutual (Figure 3.2D, 3.5), suggesting the presence of pairs of cells with some sort of affinity, either through cell-cell adhesion, or through a shared pericellular matrix. These groups seem to remain during growth through the calf to the adult stage, as the

proportion of cells in the tissue decreases dramatically but the distance to nearest cell does not change, and cells are mutual neighbors with a high incidence. Such a phenomenon may also arise from active cell fate processes of proliferation and death, where cells throughout the tissue are constantly being removed by apoptosis or necrosis, and regenerated by proliferation as the tissue expands, leading to closely situated daughter cells. Previous studies [15, 20] have investigated the role of cell death in developing articular cartilage, and identified only very localized bands of cell death near the subchondral bone and proliferation either near the bone or the articular surface [10, 15, 18-20]. A more detailed analysis of cell fates and organization during growth may uncover the role of cell-cell interactions and cell kinetics.

The angle to the nearest neighboring cell showed small variations from an isotropic organization in the femoral condyle of immature tissue. This result may suggest an earlier accelerated maturation process occurring in the femoral condyle that that in the patellofemoral groove, consistent with the previous growth related studies showing larger increases in collagen content [33] and tensile properties [32], hallmarks of maturation, from the fetal to calf stages. Further, horizontal clusters have been qualitatively shown in immature tissue from *en face* views in the superficial zone [14]. However, because of the relatively dense packing of cells in immature tissue, the nearest neighboring cell may often reside in a different cell cluster. Further development of image processing methods could allow characterization of cell clusters within densely packed groups of cells.

The change in angle of neighboring cells from horizontal to vertical from the superficial to deep zones of adult articular cartilage may be physiologically important, although this remains to be elucidated. Some authors have proposed models of articular

cartilage growth which mimic that of the growth plate, where cells in progenitor and proliferating pools progress through to the hypertrophic zone and become calcified as the bone increases in length. In such a model, the groups of cells that arise in the superficial zone, possibly from proliferation of a progenitor-like cell residing in the region [1, 6, 9, 10, 15, 18-20, 30], advance through to the deep regions, becoming aligned vertically. Also possible is a relationship between the orientation of groups of cells within a pericellular region and the local collagen fibers. In the superficial zone, the collagen is oriented parallel to the surface, arcading downward through the middle zone, eventually becoming vertical in the deep zone [3]. Thus in the superficial zone, horizontal clusters of cells may reside in between sheets of collagen, where in the deep regions, the vertical columns of cells may inter-digitate with columns of collagen fibers.

Analysis of the distance and angle to neighboring cells beyond the 1st is consistent with the presence of multi-cell units in adult cartilage (Figures 3.3, 3.4). In the superficial zone, the angle to 2nd nearest neighboring cell is 26°, suggesting that this neighbor still has a slight tendency toward a horizontal orientation to the original cell and clusters of 3 or greater cells may be present. In the deep zone, the 2nd nearest neighboring cell has an average angle of 43 degrees, reflecting columns of at least 3 cells. The scatter plots confirm this result, showing a small but distinct population of cells with a 2nd nearest neighbor still at an angle near 0° in the superficial and near 90° in the deep zone.

These quantitative metrics may be used to identify and characterize local subpopulations with distinct arrangements, as well as to describe global variations in the organization of cells in a tissue volume. The dynamics of biological tissues such as cartilage may be dependent on the activity of small distinct subpopulations of cells.

During growth, the articular surface contains progenitor cells, and may also contain an adjacent small population of 'transit amplifying' cells that are undergoing proliferation. These events may be rare, especially in more mature tissue, yet still contribute substantially to the expansion of the cell population governing tissue growth. Such rare events could potentially be identified by appropriately validated metrics, such as proximity of neighboring cell nuclei (<5μm), or orientation of mutual neighbors. Further, focal sites of pathogenic cell death could be localized by identifying cells or tissue regions relatively far from the nearest cell, amidst a population of normally arranged chondrocytes, and may be associated with tissue undergoing early yet treatable pathogenic degeneration. The identification of anomalous cell groups within a large tissue sample may reveal the rare events critical for normal growth, and those detrimental to maintenance of joint homeostasis.

This paper describes the application of 3-D imaging and analysis to deduce the changes in cell organization that occur during *in vivo* growth of a biological tissue, namely articular cartilage. This cell organization changes dramatically during growth, with the expanding articular cartilage undergoing a decrease in cell density and ultimately attaining the classical zonal organization described previously. The novel metric, determined from 3-D images, of angle to nearest neighboring cell may be particularly useful in gauging the extent and mechanisms of tissue maturation. Further investigation of chondrocyte populations in cartilage during growth, aging, injury, and degradation, may uncover the physiological significance of the cell arrangements described here. Additionally, investigation of cells at this scale within other native and engineered biological tissues may uncover tissue-specific patterns of growth, and the role

of cell populations and sub-populations in development of complex tissue geometries and microstructure as well as the propagation of tissue degeneration and disease.

3.6 Acknowledgments

This chapter, in full, was submitted by invitation to a special edition of *Biomaterials* entitled "Cellular and Molecular Biology Techniques for Biomaterials Evaluation". The dissertation author is the primary investigator and thanks co-authors Dr. Won Bae and Barbara Schumacher for their contribution. This work was supported by National Institute of Health and National Science Foundation.

3.7 References

1. Alsalameh S, Amin R, Gemba T, Lotz M: Identification of mesenchymal progenitor cells in normal and osteoarthritic human articular cartilage. *Arthritis Rheum* 50:1522-32, 2004.

2. Armstrong SR, RA. Price, R.: Topographical variation within the articular cartilage and subchondral bone of the normal ovine knee joint: a histological approach. *Osteoarthritis and Cartilage* 5:25-33, 1995.

3. Benninghoff A: Form und bau der gelenkknorpel in ihren beziehungen zur funktion. Zweiter teil: der aufbau des gelenkknorpels in seinen beziehungen zur funktion. *Z Zellforsch* 2:783-862, 1925.

4. Brakenhoff GvS, EA. van der Voort, HTM. Naninga, N.: Three-dimensional confocal fluorescence microscopy. *Methods in Cell Biology* 30:379-98, 1989.

5. Centonze VW, JG.: Multiphoton Excitation Provides Optical Sections from Deeper within Scattering Specimens than Confocal Imaging. *Biophysical Journal* 75:2015-24, 1998.

6. Dowthwaite GP, Bishop JC, Redman SN, Khan IM, Rooney P, Evans DJ, Haughton L, Bayram Z, Boyer S, Thompson B, Wolfe MS, Archer CW: The surface of articular cartilage contains a progenitor cell population. *J Cell Sci* 117:889-997, 2004.

7. Eggli PS, Hunziker EB, Schenk RK: Quantitation of structural features characterizing weight- and less-weight-bearing regions in articular cartilage: a stereological analysis of medial femoral condyles in young adult rabbits. *Anat Rec* 222:217-27, 1988.

8. Ewald AJ, McBride H, Reddington M, Fraser SE, Kerschmann R: Surface imaging microscopy, an automated method for visualizing whole embryo samples in three dimensions at high resolution. *Dev Dyn* 225:369-75, 2002.

9. Fickert SF, J. Brenner, RE.: Identification of subpopulations with characterisitics of mesenchymal progenitor cells from human osteoarthritic cartilage using triple staining for cell surface markers. *Arthritis Research and Therapy* 6:R422-R32, 2004.

10. Hayes AJ, MacPherson S, Morrison H, Dowthwaite G, Archer CW: The development of articular cartilage: evidence for an appositional growth mechanism. *Anat Embryol (Berl)* 203:469-79, 2001.

11. Huang DS, EA. Lin, CP. Schuman, JS. Stinson, WG. Chang, W. Hee, MR. Flotte, T. Gregory, K. Puliafato, CA.: Optical coherence tomography. *Science* 254:1178-81, 1991.

12. Hunziker EB: Articular cartilage structure in humans and experimental animals. In: *Articular Cartilage and Osteoarthritis,* ed. by KE Kuettner, Schleyerbach R, Peyron JG, Hascall VC, Raven Press, New York, 1992, 183-99.

13. Hunziker EB, Quinn TM, Hauselmann HJ: Quantitative structural organization of normal adult human articular cartilage. *Osteoarthritis Cartilage* 10:564-72, 2002.

14. Jadin KD, Wong BL, Bae WC, Li KW, Williamson AK, Schumacher BL, Price JH, Sah RL: Depth-varying density and organization of chondrocyte in immature and mature bovine articular cartilage assessed by 3-D imaging and analysis. *J Histochem Cytochem* 53:1109-19, 2005.

15. Kavanagh E: Division and death of cells in developing synovial joints and long bones. *Cell Biology International* 26:679-88, 2002.

16. Kerschmann R: Image recording apparatusUnited States Patent #4,960,330, October 2, 1990, 1988.

17. Li KW, Williamson AK, Wang AS, DiMicco MA, Kurtis MS, Chen SS, Sah RL: Mechanical regulation of biosynthesis in cartilage at different stages of growth. *Trans Orthop Res Soc* 26:339, 2001.

18. Mankin HJ: Localization of tritiated thymidine in articular cartilage of rabbits. I. growth in immature cartilage. *J Bone Joint Surg Am* 44-A:682-98, 1962.

19. Mankin HJ: Localization of tritiated thymidine in articular cartilage of rabbits. II. repair in immature cartilage. *J Bone Joint Surg Am* 44-A:688-98, 1962.

20. Mankin HJ: Mitosis in articular cartilage of immature rabbits. A histologic, stathmokinetic (colchicine) and autoradiographic study. *Clin Orthop Rel Res* 34:170-83, 1964.

21. Mitrovic D, Quintero M, Stankovic A, Ryckewaert A: Cell density of adult human femoral condylar articular cartilage. *Lab Invest* 49:309-16, 1983.

22. Oreja MR, MQ., Abelleira, AC. Garcia, MAG. Garcia, MAS. Barreiro, FJJ.: Variation in Articular Cartilage in Rabbits Between Weeks Six and Eight. *The Anatomical Record* 241:34-8, 1995.

23. Pal S, Tang L-H, Choi H, Habermann E, Rosenberg L, Roughley P, Poole AR: Structural changes during development in bovine fetal epiphyseal cartilage. *Collagen Rel Res* 1:151-76, 1981.

24. Paukkonen K, Selkainaho K, Jurvelin J, Helminen HJ: Morphometry of articular cartilage: a stereological method using light microscopy. *Anat Rec* 210:675-82, 1984.

25. Quinn TM, Maung AA, Grodzinsky AJ, Hunziker EB, Sandy JD: Physical and biological regulation of proteoglycan turnover around chondrocytes in cartilage explants. Implications for tissue degradation and repair. *Ann NY Acad Sci* 878:420-41, 1999.

26. Schumacher BL, Su J-L, Lindley KM, Kuettner KE, Cole AA: Horizontally oriented clusters of multiple chondrons in the superficial zone of ankle, but not knee articular cartilage. *Anat Rec* 266:241-8, 2002.

27. Sharpe J, Ahlgren, U. Perry, P. Hill, B. Ross, A. Hecksher-Sorensen, J. Baldock, R. Davidson, D.: Optical Projection Tomography as a Tool for 3D Microscopy and Gene Expression Studies. *Science* 296:541-5, 2002.

28. Stockwell RA: The interrelationship of cell density and cartilage thickness in mammalian cartilage. *J Anat* 109:411-21, 1971.

29. Stockwell RA, Meachim G: The chondrocytes. In: *Adult Articular Cartilage,* ed. by MAR Freeman, Pitman Medical, Tunbridge Wells, England, 1979, 69-144.

30. Thornemo MT, T. Sjogren Jansson, E. Larsson, A. Lovstedt, K. Nannmark, U. Brittberg, M. Lindahl, A.: Clonal Populations of Chondrocytes with Progenitor Properties Identified within Human Articular Cartilage. *Cells Tissues Organs* 180:141-50, 2005.

31. Tsai PF, B. Ifarraguerri, AI. Thompson, BD. Lev-Ram, V. Schaffer, CB. Xiong, Q. Tsien, RY. Squier, JA. Kleinfeld, D.: All-Optical Histology Using Ultrashort Laser Pulses. *Neurotechnique* 39:27-41, 2003.

32. Williamson AK, Chen AC, Masuda K, Thonar EJ-MA, Sah RL: Tensile mechanical properties of bovine articular cartilage: variations with growth and relationships to collagen network components. *J Orthop Res* 21:872-80, 2003.

33. Williamson AK, Chen AC, Sah RL: Compressive properties and function-composition relationships of developing bovine articular cartilage. *J Orthop Res* 19:1113-21, 2001.

34. Wong M, Wuethrich P, Eggli P, Hunziker E: Zone-specific cell biosynthetic activity in mature bovine articular cartilage: a new method using confocal microscopic stereology and quantitative autoradiography. *J Orthop Res* 14:424-32, 1996.

CHAPTER 4

DEPTH-VARYING GROWTH OF ARTICULAR CARTILAGE EXPLANTS REVEALED BY BIOMECHANICAL ANALYSIS OF DISPLACEMENT OF CHONDROCYTES

4.1 Abstract

Growth of articular cartilage occurs via extracellular matrix accretion and remodeling, and proliferation to maintain a high density of cells. These processes may contribute to varying degrees as a function of depth from the articular surface. The objectives of this study were to assess the spatially-varying strain due to tissue growth during in vitro culture with enzymatic or chemical modulation of the extracellular matrix. Tissue displacement and strain during growth were calculated by relative motion of cell nuclei at a vertical surface. The tissue grew in thickness by 23±4% during tissue culture, 34±12% in culture with BAPN, and 0±0% in culture after treatment with Chondroitinase ABC (C-ABC) to remove glycosaminoglycans (GAGs). The axial strain, ε_{zz}, exceeded the other strain compenents by >20 times, and varied in both the axial (z) and radial (r) directions, being highest near the articular surface (z=0) and at the disk center (r=0). The properties of cells and extracellular matrix may predispose articular cartilage to

anisotropic and heterogeneous growth in vitro, and these characteristics may also dictate growth in vivo.

4.2 Introduction

Articular cartilage growth is associated with changes in the depth-variation in tissue composition, structure, and function. During *in vivo* growth, the constituents of the extracellular matrix (ECM), including proteoglycans and collagen, are synthesized and remodeled by the chondrocytes in different depth zones in precise ways to increase the tissue volume and achieve functional maturation [26, 27]. These changes are mediated by a relatively dense population of cells, each of which maintain a small matrix domain [7, 8] in which matrix turnover may be relatively rapid [22].

The cellular and ECM properties vary as a function of depth from the articular surface, leading to description of three classical depth zones in mature tissue: the superficial (tangential) zone, the middle (transitional) zone, and the deep (radial) zone[2, 3, 7]. In the superficial zone, the tissue is more soft and prone to deformation by compression [23] or osmotic loading [21], and less resistive to fluid flow [13] than deep zone cartilage. The cell organization also varies with depth, being particularly dense near the surface, and organized into horizontal clusters, and sparse deeper into the tissue with vertical columns of cells present [8]. The depth-varying properties of cartilage begin to arise early in the maturation process, particularly in post-natal animals [8, 11], although it is unclear how these progress to the mature adult. Ultimately, the cell and ECM structure and composition develop in articular cartilage to achieve complex depth-varying properties essential for providing and maintaining a load-bearing, low friction, wear-resistant surface for joint articulation.

The way in which cartilage grows may be critical to allowing both joint expansion and functional maturation, and understanding this process may lead to more effective strategies for generating viable repair tissue in vitro. It has been suggested that cartilage growth occurs appositionally by proliferation of cells near the articular surface [5, 15-17]. Also, because of a drop in cell density as the tissue progresses through stages of growth [8] in the absence of widespread cell death [10], it is also likely that the tissue grows interstitially throughout by accretion and remodeling of extracellular matrix molecules, particularly proteoglycans. Such growth may also be depth-dependent due to varying biosynthesis rates in cells in different depth zones of immature tissue [6]. The relative extent of different growth mechanisms in the depth zones is not clear, although they likely contribute to combined growth and maturation in distinct ways.

In vitro growth may be regulated by chemical agents that alter extracellular matrix function by directly changing the composition and structure. In articular cartilage, the mechanical function and hydration of the tissue are related to a balance between the swelling pressure of the negatively charged proteoglycan aggregates and the restraining force of the collagen network [19]. Disrupting the balance between these forces in favor of the swelling pressue is predicted to allow tissue growth [12]. Thus, the extents of cartilage growth *in vitro* may be directly affected by alteration of extracellular matrix components by enzymatic and chemical treatments. One such treatment, enzymatic digestion with Chondroitinase ABC (C-ABC), can deplete the GAG within articular cartilage explants by selectively depolymerizing chondroitin and dermatin sulfate[29]. This treatment has been shown to inhibit growth of articular cartilage explants in culture [1]. Another agent, B-aminopropionitrile (BAPN), effectively blocks formation of lysyl

oxidase mediated collagen crosslinks [9], thus attenuating the restraining force of the collagen network. In this case, the swelling pressure of the negatively charged proteoglycans overcome the restraining force, and the articular cartilage shows expansive growth greater than untreated tissue [1]. The growth of articular cartilage can be directly modulated *in vitro* by application of chemical agents that disrupt the balance between the restraining force of the collagen network and the swelling pressure of sGAG molecules.

Displacement fields within articular cartilage have previously been analyzed by tracking motion of intrinsic or extrinsic surface markers and may also be useful to analyze cartilage growth kinematics *in vitro* as well as *in vivo*. The spatially-varying tissue strain induced during osmotic swelling of cartilage bathed in a hypotonic solution was assessed by tracking enamel markers applied on the tissue surface [21]. In other studies, the displacement of tissue as a result of unconfined compression was quantified by mapping the relative motion of labeled cell nuclei as fiducial markers at a tissue surface [11, 24]. Cartilage growth occurs *in vitro* [28], with cell death at the cut surfaces [25], and these cells may be used as intrinsic markers for bulk deformation during growth.

Overall, the specific depth-dependent properties of articular cartilage that exist in immature tissue may predispose it to growth deformation that varies from the articular surface to the deep regions, and this may in turn be directly affected by selective alteration of the content or assembly of ECM components. The objectives of this study were (1) to assess the growth kinematics of articular cartilage explants *in vitro* by tracking chondrocyte nuclei, and (2) to quantify the depth variation in growth-associated

tissue strain under control conditions, in the presence of BAPN, and after C-ABC treatment.

4.3 Materials and Methods

Cartilage Culture and Imaging.

Articular cartilage from the stifle joint of immature (1-3 week old) bovine animals was harvested, and growth was characterized during subsequent culture by tracking non-viable cells at one of the cut surfaces. A total of 12 cartilage disks, 2 mm in diameter and ~0.9 mm thick, including the intact articular surface, were collected from each of 3 animals. Four disks were incubated for 2 days in either: 1) medium (DMEM with 20% FBS and 50 μg/mL ascorbate), 2) medium with 0.5 U/mL protease-free chondroitinase-ABC (C-ABC) (Associates of Cape Cod, East Falmouth, MA) to deplete GAGs, or 3) medium with 0.1 mM BAPN (Sigma, St. Louis, MO) to inhibit lysyl oxidase mediated collagen crosslinking. Disks incubated for 2 days with C-ABC disks were rinsed with 50x tissue volumes media (3 times for 20 min.) to remove residual enzyme.

Samples were processed and imaged to allow *in vitro* tracking of cells during explant culture. Disks were cut perpendicular to the articular surface with a scalpel to form two half-disks. One half from each parent disk was transferred to either tissue culture wells with medium as an unprocessed control, or stained with Live/Dead solution (Invitrogen, Corp., Carlsbad, CA) for analysis of cell viability, or fixed with 4% paraformaldehyde for 1 day for histological analysis. The other half was stained for 1 hour with media containing 0.5 mM Ethidium Homodimer (Invitrogen Corp.), a

fluorescent nuclear label that penetrates the cell membranes of dead cells, and then rinsed with media (3 times for 10 min.). These disk halves were placed in coverglass chambers with the cut surface flush with the bottom and held in place by suspension in 0.25 mL of 1% low-melting point agarose (FMC Bioproducts, Rockland, ME) in medium (Figure 4.1A). After a brief gelling period (~2 min.), concentrated tissue culture media was added to make a final concentration of 20% FBS and 50 μg/mL ascorbate, including 0.1 mM BAPN[4] for those disks previously cultured in BAPN containing media (group 2). All samples were incubated from day 2 to day 16 with media changes every two days. The stained samples were imaged on days 2, 8, 12 and 16 with an inverted Nikon epi-fluorescence microscope at 4x or 10x magnification. Images were taken spanning the full width (r) and depth (z) of the sample, and then stitched together by overlapping visible cell nuclei in Adobe Photoshop 7.0 (Adobe Systems, Inc. San Jose, CA). At termination of the culture, disks were placed cut side down on a glass coverslip and imaged under brightfield illumination to determine axial thickness and radial width. Disk halves were either cut in half again (to form quarters) and stained with Live/Dead solution (Invitrogen, Inc.) for analysis of cell viability, or fixed in 4% paraformaldehyde for 1 day for histology.

Image Analysis to Determine Growth Strain.

Images were analyzed to determine the geometrical changes in the axial and radial directions during the growth period. First, the change in radius and thickness of unprocessed controls versus imaged specimens was determined to assure that processing did not affect the magnitude of growth. A series of 3 equally spaced measurements of

radial width (r) and axial thickness (z) were taken between day 2 fluorescent images and day 16 brightfield images, with n=3. Next, the axial (z) thickness of samples was assessed at each time point for two animals to determine the approximate time course of growth. From this analysis, the majority of the axial growth (>70%) occurred from day 2 to day 8, so this period was used for analysis of spatially-varying growth.

Images were processed to determine displacement of fluorescently tagged non-viable cells as an indicator of local strain due to growth over the culture duration (Figure 4.1B, C). A sample of ~40-60 stained cells were identified and marked in each image series (day 2 and day 8) from 2 samples from each of the 3 groups, from 3 animals, for a total of 18 image pairs. Cell nuclei were chosen based on visibility at both time points, spanning the entire sample face, and included points at or near the tissue surfaces. Using Matlab 7.0 (The Mathworks, Inc., Natick, MA), images were imported and the centroids of marked cells were determined. Images from each day were rotated to a constant orientation, with the articular surface roughly parallel to the image axis, based on the line segment between 2 cell nuclei spanning the image width and approximately at the midpoint between the superficial and deep surfaces of the sample. The top most point in the day 2 image, and the corresponding point in the day 8 image, was used as a reference in the axial direction (z=0). The nucleus at the median position in the r direction in the day 2 image, and the same nucleus in the day 8 image, was defined as r=0. Points were manually matched between the pair of images to allow tracking of the same cell nucleus from day 2 to day 8. The radial and axial displacements, u_r and u_z, of each nucleus were determined for each image relative to the day 2 image. The displacement data were interpolated to form continuous displacement fields, $u_r(r,z)$ and $u_z(r,z)$, with points spaced

at 20 μm increments in the r and z directions. The gradient of each of these fits was found and the strain calculated at 20 μm increments in the longitudinal direction, $\varepsilon_{zz}=\partial u_z/\partial z$, in the radial direction, $\varepsilon_{rr}=\partial u_r/\partial r$, and in shear, $\varepsilon_{rz}=0.5(\partial u_r/\partial z+\partial u_z/\partial r)$. The average strain was calculated in 0.1 mm bins 1) as a function of radial distance (r) from the center of the disk to within ~0.1 mm of the disk edge, and 2) with depth from the articular surface (z) to within ~0.1 mm of the deep surface.

Statistical Analysis

Data are presented as the mean±SEM. The effects of staining, embedding and imaging on tissue thickness and cell viability were assessed by ANOVA. The effects of radial distance (r) and depth (z) on growth strain, $\varepsilon_{rr}(z)$, $\varepsilon_{rz}(z)$, $\varepsilon_{zz}(z)$ were assessed by repeated measures ANOVA.

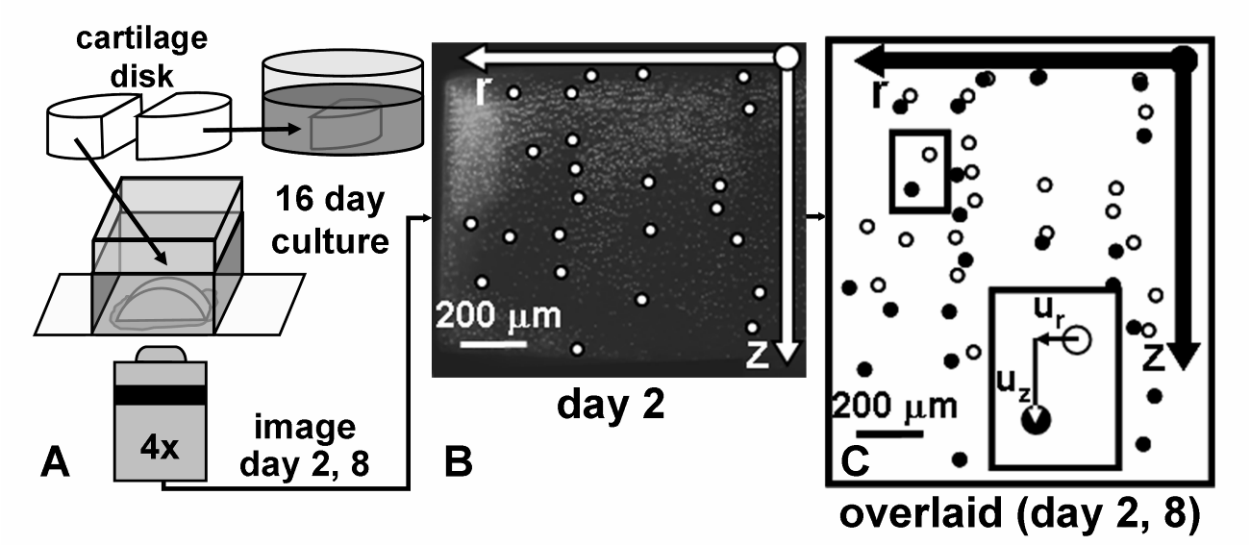

Figure 4.1. Tracking cell displacement in articular cartilage at a cut surface during *in vitro* growth. (A) Schematic of culture and imaging method. (B) Representative image result at day 2 with some cells marked. (C) Marked cells from day 2 (○) and day 8 (●) overlaid, showing relative displacement during in vitro growth as a function of depth.

4.4 Results

Tissue growth was evident in all specimens after 16 days of culture by increase in the half-disk edge thickness, and was not significantly altered by staining, embedding, and imaging. A subset of disks grew in thickness from day 2 to day 16 in a time-dependent manner (Figure 4.2), although a large proportion of growth occurred between days 2 and 8 (~70%), the time period focused on for further analysis. Overall growth of a subset of half-disks was not affected by staining, embedding, and imaging ($p=0.71$), with a change in axial thickness of 42±11% (n=3) in these processed specimens versus 48±13% (n=3) in their partnered control specimens over the 14 day incubation period. Deposition of new tissue occurred outside the original tissue area, likely by cellular outgrowth as observed in previous studies [14], but was excluded from all subsequent analysis.

The dead cells of the labeled disks were prominent at the cut edges, and easily visualized during subsequent imaging through 6 days of culture (Figures 4.1, 4.3). The intensity of Ethidium Homodimer stain decreased during the culture period, requiring increased exposure time for image capture. At different times of the culture period, the cut surfaces of some samples were no longer flush with the coverglass, preventing further image analysis.

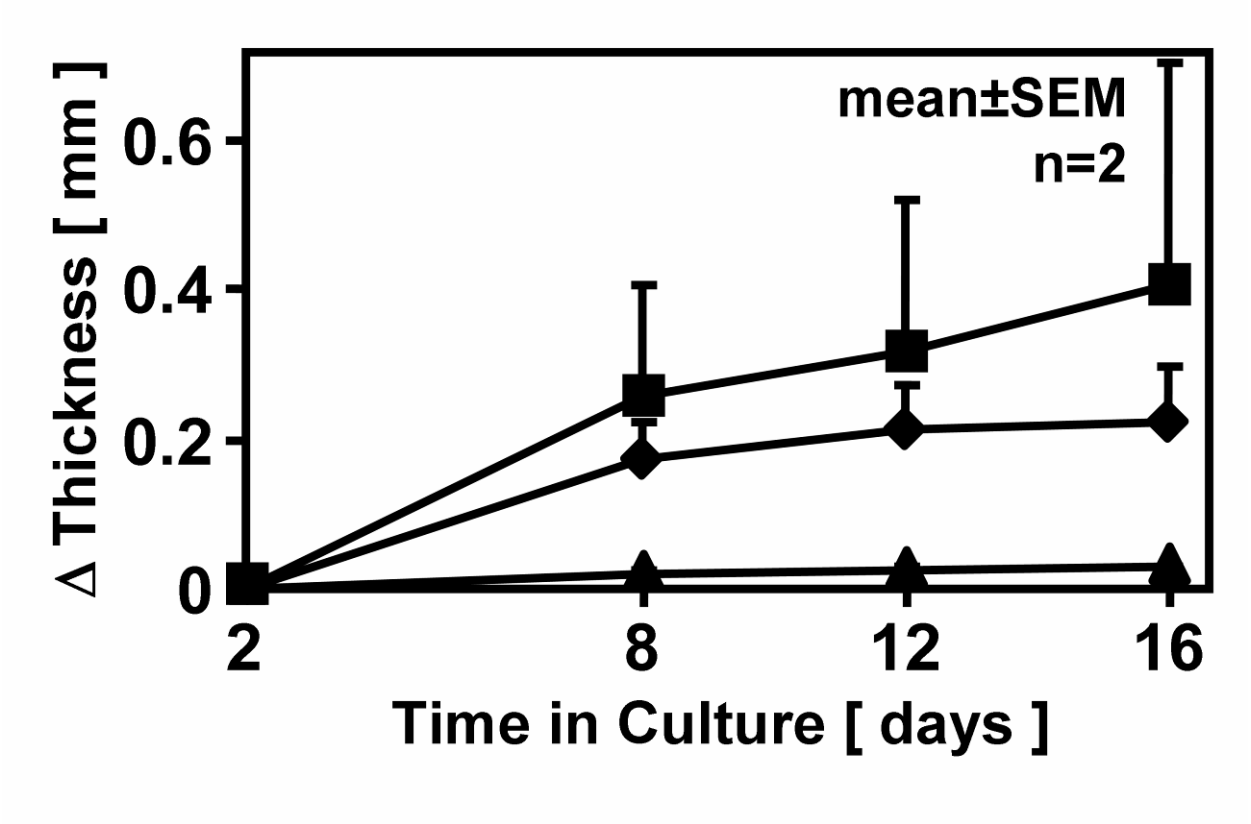

Figure 4.2. Time course of growth in axial thickness of a subset of half disks. Change in thickness relative to day 2 thickness for control (◆), BAPN (■), and C-ABC treated (▲) samples.

In contrast to the high percentage of dead cells at the cut surface, cell viability in the tissue was maintained. Viability at the intact articular surface after the 2 day preculture was high (79±10%, n=3), with no significant difference among experimental groups (p=0.17). Also, viability of cells within the cartilage was maintained, with 65±15% of cells viable at the new vertically cut surface of the disk quarter after 16 days of culture, and no significant difference among groups (p=0.24).

The interpolated continuous displacement fields (u_r and u_z) varied with depth from the articular surface (Figure 4.4). The continuous fits of raw data resulted in close fits of data points, with no apparent outliers, as expected. The axial displacement, u_z, increased monotonically with depth and exceeded the radial displacement, u_r, by an order of magnitude.

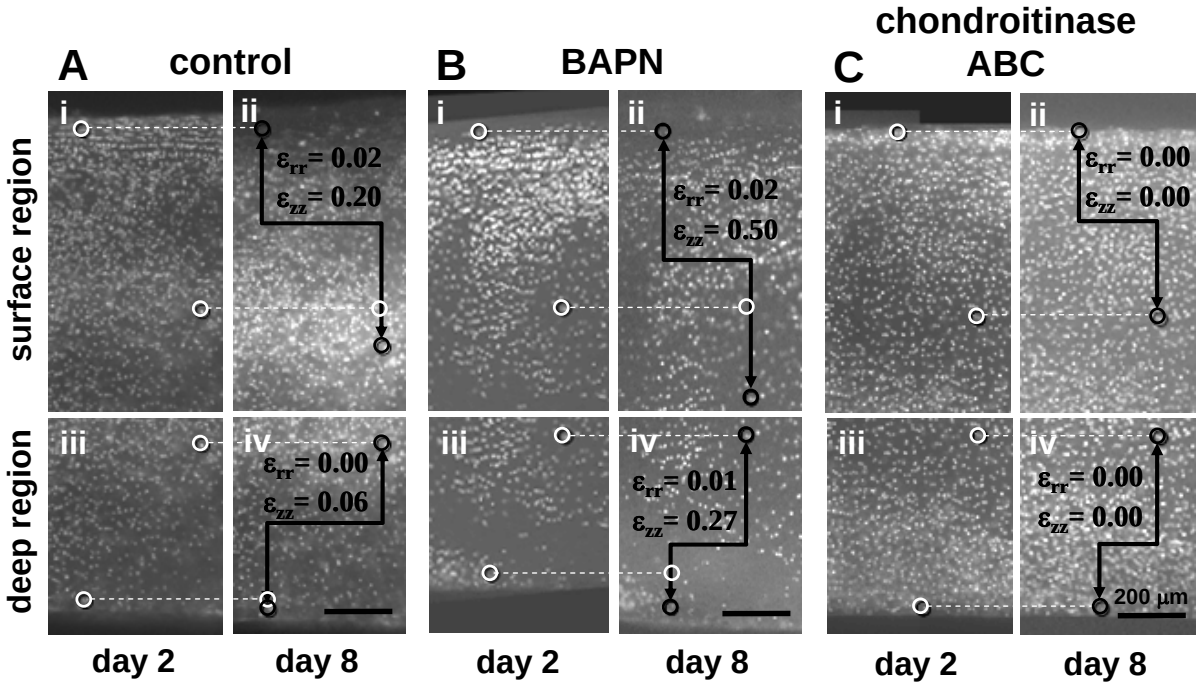

Figure 4.3. Relative positions of cells during growth for control (A), BAPN (B), and C-ABC treated samples (C). Marked cells in images at day 2 (white) and day 8 (black) in the surface and deep tissue regions. Strain (ε_{rr} and ε_{zz}) calculated between the points, with the top point as a reference, illustrate depth-dependent tissue strain.

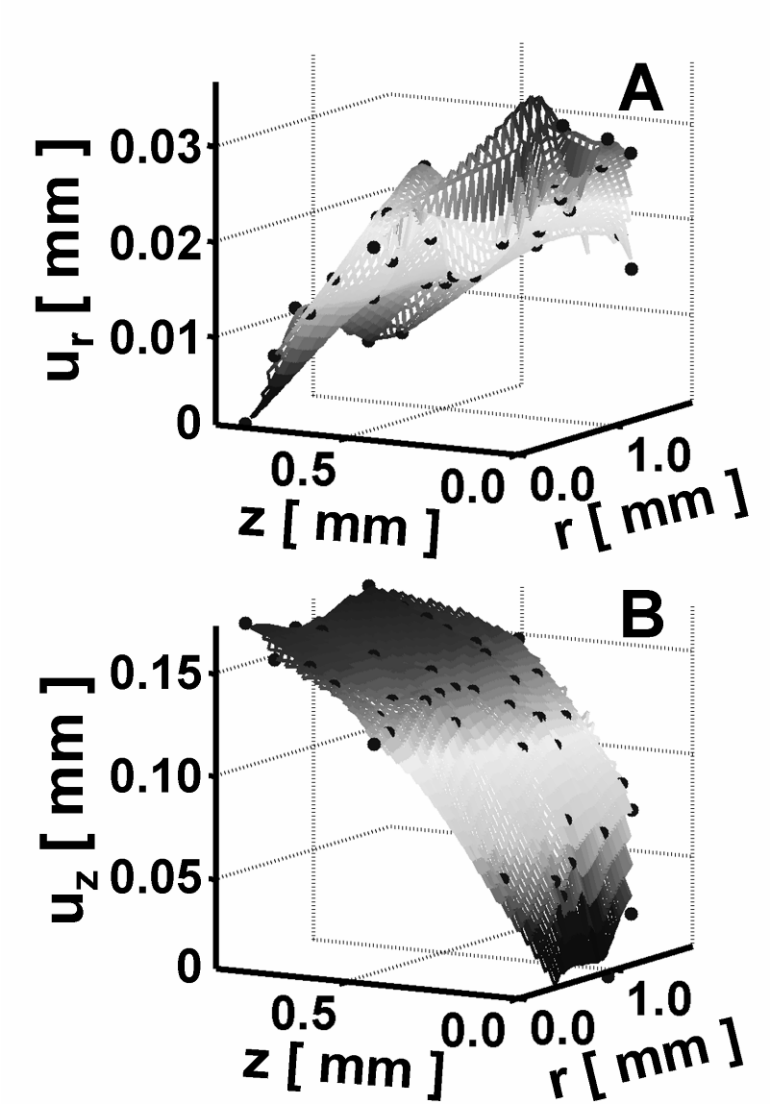

Figure 4.4. Representative growth displacement fields, (A) $u_r(r,z)$ and (B) $u_z(r,z)$, from one control specimen. Points represent displacement of an object from day 2 to day 8 at its original (r,z) position. Surface represents cubic interpolation of displacement data.

The growth strain was also predominantly in the axial direction, and showed a significant spatial variation (Figures 4.3, 4.5). The axial strain, ε_{zz}, decreased with depth from the articular surface to 0.8 mm ($p<0.001$), from 64±17% to 12±8% in BAPN treated samples and 49±5% to 7±2% in control samples. The axial strain also varied radially ($p<0.001$), being higher in the disk center and decreasing slightly towards the edge, reflecting the slight bulging of the articular surface. The radial strain, ε_{rr}, and shear, ε_{rz}, were an order of magnitude lower than the axial strain, and did not change significantly with radial distance or depth.

Tissue growth was affected by alteration of the extracellular matrix components (Figure 4.3, 4.5). Depletion of GAG's via C-ABC resulted in near zero growth, as confirmed by images (Fig. 4.3C) and the calculated strain components (Figure 4.5), over 16 days of culture. The axial strain was affected by extracellular matrix alterations ($p<0.05$), with a significant difference between chondroitase ABC treated and BAPN treated samples ($p<0.05$). On the other hand, inhibition of collagen crosslinks by treatment with BAPN did not significantly affect the geometric changes of cartilage explants in culture relative to the controls ($p=0.60$), although the magnitude of all strain components was higher in these samples.

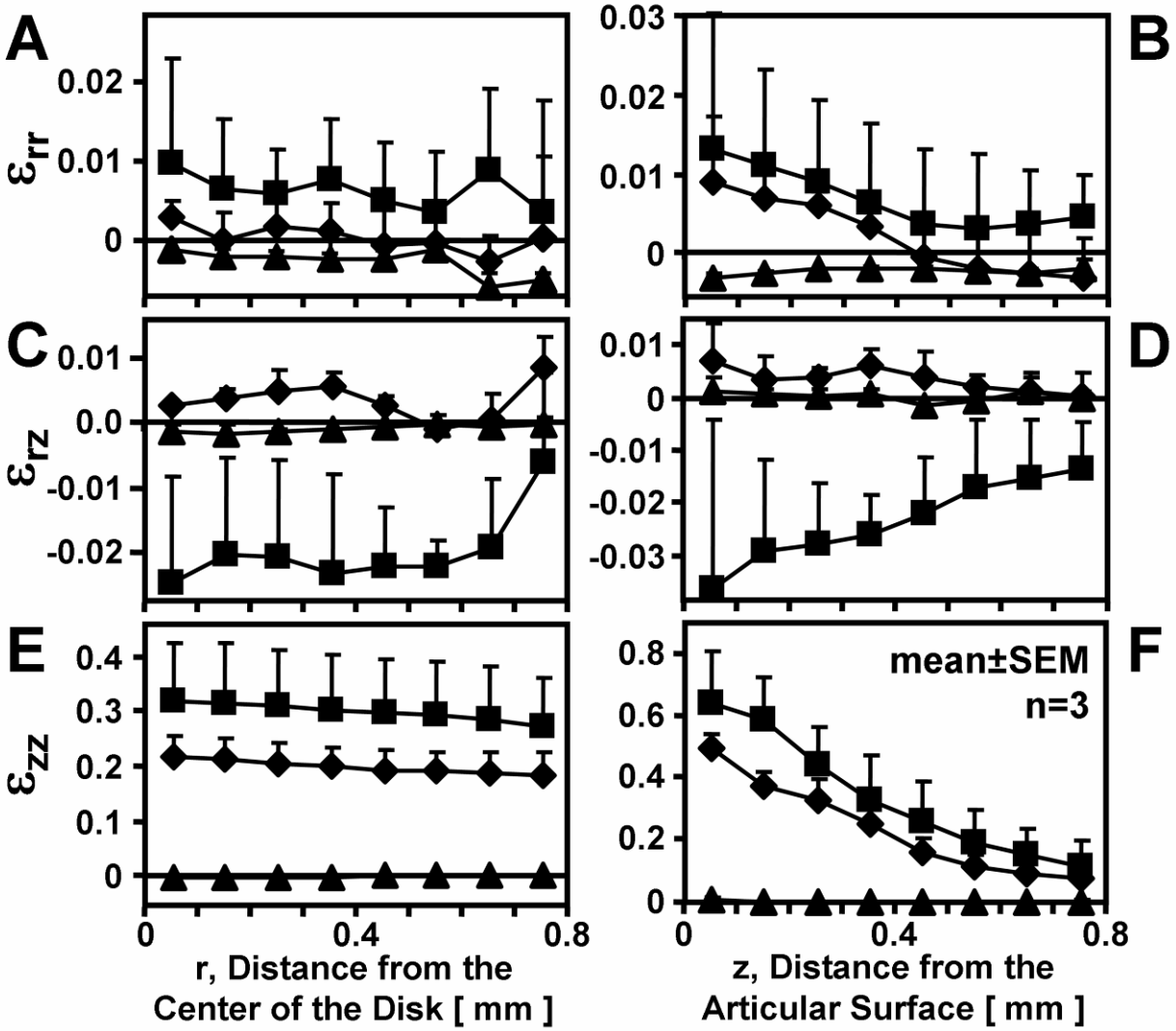

Figure 4.5. Average strains calculated as a function of r (A,C,E) and z (B,D,F). (A,B) ε_{rr}, (C,D) ε_{rz}, and (E,F) ε_{zz} were calculated in 0.1 mm bins from the disk center (r=0) to the disk edge and the articular surface (z=0) to the deep surface, excluding ~0.1 mm at the cut disk edge and deep surface. Control (◆), BAPN (■), and C-ABC treated (▲).

The presence of GAG molecules in the tissue, as assessed by alcian blue staining of sagittal tissue sections, illustrated the effects of chemical treatments and tissue culture time (Figure 4.6). Sections from samples after harvest, and after 2 and 16 days of culture with or without BAPN appeared deep blue, indicating a high concentration of GAG molecules (Figs. 4.6A, B, D, E). On the contrary, samples digested with C-ABC showed no staining (Fig. 4.6C), indicating full digestion and removal of the proteoglycans. The depleted molecules recovered partially after 14 days in culture by synthesis by the chondrocytes, with concentrated regions of staining surrounding cells, especially in the deeper tissue regions (Fig. 4.6F).

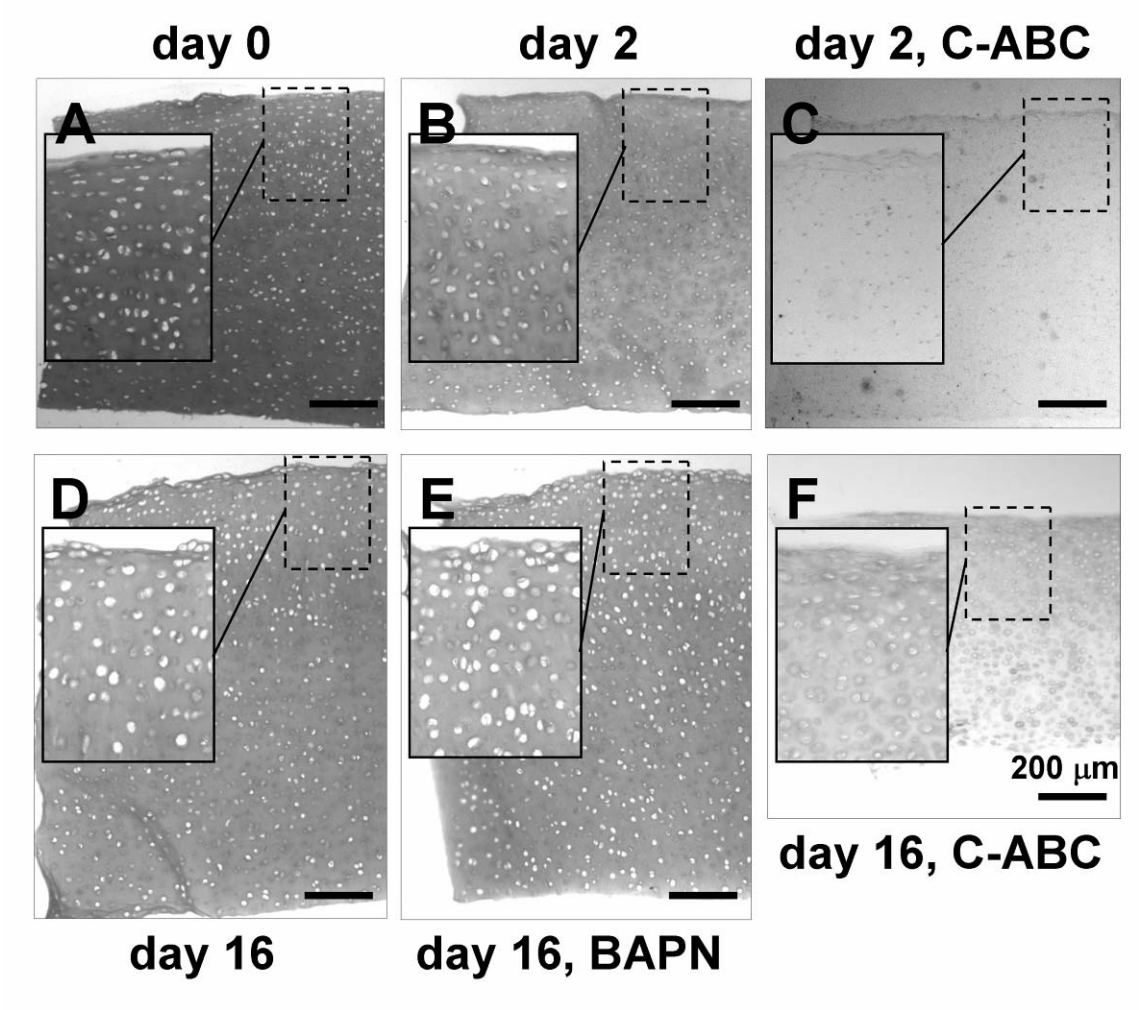

Figure 4.6. Alcian blue stained vertical sections from within half disks before and after growth. Samples analyzed before growth at day 0 (A), after 2 days in culture (B) and after 2 days of chondroitinase ABC digestion (C). Sections from disks after 16 days of culture with tissue culture media (D), including BAPN (E), and after chondroitase ABC treatment (F).

4.5 Discussion

The objective of this study was to assess the spatially-varying strain due to enzymatically or chemically modulated growth of articular cartilage explants. Explants grew in a time-dependent manner from initially after the 2 day preculture period to 16 days, but mostly from day 2 to day 8 (Figure 4.2). The axial strain, ε_{zz}, (perpendicular to the articular surface) between day 2 and day 8 exceeded the radial strain by ~20 times (Figures 4.3, 4.5), and decreased with depth from the articular surface from 50% to 7% in control samples. Growth was also affected by chemical treatment, with significantly higher overall axial strain (~34%) in samples incubated with BAPN (a blocker of collagen cross-link formation) during culture than those cultured after treatment with C-ABC to deplete proteoglycan molecules (0%). Articular cartilage explants are predisposed to growth that is anisotropic (primarily in the axial direction) and heterogenous (growth strain decreases as a function of depth and distance from the disk center), which can be modulated by directly altering extracellular matrix composition and structure.

The effects of tissue swelling, as opposed to growth and remodeling, were masked by beginning tracking of displacements after 2 days in culture. Deformation of articular cartilage explants after tissue harvest may occur as a result of changing osmotic forces or the removal of restraining function of the surrounding tissue [20]. This may occur on the order of a few hours, thus, any short-term effects of relieving the prestrain from the tissue block were bypassed by implementing a preculture period of 2 days.

Thus, any deformation measured in this study can be attributed to growth and remodeling.

The application of 2-D imaging of a cut surface accurately represents 3-D growth of small diameter disks. Immediate cell death via apoptosis at a cut surface has been demonstrated previously, with additional death occurring over time in culture to a distance of ~100 μm in cartilage [25]. Outside of this region, a repair response is elicited leading to proliferation of cells and formation of clonal groups. These responses result in a heterogeneous profile of cell death, cell cloning, and normal *in vitro* cell behavior across the disk surface, possibly leading to bulging in the center of the half disk. In this study, tissue disks were cut to 2 mm in diameter, so that growth occurring at the disk center was in close proximity to the disk edges, so translated to deformation of this edge. Although bulging was observed in the image plane across the 2 mm disk edge, cross sections of the half-disks orthogonal to the image plane show only a slight non-uniform growth occurring over the radius of 1 mm. Next, because of the complex 3-D geometry of the tissue half disk, the concentration of essential molecules for cell survival and function is not uniform throughout the tissue due to limited diffusion through the cartilage matrix. However, studies have shown that diffusion is sufficient to supply chondrocytes in human articular cartilage with glucose at a rate equal to consumption at a distance of up to 1.7 mm [18]. In our studies, with more permeable calf bovine tissue with a half-disk radius of 1 mm and thickness of ~1 mm, the maximum distance from a free surface is only 0.5 mm. Again, by inspection, the tissue disks maintain their bulk geometry throughout the 16 day culture period. Thus it appears that cell death and

transport limitations have small effects on bulk tissue growth for small disks for the duration of this experiment.

The higher levels of growth near the articular surface may be due to spatially-varying tissue mechanical properties. From similar studies conducted to ascertain the depth-varying mechanical properties of tissue under compression, the compressive modulus is lowest near the articular surface [11], and most prone to osmotic swelling [21]. This may result in a larger magnitude of growth near the surface when the swelling pressure is increased by accumulation of negatively charged proteoglycans. Also, the permeability of cartilage near the articular surface may be highest in the superficial zone [13], such that newly synthesized molecules can diffuse out and contribute to a more homogeneous extracellular matrix. This is illustrated in alcian blue stained images of matrix-depleted cartilage after 16 days in culture (Figure 4.6), where dark halos are observed around cells and dim staining farther from cells in the deep region, and moderately intense continuous staining around cells near the articular surface.

Changes in growth and remodeling with depth may also reflect depth-varying biological properties of the indwelling cells, and may reflect normal *in vivo* mechanisms of growth. From 3-D histology of immature articular cartilage, the density of cells decreases as a function of depth from the surface to 0.8 mm [8], so that although individual cell metabolism may be lowest near the surface of immature tissue [6], the net metabolism and consequent matrix deposition may be higher. Also, expansion of the cells within growing tissue by cell proliferation, thought to occur primarily near the surface in immature tissue [5, 10, 15-17] may contribute to accelerated growth by maintaining a high cell density while the tissue expands. Further investigation of cell proliferation and

matrix synthesis by cells in this culture configuration may reveal the contribution of each of these to local tissue growth.

The large difference in growth strain between the axial direction and the radial direction suggests anisotropy of tissue mechanical properties and chondrocyte biosynthesis and remodeling dynamics. In both osmotic pressure and mechanical compression experiments [21, 23], the strain in the radial direction was small compared to that in the axial direction, by a factor greater than 3 and 10, respectively. This may reflect a significantly stiffer cartilage matrix in the radial direction that is resistant to forces generated by osmotic forces or radial tension as a result of axial compression. Our results are consistent with this trend, and show even greater anisotropy, with more than 20 times the tissue strain due to growth from the axial to radial directions. While similar material properties may be governing this phenomenon, other factors such as directionality of matrix assembly and degradation, as well as cell proliferation may be significant.

These studies investigate the depth-varying growth of articular cartilage explants, and the effects of enzymatic or chemical modulation of the extracellular matrix on subsequent growth. The axial strain, ε_{zz}, due to growth was highest near the surface and decreased as a function of depth. Inhibition of collagen crosslinking by BAPN enhanced growth, while depletion of GAG within the tissue prior to culture prevented growth up to 16 days. The depth-dependent growth of articular cartilage may be due to intrinsic properties of the local extracellular matrix and cells. Mechanisms that involve this spatially-varying growth may allow maturation within the deeper regions of the tissue concurrent with overall expansion of the tissue concentrated near the surface.

Recapitulating such a mechanism with engineered or donor cartilage may ultimately be critical for achieving desired mechanical properties while increasing tissue volume. The assessment of 3-D growth strain by tracking motion of points on a 2-D surface allows one to characterize spatially-varying growth *in vitro,* and may also be applicable *in vivo* in conjunction with appropriate imaging methods. Further, the methodology described here may be extended to analysis of growth of a variety of tissues.

4.6 Acknowledgments

This work was supported by the National Institute of Health and the National Science Foundation. The dissertation author (primary investigator) thanks the coauthors of the manuscript for their contributions: Anna Asanbaeva and Scott Tcheng.

4.7 References

1. Asanbaeva A, McGowan KB, Masuda K, Klisch SM, Thonar EJ-MA, Sah RL: Mechanisms of cartilage growth: alteration and function and composition in vitro by deposition of collagen and proteoglycan matrix components. *Trans Orthop Res Soc* 29:554, 2004.

2. Aydelotte MB, Greenhill RR, Kuettner KE: Differences between sub-populations of cultured bovine articular chondrocytes. II. Proteoglycan metabolism. *Connect Tissue Res* 18:223-34, 1988.

3. Aydelotte MB, Kuettner KE: Differences between sub-populations of cultured bovine articular chondrocytes. I. morphology and cartilage matrix production. *Connect Tissue Res* 18:205-22, 1988.

4. DiMicco MA, Waters SN, Akeson WH, Sah RL: Integrative articular cartilage repair: dependence on developmental stage and collagen metabolism. *Osteoarthritis Cartilage* 10:218-25, 2002.

5. Hayes AJ, MacPherson S, Morrison H, Dowthwaite G, Archer CW: The development of articular cartilage: evidence for an appositional growth mechanism. *Anat Embryol (Berl)* 203:469-79, 2001.

6. Hidaka C: Maturation differences in superficial and deep zone articular chondrocytes. *Cell and Tissue Research* 323:127-35, 2006.

7. Hunziker EB: Articular cartilage structure in humans and experimental animals. In: *Articular Cartilage and Osteoarthritis,* ed. by KE Kuettner, Schleyerbach R, Peyron JG, Hascall VC, Raven Press, New York, 1992, 183-99.

8. Jadin KD, Wong BL, Bae WC, Li KW, Williamson AK, Schumacher BL, Price JH, Sah RL: Depth-varying density and organization of chondrocyte in immature and mature bovine articular cartilage assessed by 3-D imaging and analysis. *J Histochem Cytochem* 53:1109-19, 2005.

9. Kagan HM, Sullivan KA: Lysyl oxidase: preparation and role in elastin biosynthesis. *Methods Enzymol* 82:637-49, 1982.

10. Kavanagh E: Division and death of cells in developing synovial joints and long bones. *Cell Biology International* 26:679-88, 2002.

11. Klein TJ, Chaudhry M, Bae WC, Sah RL: Depth-dependent biomechanical and biochemical properties of fetal, newborn, and tissue-engineered articular cartilage. *J Biomech*, 2005.

12. Klisch SM, Chen SS, Sah RL, Hoger A: A growth mixture theory for cartilage with applications to growth-related experiments on cartilage explants. *J Biomech Eng* 125:169-79, 2003.

13. Leddy H: Site-specific molecular diffusion in articular cartilage measured using fluorescence recovery after photobleaching. *Annals of Biomedical Engineering* 31:753-60, 2003.

14. Luyten FP, Hascall VC, Nissley SP, Morales TI, Reddi AH: Insulin-like growth factors maintain steady-state metabolism of proteoglycans in bovine articular cartilage explants. *Arch Biochem Biophys* 267:416-25, 1988.

15. Mankin HJ: Localization of tritiated thymidine in articular cartilage of rabbits. I. growth in immature cartilage. *J Bone Joint Surg Am* 44-A:682-98, 1962.

16. Mankin HJ: Localization of tritiated thymidine in articular cartilage of rabbits. II. repair in immature cartilage. *J Bone Joint Surg Am* 44-A:688-98, 1962.

17. Mankin HJ: Mitosis in articular cartilage of immature rabbits. A histologic, stathmokinetic (colchicine) and autoradiographic study. *Clin Orthop Rel Res* 34:170-83, 1964.

18. Maroudas A, Bullough P, Swanson SA, Freeman MA: The permeability of articular cartilage. *J Bone Joint Surg Br* 50:166-77, 1968.

19. Maroudas A, Venn M: Chemical composition and swelling of normal and osteoarthrotic femoral head cartilage. II. Swelling. *Ann Rheum Dis* 36:399-406, 1977.

20. Myers ER, Lai WM, Mow VC: A continuum theory and an experiment for the ion-induced swelling behavior of articular cartilage. *J Biomech Eng* 106:151-8, 1984.

21. Narmoneva DA, Wang JY, Setton LA: Nonuniform swelling-induced residual strains in articular cartilage. *J Biomech* 32:401-8, 1999.

22. Quinn TM, Maung AA, Grodzinsky AJ, Hunziker EB, Sandy JD: Physical and biological regulation of proteoglycan turnover around chondrocytes in cartilage explants. Implications for tissue degradation and repair. *Ann NY Acad Sci* 878:420-41, 1999.

23. Schinagl RM, Gurskis D, Chen AC, Sah RL: Depth-dependent confined compression modulus of full-thickness bovine articular cartilage. *J Orthop Res* 15:499-506, 1997.

24. Schinagl RM, Ting MK, Price JH, Sah RL: Video microscopy to quantitate the inhomogeneous equilibrium strain within articular cartilage during confined compression. *Ann Biomed Eng* 24:500-12, 1996.

25. Walker EA, Verner A, Flannery CR, Archer CW: Cellular responses of embryonic hyaline cartilage to experimental wounding in vitro. *J Orthop Res* 18:25-34, 2000.

26. Williamson AK, Chen AC, Masuda K, Thonar EJ-MA, Sah RL: Tensile mechanical properties of bovine articular cartilage: variations with growth and relationships to collagen network components. *J Orthop Res* 21:872-80, 2003.

27. Williamson AK, Chen AC, Sah RL: Compressive properties and function-composition relationships of developing bovine articular cartilage. *J Orthop Res* 19:1113-21, 2001.

28. Williamson AK, Masuda K, Thonar EJ-MA, Sah RL: Growth of immature articular cartilage in vitro: correlated variation in tensile biomechanical and collagen network properties. *Tissue Eng* 9:625-34, 2003.

29. Yamagata T, Saito H, Habuchi O, Suzuki S: Purification and properties of bacterial chondroitinases and chondrosulfatases. *J Biol Chem* 243:1523-35, 1968.

CHAPTER 5

CELL PROLIFERATION IN ARTICULAR CARTILAGE: CONTRIBUTION OF DYNAMICS OF CARTILAGE CELLULARITY DURING GROWTH

5.1 Abstract

Articular cartilage growth is associated with proliferation of cells to maintain a high density during tissue expansion, and this may vary both spatially and temporally to mediate proper joint development. The objective of this study was to use a combined theoretical and experimental approach to assess mechanisms of cartilage growth. To this end, the aims were to develop a cellular model of tissue growth and to localize cell proliferation events occurring in fetal, calf, and adult articular cartilage during *in vitro* growth, and in regions of high proliferative activity, probe both cultured and native tissue for mitotic cells. Tissue was harvested and cultured for 6 days in the presence of BrdU, which is incorporated into actively dividing cells. BrdU positive cells were localized by immunohistochemistry as a function of depth from the articular surface. This tissue, as well as freshly harvested native tissue, was labeled and imaged *en face* to identify cells in mitosis based on cytoskeletal and nuclear morphology. Proliferating cells were concentrated near the articular surface at all growth stages, and the number of BrdU

positive cells decreased from Fetal→Calf and Calf→Adult. Mitotic cells were observed in cultured tissue at all stages, and in immature native tissue. Integration of modeling and experimental results highlighted the important role of cell proliferation in maintaining cell density during growth, especially near the articular surface.

5.2 Introduction

During articular cartilage development, the indwelling chondrocytes guide tissue growth and maturation through extracellular matrix metabolism. Articular cartilage undergoes growth through accretion of tissue and remodeling through alterations to the extracellular matrix, and these collectively can be referred to as *growth* [3, 4], and occurs both *in vivo* and *in vitro* [26-28]. On the other hand, maturation involves differentiation of cells and tissues, which occurs in native tissues *in vivo,* but is not normally achieved *in vitro*. In the immature state, the population of cells is maintained at a high density [13] allowing for a highly anabolic state that leads to net accretion of extracellular matrix proteins [26, 27], and concomitant growth and maturation. By adulthood, tissue growth and maturation have ceased and chondrocytes become sparse as their role shifts to maintenance of homeostasis. The cell density in articular cartilage is generally consistent with growth and maturation in immature tissues and ultimately homeostasis in mature cartilage.

As cartilage development progresses, the organization of cells changes by displacement associated with extracellular matrix growth and addition of new cells by proliferation. As the tissue grows in volume, the cell density decreases [13, 26, 27], and the matrix domain, or tissue volume under control of an individual cell [10], becomes increasingly large, so that further expansion and remodeling become less and less effective [22]. On the other hand, from 3-D histology, a relatively high cell density is maintained in the cartilage layer during growth [13]. Although the volume of the joint increases substantially from birth to maturity, the cell density decreases proportionally

much less [13, 26, 27], indicating that new cells are being introduced, likely by proliferation of existing cells. Alteration in cell density due to tissue expansion and cell proliferation may occur differentially with depth, leading to the changes in the depth-dependent density and organization of cells that are observed from young to adult bovine animals [13]. The precise way in which tissue expansion and cell proliferation contribute to alterations in cell organization is not clear, but may be better understood by localizing proliferative events in growing tissues and analyzing these results in the context of a cellular model of tissue growth.

Cell proliferation occurs in immature articular cartilage in specific regions, as identified by biosynthetic incorporation of precursors into DNA during the cell cycle and by cell morphology, and may be associated with accelerated growth. Mankin [16-19] described 2 bands of proliferating chondrocytes in the immature rabbit, one at the articular surface and the other near the subchondral bone, by incorporation and localization of radiolabeled thymidine and by identification of mitotic cell nuclei. More recent studies have identified proliferating cells by localizing the proliferating cell nuclear antigen (PCNA) [14] and by uptake of the thymidine analog, bromodeoxyuridine (BrdU) [2] during the S phase of the cell cycle. Using these markers, proliferating cells have been identified near the articular surface, but not near the subchondral bone, and as such this region has been implicated as a source of growth by apposition [9]. Such cell proliferation events may arise from progenitor or stem cells that reside in this region [1, 6, 7, 25]. Disruption of the cell cycle by chemical agents leads to thinner articular cartilage, especially in the region of proliferation. Furthermore, growth factors such as IGF-1 and TGF-β, are more highly localized in cells in the superficial-most half of

immature *Monodelphis domestica* articular cartilage [9]. The cell proliferation events near the articular surface may be consistent with localized growth through maintenance of a relatively high cell density during tissue expansion.

The changes in the density of cells in articular cartilage during growth by tissue expansion and cell processes such as migration, division and death can be modeled by cell conservation equations, where each cell in a volume is considered (Figure 5.1). In a study by Wilsman et al [30] the differential growth (rates differing by region) of the growth plate was assessed, and chondrocytes in the growth plate cartilage were conserved; i.e., the number of chondrocytes lost by calcification (differentiation) was nearly the same as those gained by proliferation. However, cells were only conserved if the control volume was increased to encompass tissue growth, illustrating that changes in cell content can theoretically be described by tracking the fates of all cells and the displacement of cells due to tissue expansion.

The objectives of this study were 1) to develop a theoretical model to predict changes in cell organization due to tissue expansion and cell fates, 2) to localize subpopulations of cells with the capacity to rapidly divide in cultured fetal, calf, and adult bovine articular cartilage, 3) to probe the region(s) of high proliferative activity for cells in mitosis in both native and cultured tissue at the different growth stages, and 4) to use cell fate and tissue growth data with the theoretical model to predict how cell density would be altered during extended growth.

5.3 Theoretical Methods

Model

The density of cells in a tissue volume changes due to displacement during tissue growth, influx and efflux of cells by migration, and addition or removal of cells by proliferation and death (Figure 5.1).

$$\left\{\begin{matrix}\text{rate of}\\ \text{cell}\\ \text{accumulation}\end{matrix}\right\} = -\left\{\begin{matrix}\text{rate of cell}\\ \text{loss by tissue}\\ \text{expansion}\end{matrix}\right\} - \left\{\begin{matrix}\text{net rate of cell}\\ \text{loss by}\\ \text{migration}\end{matrix}\right\} + \left\{\begin{matrix}\text{rate of cell}\\ \text{generation}\end{matrix}\right\}$$

This differential form for conservation of cells can be obtained by considering the change in the number of cells in a small volume element over time, and taking the limit as the volume goes to zero, resulting in Eq. 1, with variables defined in Table 1:

$$\frac{\partial n}{\partial t} = -\left(\vec{\nabla}\cdot n\vec{v}\right) - \left(\vec{\nabla}\cdot n\vec{m}\right) + n\left(P - D\right) \qquad (1)$$

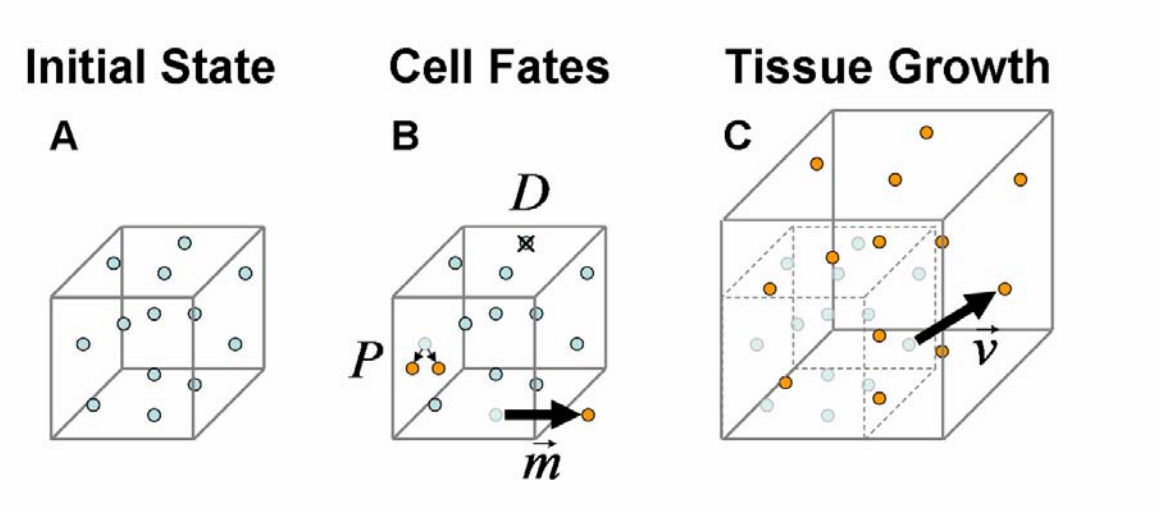

Figure 5.1. Schematic of cells in a small volume of articular cartilage A) in the initial state, B) after cell proliferation, death, and migration, and C) after tissue growth.

Table 5.1. Variables describing the alterations in cell organization due to cell fates and tissue growth.

Variable	Description	Units
x, y, z	spatial position	cm
t	time	day
$n\ (x, y, z, t)$	cell density	#/cm^3
$\vec{\boldsymbol{v}}\ (x, y, z)$	growth velocity	cm/day
$\vec{\boldsymbol{m}}\ (x, y, z)$	migration velocity	cm/day
$P\ (x, y, z, t)$	proliferation rate	proportion/day
$D\ (x, y, z, t)$	death rate	proportion/day

Determination and Use of Model Parameters

The parameters of these equations can be calculated on average to predict the change in cell density as a function of depth during growth of a tissue volume, from $V(t_0) \rightarrow V(t)$. This analysis can be implemented *in vitro* on cartilage explants using fluorescent labeling of cell nuclei and cell kinetics. Cells have been localized in 3-D cartilage volumes [11, 13], so at t_0, n_0 can be determined as a function of depth from the surface on average for a group of animals. Previous studies have used BrdU uptake by proliferating cells in animals labeled for different durations to assess the rate of proliferation in specific depth zones, P [29, 30]. In theory, kinetics of cell death and differentiation can be assessed with similar time-labeling techniques. Finally, the spatially-varying displacement of tissue due to deformation can be tracked by imaging points on a surface, and this can applied to cartilage at different time points of *in vitro* culture [12]. Taken together, Eq. 1 can be solved to predict the density of cells in a given tissue volume after a period of growth.

Ideal Cases

The growth of articular cartilage may be broadly characterized by heterogeneity (varying spatially) and anisotropy (occurring in preferred direction) of matrix assembly and cell processes. The effects of these complexities of growth on the depth-varying cell density of cartilage are clarified by first considering the following simplified cases:

Case 1: Uniform, Steady Matrix Growth with Uniform, Static Cell Population.

In the absence of proliferation, migration and death ($P = M = D = 0$), Eq. 1 can be simplified to Eq. 2, and with uniform spatial and constant temporal growth displacement rates, $\vec{v} = v_0(x\hat{i}_x + y\hat{i}_y + z\hat{i}_z)$ and cell density, *n*, to Eq. 3.

$$\frac{\partial n}{\partial t} = -\left(\vec{\nabla} \cdot n\vec{v}\right) \tag{2}$$

$$\frac{\partial n}{\partial t} = -n\left(\frac{\partial v_x}{\partial x} + \frac{\partial v_y}{\partial y} + \frac{\partial v_z}{\partial z}\right) \tag{3}$$

$$\frac{dn}{dt} = -3nv_0 \tag{4}$$

$$\int_{n_0}^{n} \frac{dn}{n} = -\int_{t_0}^{t} 3v_0 dt \tag{5}$$

$$\ln n - \ln n_0 = -3v_0(t - t_0) \tag{6}$$

$$n = n_0 e^{-3v_0(t-t_0)} \tag{7}$$

where n_0 and n are the cell density at time t_0 and arbitrary time t. This specialized case of tissue growth results in an exponential decrease in cell density.

Case 2: No Matrix Growth with Uniform and Steady Cell Proliferation.

On the other hand, if cells are proliferating within a tissue that is not expanding, the cell density increases exponentially.

$$\frac{\partial n}{\partial t} = n(P) \tag{8}$$

$$n = n_0 e^{P(t-t_0)} \tag{9}$$

Case 3: Uniform, Steady Matrix Growth and Proliferation.

Considered together, uniform and steady matrix growth with proliferation leads to Eq. 11, which illustrates that depending on the relative rates of proliferation, P, and growth, v_0, the cell density may increase or decrease:

$$\frac{\partial n}{\partial t} = -\left(\vec{\nabla} \cdot n\vec{v}\right) + n(P) \tag{10}$$

$$n = n_0 e^{(P-3v_0)(t-t_0)} \tag{11}$$

5.4 Experimental Methods

Detection of S Phase passage by labeling incorporated BrdU

Articular cartilage was harvested from bovine animals at different stages of growth to spatially localize cell proliferation during *in vitro* culture. Cartilage disks 3 mm in diameter and 2 mm in depth, with the articular surface intact, were harvested from the lateral femoral condyle of 3 each of immature fetal (2nd trimester) and calf (1-3 weeks), and mature adult (1-2 years) bovines. Disks were soaked in PBS and P/S/F and incubated in medium supplemented with 20% FBS, 50 µg/mL ascorbate, and bromodeoxyuridine (BrdU) (per the manufacturer instructions, Invitrogen, Inc., Carlsbad, CA) for 6 days with medium changes every other day. Disks were rinsed 3x in PBS to remove unbound BrdU and fixed for 1 day in 4% paraformaldehyde. Some samples were cut in half perpendicular to the articular surface and processed whole mount with a BrdU labeling kit (Invitrogen, Inc.), except with detection by primary AlexaFluor-conjugated anti-BrdU (Invitrogen, Inc.) by incubating for 18 hours at a 1:20 dilution (as per manufacturer's

suggestion). Samples were rinsed in PBS + 0.1% Tween 3 times for 20 minutes, counterstained with Hoescht for 1 hour, and then subjected to a final rinse for 30 minutes in PBS + 0.1% Tween.

Samples were imaged and then analyzed to determine the proportion of BrdU-positive cells as a function of depth from the articular surface. Half disks were imaged from a sagittal view on a Bio-Rad laser scanning confocal microscope at 10x magnification. A 5x5 Mexican hat filter was applied to enhance labeled cell nuclei relative to the background, and then color segmented using a threshold value two times the background, based on histogram analysis. The number and proportion of BrdU labeled cells were tabulated in 0.1 mm depth bins from the articular surface to 0.9 mm in depth.

Identification of cells in mitosis in freshly harvested explants

Freshly harvested articular cartilage, as well as after 6 days of culture from above, were processed to label cellular tubulin and nuclear DNA to highlight cell mitoses. Fetal, calf, and adult knee joints (n=2-3) were maintained at 4°C until tissue harvest 1-4 days after slaughter. Cartilage disks 3 mm in diameter and ~2 mm in depth, with the articular surface intact, were excised from the medial femoral condyle of fetal (2^{nd} trimester), calf (1-3 weeks), and adult (1-2 years) bovines. The cartilage disks were fixed in 4% paraformaldehyde overnight, rinsed 3x in PBS, and then treated with DNA-ase free RNA-ase (Roche Diagnostics, Basel, Switzerland) to remove nuclear RNA for nuclear labeling of DNA. Next, the disks were digested for 2 days with 0.5 U/mL chondroitinase in supplemented tissue culture media to deplete sulfated glycosaminoglycans and

enhance antibody penetration into the tissue. Samples were rinsed 5 times for 20 minutes with PBS and permeabilized for 3 hours in PBS + 0.1% Tween. Non-specific binding sites were blocked with PBS + 0.1% BSA + 1.2 μg/mL mouse IgG + 0.1% Tween for 3 hours. Samples were incubated with FITC conjugated anti-β-tubulin (1:50 dilution) in PBS + 0.1% Tween for 18 hours. After rinsing 3 times in PBS for 20 minutes, nuclear DNA was labeled with 10 μg/mL Propidium Iodide in PBS and then rinsed (3 times for 10 minutes).

The superficial zone of cultured and fresh disks was imaged to detect cells at different stages of mitosis. Disks were placed on a glass coverslip and imaged from an *en face* view on an inverted Bio-Rad laser scanning confocal microscope with a 40x/NA 1.3 oil objective. Serial images were captured in 1 μm increments from the articular surface to a depth of up to ~50 μm and in a series of fields of view across the diameter of the disk, excluding 200 microns from the edge. Images were inspected for the appearance of mitotic events, identified by condensed or flattened nuclei or nuclei pairs and a tubulin rich mitotic spindle. Approximately >10,000 cells were scanned for fresh and cultured tissue at each growth stage for each animal.

Statistics

Values are reported as mean±SEM. The effects of developmental stage on BrdU incorporation was analyzed by repeated measures ANOVA with developmental stage as a main factor and depth as a repeated factor.

5.5 Results

BrdU positive cells were identified by bright red staining co-localized with Hoescht DNA binding dye (blue) in a small population of cells (Figure 5.2). Positive labeling of cells indicates incorporation of BrdU into the DNA of cells during the S phase of the cell cycle during the 6 day culture period. Cells that were only labeled blue did not pass through S phase over the culture period and may be considered in G_0, or growth arrest, where cell division does not occur.

BrdU positive cells were present in all growth stages and depth zones, but the number varied markedly (Figures 5.2, 5.3). Positively labeled cells made up a small proportion of total cells, but were concentrated near the articular surface, with greater than 20% positively labeled in fetal and calf tissue. Positive cells decreased as a function of depth ($p<0.01$), changing in proportion from 0.20 ± 0.02 to 0.01 ± 0.01 in fetal, 0.26 ± 0.05 to 0.01 ± 0.003 in calf, and 0.08 ± 0.04 to 0.02 ± 0.02 in the adult from the surface to 900 μm in depth. The number of cells labeled with BrdU varied with growth stage ($p<0.05$), although the proportion did not change significantly.

Cell nuclei stained with Propidium Iodide and cellular tubulin localized with FITC-conjugated antibody were bright relative to the background, allowing detection of mitotic cells. Mitotic cells at all stages of division were evident compared to cells at other stages of the cell cycle (Figure 5.4), with condensed nuclear DNA, opposed nuclei pairs, a symmetric mitotic spindle aligned with nuclei, or an intense concentrated midbody between pairs. In contrast, cells in G_0 had large and rounded cell nuclei, and a more

diffuse tubulin network making up a larger volume. Cell mitoses appeared to occur mostly parallel to the articular surface, with only a couple detected more oblique to it.

Cells that appeared mitotic were detected in the superficial zone with a small incidence in all samples, with higher prevalence in tissue that was cultured. Mitotic cells were observed 0-50 μm from the articular surface (Figure 5.4) in cartilage that was freshly-harvested (fetal-0.04±0.02%, calf-0.08±0.05%, adult-0.00±0.00%) and cultured for 6 days (fetal-0.08±0.01%, calf-0.20±0.13%, and adult-0.06±0.01%).

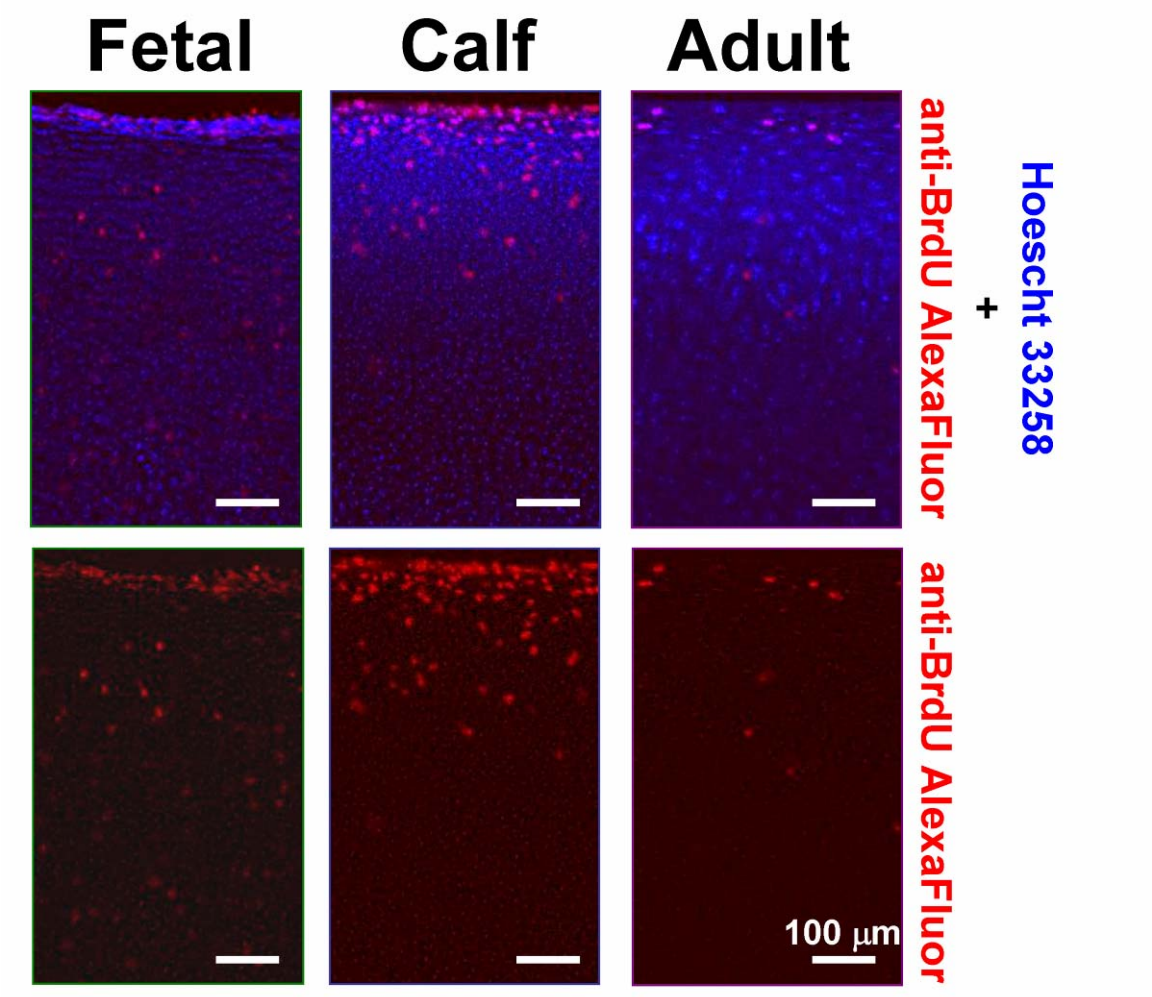

Figure 5.2. Bovine calf articular cartilage labeled with BrdU for 6 days in culture. Images depict labeling of Hoescht nuclei binding dye (blue) and AlexaFluor anti-BrdU (red).

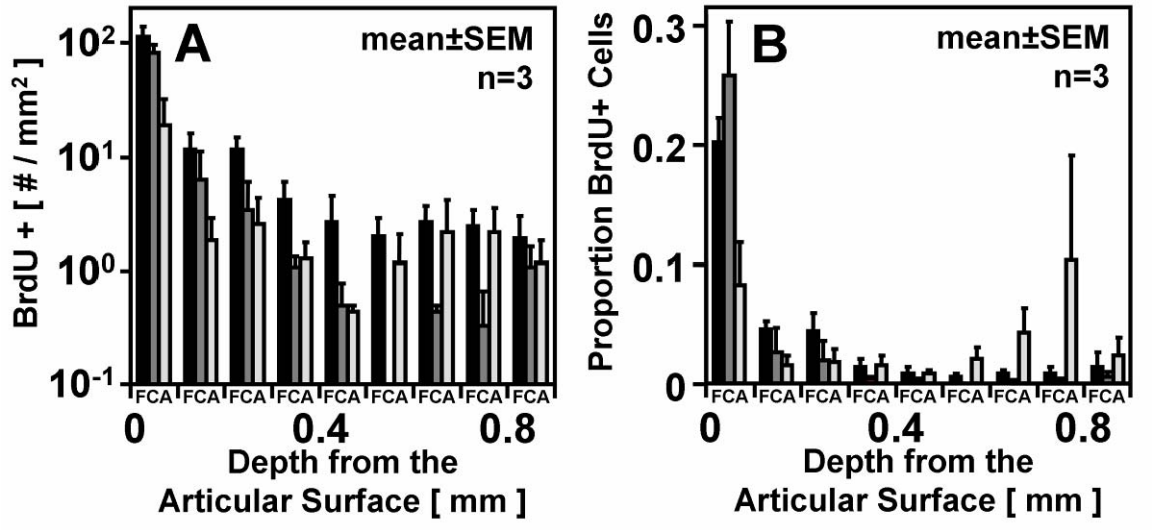

Figure 5.3. BrdU positive cells quantified for Fetal (F), Calf (C), and Adult (A) tissue. Positive cells presented as A) number (on Log scale) and B) proportion of total cells as a function of depth in 0.1 mm depth bins.

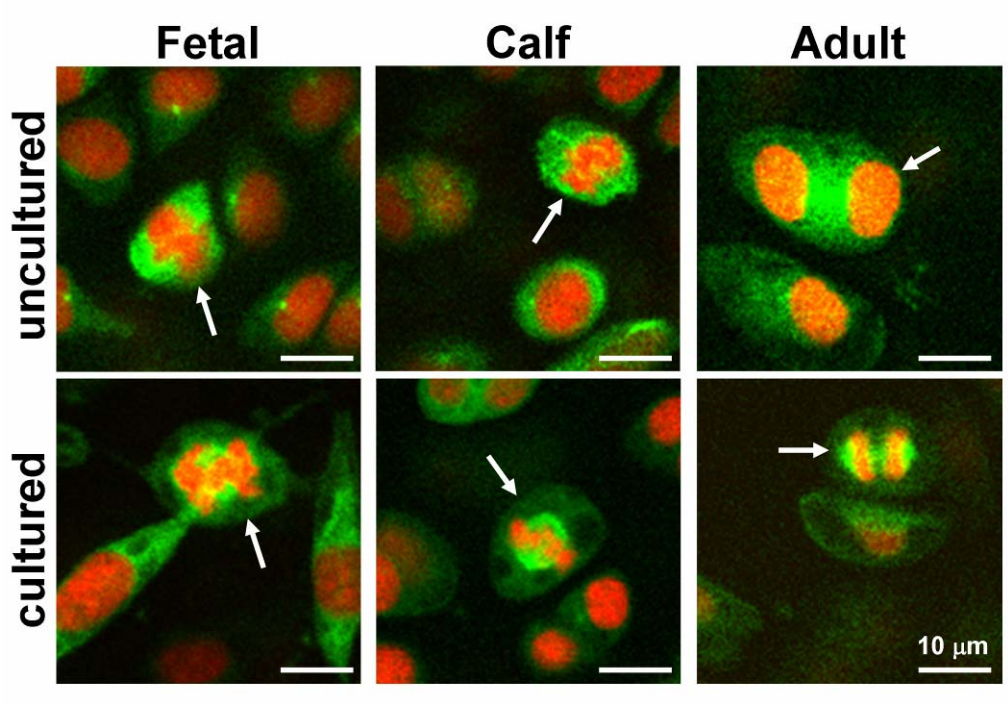

Figure 5.4. *En face* views of cell nuclei (propidium iodide) and tubulin (anti-β-tubulin FITC) in the superficial zone of Fetal, Calf, and Adult articular cartilage either freshly harvested or after 6 days in culture. Cells (arrows) are at different stages of mitosis, but are characterized by condensed cell nuclei and a distinct symmetric mitotic spindle. (Adult uncultured not in mitosis, but possibly former division)

Evaluation of Model

The cellular model of tissue growth outlined above was applied with estimates of cell fates and tissue growth displacement data from short-term *in vitro* studies to predict how the cell density changes. Such snapshots of *in vitro* tissue dynamics were then extrapolated over an extended *in vitro* growth period to estimate the effects on cell density. Finally, estimates of total growth and proliferation were modified to be consistent with *in vivo* data, and the changes in cell density were compared to those observed from the fetal to calf stages of *in vivo* growth [11]. The following parameters and assumptions were used to test each of 3 growth cases.

Parameters:

n(z): cell density in 1-3 week Calf [11]

cell density in 2nd trimester Fetal, 229/282 days gestation

P(z): proportion of cells proliferating per day (calf, fetal from the current study)

$t - t_0$ (in vitro): 6 days

$t - t_0$ (in vivo): 60 days (~53 days pre-natal to ~7 days post-natal)

$\vec{v}(z)$ (in vitro): growth displacement over 6 day culture [12]

Radial growth rate (%/day): 0.7%

from diameter of femoral condyle, medial to lateral:

Fetal: 2.6 cm, Calf: 3.7

Assumptions:

1. The cartilage grows axially (perpendicular to the articular surface, or the z direction) and there is no lateral growth velocity component [12].

   $v_x = v_y = 0 \qquad v_z = f(z,t)$

2. Growth is heterogeneous, with the proportion of growth being highest near the surface and decreasing as a function of depth from the articular surface [12] with the following additional assumptions:
    a. Growth occurs uniformly over 6 days
    b. Growth occurs as a constant proportion (the first 100 μm grows by 10% on day one to 110 μm, then the first 100 μm of tissue at day one grows to 110 μm by day two)
    c. Growth occurs as a function of absolute depth from the articular surface (i.e. tissue originally near the surface is displaced farther away by growth, and takes on the growth rate of deeper tissue)
3. Net cell migration is equal to zero, $\vec{m} = 0$
4. Cell death is negligible, $D = 0$
5. The proportion of new cells from proliferation per day is derived from the # of BrdU positive cells after 6 days with the following assumptions:
    a. 1 cell division creates 2 BrdU+ cells, and a net gain of only 1 cell, so BrdU+ cells are divided by 2.
    b. Cells proliferate steadily over the 6 day culture period
    c. Cells do not divide more that once, due to inhibitory effects of BrdU [9]
    d. Proliferation occurs as a proportion of cells present and as a function of absolute depth from the articular surface (i.e. cells originally near the surface are displaced away from the surface by growth, and lose their proliferative phenotype)

Application of Model

The cellular model of tissue growth can theoretically be applied to large tissue volumes with all parameters varying in time and space to describe changes in the organization of cells. In this study, a numerical solution was found over incremental time periods and control volumes, where the parameters approach uniformity and the expressions are simplified. As data are presented in these studies in 100 μm bins from the surface to 0.8-1 mm, the initial volume elements were thin slices with a thickness of 100 μm from the articular surface to 0.9 mm. The time increments were 1 day, as only small changes in tissue volume and proliferating cells occur over this time scale.

First, the parameters of proliferation and growth were found on a per day basis relative to the changing tissue geometry. Based on the assumptions that proliferation is steady and cells do not divide more than once, the proliferation rate was considered linear over the short duration (6 days) of this study, so daily proliferation was 1/6 of these values in each depth bin. Proliferating cells were then localized back to their initial position by tracing the depth-varying growth backwards. This depth profile was then averaged with that at day 6 to achieve a representative rate of proliferation in each depth bin over the time course of growth. Similarly, the daily growth rate was found as a function of depth that would result in the final growth calculated after 6 days in culture.

Next, the cell proliferation and tissue growth were simulated in incremental volumes and durations to investigate changes in cell density (Figure 5.5). For every 100 μm, new cells were added by proliferation, P, and then all of the cells were displaced according to the growth velocity, $\vec{v}$. This process was repeated daily to a final duration equal to the *in vitro* growth period (6 days) (Figure 5.5A) and for an extended period of growth of 60 days (Figure 5.5B). *In vivo* growth from fetal to calf tissue was then simulated by starting with the cell density profile for fetal tissue, and growing the tissue

incrementally over 60 days. Here, the rate of growth *in vitro* was corrected to accurately reflect geometry changes from the fetal→calf stages (joint radius increases by 0.7% per day, Jadin unpublished)(Figure 5.5C). Finally, the *in vitro* proliferation rate was corrected by a factor of ½ to reflect the smaller incidences of mitotic cells in native (0.04 and 0.08, fetal and calf) relative to cultured (0.08 and 0.20) tissue (Figure 5.5D).

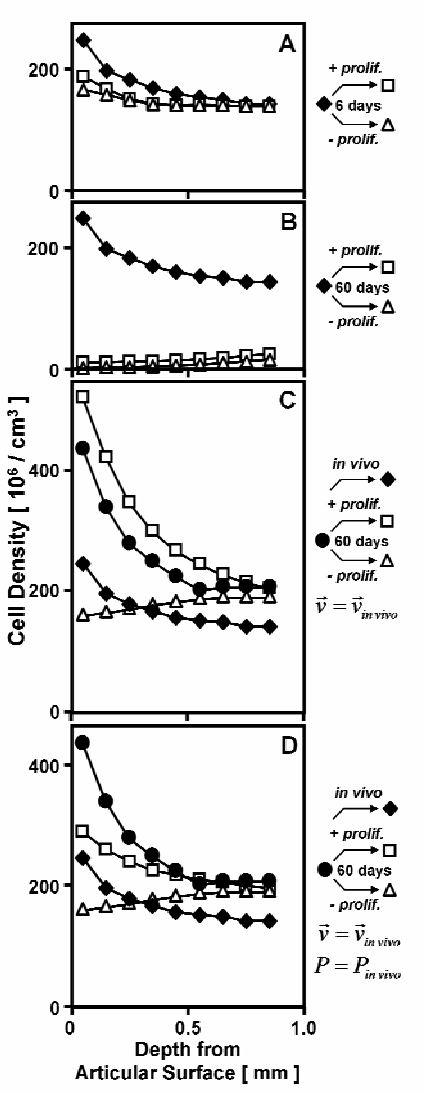

Figure 5.5. Cell density depth profiles for articular cartilage before and after simulated growth. Simulated *in vitro* growth is presented for calf tissue (◆) for 6 days (A) and 60 days (B), with (□) and without (△) cell proliferation with equal growth rates. Simulated growth from the fetal (●) →calf tissue is presented, after the growth rate was corrected to the same as native tissue (C), and further with correction for proliferation (D) based on the ratio between native and cultured tissue in the superficial zone.

5.6 Discussion

Cell proliferation in articular cartilage, although rare, may contribute significantly to immature tissue growth, and to maintenance of homeostasis in the mature adult. The goals of this study were to identify proliferating cells in native and cultured articular cartilage, and to develop a cellular model for tissue growth to assess the effects of tissue expansion and cell proliferation on cell density. The capacity for proliferation at various growth stages was assessed by localizing proliferating cells by BrdU incorporation in cultured tissue. The extent of proliferation in the superficial zone of native and cultured tissue was investigated by identifying cell mitoses morphologically. After 6 days in culture, cells positively labeled for BrdU incorporation were detected at a low incidence, but were concentrated near the articular surface, with ~20% of cells positively labeled (Figures 5.1, 5.2). Cells were detected at various stages of mitosis in the superficial zone of fetal, calf, and adult cultured cartilage, but in the native state occurred only in the immature fetal and calf tissue (Figure 5.3). These studies provide direct evidence for proliferation of chondrocytes in immature articular cartilage, and a capacity for proliferation at all growth stages.

The cellular model of tissue growth describes the conservation of cells with all of the kinematic and cell fate parameters defined. This model does not encompass classical growth theory, where the growth of tissues is related to accretion and remodeling of extracellular matrix molecules, as in previous studies [15]. Further, the relationship between matrix composition and kinematics is not addressed using this model. A model

involving all of the complex interactions between extracellular matrix composition and structure, and cellular kinetics in immature tissues could provide a detailed description of the dynamics of tissue growth and maturation, although such a model would be exceedingly difficult to evaluate and interpret. The assumptions made in the current study dealing with cell fates, such as insignificant migration and death, may not be entirely accurate, although cell migration is thought to not take place in cartilage, and cell death is localized near the subchondral bone [14]. Finally, extrapolating the *in vitro* cell proliferation and growth displacement profiles from previous studies to an *in vivo* growth model may not be valid, although displacement was corrected to be consistent with joint expansion, and proliferation modified with relative rates of mitosis at the articular surface. Although the assumptions made in this study are not validated, the simulations provide a better understanding of the relative effects of tissue expansion and cell proliferation in both an *in vivo* and *in vitro* growth context. Further studies can be conducted to evaluate all of the kinetic parameters of the model *in vivo*.

Articular cartilage disks were processed to capture mitotic events occurring during *in vivo* growth and homeostasis. Although the knees were analyzed 1-4 days post-mortem, mitotic events were still detected in immature tissue, and this seemed to be independent of holding time between 1 and 4 days. From the time of slaughter to harvest and fixation, the knees were maintained at 4°C to slow cellular processes. This condition may result in slowing of the cell cycling rate, both by effects of the lowered temperature on cells, and by lessening of fresh nutrient supply post-mortem. For these reasons, the mitosis rates calculated in this study should be interpreted as baseline values, which may be much higher *in vivo*. Further studies on other animals in which BrdU labeling can be

done *in vivo*, and tissue can be obtained from freshly slaughtered animals, may more accurately represent native mitotic activity.

The articular surface region was focused on for detection of mitotic events in native and cultured cartilage because of evidence that cell proliferation may be most prevalent there. From the current study, a high concentration of BrdU positive cells were detected in the superficial zone of cultured tissue, decreasing in the deeper layers. *In vivo* studies employing similar methods, but in different species, found similar patterns, although with dividing cells more concentrated in the slightly deeper transitional zone [9, 14, 16, 17, 19]. Future studies may be conducted to determine the role of rare proliferation in full thickness articular cartilage from large mammals, in which cell density is lower. These may include analysis of *in vivo* BrdU incorporation or antibody labeling for markers of cell division, in conjunction with high throughput 3-D imaging and automated analysis.

The finding of a population of dividing cells near the articular surface of immature calf tissue in explant culture agrees with previous *in vivo* studies of other animals. Mitotic cells and those labeled with tritiated thymidine were seen everywhere in newborn cartilage and localized into two discrete bands in immature rabbits, one near (but excluding the articular surface), and one near the calcified cartilage region adjacent to the subchondral bone [16, 17, 19]. Such events near the bone have not been repeated in recent studies, although cell division is consistently found near the articular surface using PCNA and BrdU labeling techniques [9, 14] and mostly excludes the very articular surface. In the *Monodelphis domestica,* those cells at the articular surface became positively labeled only after 10 days, consistent with a slower dividing progenitor

population localized at the surface [9]. The preponderance of dividing cells at the very articular surface in the current work may reflect species-specific cellular properties or activation of surface progenitor cells in explant culture in the presence of serum containing media. In the native tissue, it is possible that the low incidence detected here may be indicative of a slowly dividing progenitor population, while more rapidly dividing cells may be detected slightly deeper.

The incidence of mitoses in native immature articular cartilage is also in general agreement with previous studies. Mitotic cells were identified in immature rabbit cartilage by a condensed nucleus or apposed nuclei pairs [19] throughout the tissue. The proportion of mitotic cells in the previous work was ~0.03% in immature murine tissue, while in the current study mitoses incidences were 0.04% in fetal tissue and 0.08% in calf tissue. Although these results are on the same order, cell proliferation may be highly dependent on the exact stage of growth, species, depth from the articular surface, and site on the joint.

Populations of cells with progenitor-like properties are prevalent during growth of biological tissues, and may persist on into adulthood. Recent studies have localized a progenitor population to the articular cartilage surface in immature animals [1, 6, 7, 25]. Such populations exist in stem cell niches in other mesenchymal tissues, such as in the bone marrow [21], synovium [5], periosteum [8], adipose [32] and muscle [24], and contribute to tissue growth and persist through adulthood to elicit a repair or regenerative response. These cells may be precursors to a population of more rapidly dividing 'transit-amplifying' cells for growth, and exist in a quiescent state in adulthood until injury or degradation occurs nearby [23, 24, 31]. Such a response is consistent with the formation

of cell clones (clusters) in cartilage after injury or fibrillation of the articular surface in osteoarthritis [20]. The presence of progenitor and proliferating cells in articular cartilage may be critical for growth, as well as maintenance of joint homeostasis and repair of cartilage defects.

The role of cell proliferation in maintaining a population of cells was illustrated by simulating tissue growth using the cellular model. Over a short period of *in vitro* growth, the cell density was lowered slightly by expansion of tissue, and cell proliferation maintained a higher density very near the articular surface due to a high proliferation rate there (Figure 5.5A). After carrying this out to 60 days, the cell density was significantly reduced, and cell proliferation played an insignificant role (Figure 5.5B). This type of expansive growth may not actually be sustainable over long periods, especially with the large reduction in cell density. Certainly, after adjusting growth to a more physiological rate beginning with fetal tissue, cell density remained high, and actually increased with *in vitro* proliferation rates (Figure 5.5C). Again, this high rate of proliferation likely does not occur *in vivo* as evidenced by the smaller incidences of mitotic cells in native relative to cultured tissues. Therefore, after adjusting both growth and proliferation to more physiological rates, the resulting cell density depth profile resembles that of native calf tissue (Figure 5.5D). Application of a cellular model of tissue growth highlights the effects of accelerated growth relative to proliferation on maintenance of a dense population of cells, which may be essential for long-term growth.

This model may be applied *in vivo* to ascertain the anisotropic and heterogeneous mechanisms that may be involved in growth of soft tissues. Cell proliferation kinetics have been assessed for growth plate cartilage of immature mice [29, 30], and this may be

applied to a number of tissues. These results can be used together with changes in the 3-D organization of cells, as assessed by 3-D histological studies [11, 13], to describe the growth velocity fields throughout tissues. Such a detailed description of growth may lead to understanding of the mechanisms of normal growth, which may be useful to understand and more effectively manipulate the effective growth of engineered tissues *in vitro*.

Cell proliferation may play an important role in articular cartilage growth and homeostasis, with differential contributions in the fetal, calf, and adult stages of development and as a function of depth. The high concentration of cells near the articular surface of immature tissue suggests that tissue metabolism by cells during growth may be concentrated here. From simulations of cell organization during tissue growth, the cell density is maintained at a high level in the superficial zone by proliferation, even with concentrated growth here. Further studies may address how proliferation and death occur throughout the joint during development and growth. Such 'fate mapping' can be used to characterize the contribution of a population of cells to expansion and maturation of articular cartilage. Chondrocyte population kinetics can then be used in conjunction with cell organization and density to provide a mechanistic model of cell population changes in growing cartilage, which may be useful for tissue engineering efforts. Further, the role of proliferation in mature tissue homeostasis and repair may be better understood, and treatments devised, by application of similar methods in injured or arthritic tissue or in animal models.

5.7 Acknowledgments

This work was supported by the National Institutes of Health and the National Science Foundation. The dissertation author (primary investigator) thanks the coauthors of the manuscript for their contributions: Scott Tcheng and Barbara Schumacher.

5.8 References

1. Alsalameh S, Amin R, Gemba T, Lotz M: Identification of mesenchymal progenitor cells in normal and osteoarthritic human articular cartilage. *Arthritis Rheum* 50:1522-32, 2004.

2. Apte SS: Validation of bromodeoxyuridine immunohistochemistry for localization of S-phase cells in decalcified tissues. A comparative study with tritiated thymidine autoradiography. *Histochem J* 22:401-8, 1990.

3. Asanbaeva A, McGowan KB, Masuda K, Klisch SM, Thonar EJ-MA, Sah RL: Mechanisms of cartilage growth: alteration and function and composition in vitro by deposition of collagen and proteoglycan matrix components. *Trans Orthop Res Soc* 29:554, 2004.

4. Asanbaeva A, Schumacher BL, Klisch SM, Masuda K, Sah RL: Articular cartilage tensile integrity: modulation by matrix depletion is maturation-dependent. *Trans Orthop Res Soc* 32:Submitted, 2007.

5. De Bari C, Dell'Accio F, Tylzanowski P, Luyten FP: Multipotent mesenchymal stem cells from adult human synovial membrane. *Arthritis Rheum* 44:1928-42, 2001.

6. Dowthwaite GP, Bishop JC, Redman SN, Khan IM, Rooney P, Evans DJ, Haughton L, Bayram Z, Boyer S, Thompson B, Wolfe MS, Archer CW: The surface of articular cartilage contains a progenitor cell population. *J Cell Sci* 117:889-997, 2004.

7. Fickert SF, J. Brenner, RE.: Identification of subpopulations with characterisitics of mesenchymal progenitor cells from human osteoarthritic cartilage using triple staining for cell surface markers. *Arthritis Research and Therapy* 6:R422-R32, 2004.

8. Fukumoto T, Sperling JW, Sanyal A, Fitzsimmons JS, Reinholz GG, Conover CA, O'Driscoll SW: Combined effects of insulin-like growth factor-1 and transforming growth factor-beta1 on periosteal mesenchymal cells during chondrogenesis in vitro. *Osteoarthritis Cartilage* 11:55-64, 2003.

9. Hayes AJ, MacPherson S, Morrison H, Dowthwaite G, Archer CW: The development of articular cartilage: evidence for an appositional growth mechanism. *Anat Embryol (Berl)* 203:469-79, 2001.

10. Hunziker EB: Articular cartilage structure in humans and experimental animals. In: *Articular Cartilage and Osteoarthritis,* ed. by KE Kuettner, Schleyerbach R, Peyron JG, Hascall VC, Raven Press, New York, 1992, 183-99.

11. Jadin KD, Bae WC, Schumacher BL, Sah RL: 3-D imaging of chondrocytes in articular cartilage: growth-associated changes in cell organization. *Biomaterials*, 2006.

12. Jadin KD, Tcheng SW, Sah RL: Depth-varying growth of articular cartilage explants revealed by biomechanical analysis of displacement of chondrocytes. *Trans Orthop Res Soc* 52:1495, 2006.

13. Jadin KD, Wong BL, Bae WC, Li KW, Williamson AK, Schumacher BL, Price JH, Sah RL: Depth-varying density and organization of chondrocyte in immature and mature bovine articular cartilage assessed by 3-D imaging and analysis. *J Histochem Cytochem* 53:1109-19, 2005.

14. Kavanagh E: Division and death of cells in developing synovial joints and long bones. *Cell Biology International* 26:679-88, 2002.

15. Klisch SM, Chen SS, Sah RL, Hoger A: A growth mixture theory for cartilage with applications to growth-related experiments on cartilage explants. *J Biomech Eng* 125:169-79, 2003.

16. Mankin HJ: Localization of tritiated thymidine in articular cartilage of rabbits. I. growth in immature cartilage. *J Bone Joint Surg Am* 44-A:682-98, 1962.

17. Mankin HJ: Localization of tritiated thymidine in articular cartilage of rabbits. II. repair in immature cartilage. *J Bone Joint Surg Am* 44-A:688-98, 1962.

18. Mankin HJ: Localization of tritiated thymidine in articular cartilage of rabbits. III. mature articular cartilage. *J Bone Joint Surg Am* 45-A:529-40, 1963.

19. Mankin HJ: Mitosis in articular cartilage of immature rabbits. A histologic, stathmokinetic (colchicine) and autoradiographic study. *Clin Orthop Rel Res* 34:170-83, 1964.

20. Mankin HJ, Dorfman H, Lipiello L, Zarins A: Biochemical and metabolic abnormalities in articular cartilage from osteoarthritic human hips. *J Bone Joint Surg Am* 53-A:523-37, 1971.

21. Prockop DJ: Marrow stromal cells as stem cells for nonhematopoietic tissues. *Science* 276:71-4, 1997.

22. Quinn TM, Maung AA, Grodzinsky AJ, Hunziker EB, Sandy JD: Physical and biological regulation of proteoglycan turnover around chondrocytes in cartilage

explants. Implications for tissue degradation and repair. *Ann NY Acad Sci* 878:420-41, 1999.

23. Reynolds SD, Giangreco A, Power JH, Stripp BR: Neuroepithelial bodies of pulmonary airways serve as a reservoir of progenitor cells capable of epithelial regeneration. *Am J Pathol* 156:269-78, 2000.

24. Seale P, Rudnicki MA: A new look at the origin, function, and "stem-cell" status of muscle satellite cells. *Dev Biol* 218:115-24, 2000.

25. Thornemo MT, T. Sjogren Jansson, E. Larsson, A. Lovstedt, K. Nannmark, U. Brittberg, M. Lindahl, A.: Clonal Populations of Chondrocytes with Progenitor Properties Identified within Human Articular Cartilage. *Cells Tissues Organs* 180:141-50, 2005.

26. Williamson AK, Chen AC, Masuda K, Thonar EJ-MA, Sah RL: Tensile mechanical properties of bovine articular cartilage: variations with growth and relationships to collagen network components. *J Orthop Res* 21:872-80, 2003.

27. Williamson AK, Chen AC, Sah RL: Compressive properties and function-composition relationships of developing bovine articular cartilage. *J Orthop Res* 19:1113-21, 2001.

28. Williamson AK, Masuda K, Thonar EJ-MA, Sah RL: Growth of immature articular cartilage in vitro: correlated variation in tensile biomechanical and collagen network properties. *Tissue Eng* 9:625-34, 2003.

29. Wilsman NJ, Farnum CE, Green EM, Lieferman EM, Clayton MK: Cell cycle analysis of proliferative zone chondrocytes in growth plates elongating at different rates. *J Orthop Res* 14:562-72, 1996.

30. Wilsman NJ, Farnum CE, Leiferman EM, Fry M, Barreto C: Differential growth by growth plates as a function of multiple parameters of chondrocytic kinetics. *J Orthop Res* 14:927-36, 1996.

31. Zhang YQ, Kritzik M, Sarvetnick N: Identification and expansion of pancreatic stem/progenitor cells. *J Cell Mol Med* 9:331-44, 2005.

32. Zuk PA, Zhu M, Mizuno H, Huang J, Futrell JW, Katz AJ, Benhaim P, Lorenz HP, Hedrick MH: Multilineage cells from human adipose tissue: implications for cell-based therapies. *Tissue Eng* 7:211-28, 2001.

CHAPTER 6

CONCLUSIONS

6.1 Summary of Findings

The overall objective of this dissertation work was to contribute to an understanding of the role of cell organization and proliferation in mediating the growth of articular cartilage through matrix accretion and expansion of the cell population. The major findings of this work, related to these objectives, are:

1. Cells in articular cartilage at different growth stages can be accurately localized in 3-D using digital volumetric imaging and image processing techniques, leading to a detailed description of the variations in cell organization with growth (Chapter 2).
    a. The cell density decreased with distance from the articular surface to one millimeter in depth in all growth stages. The cellularity of articular cartilage also decreased from immature to mature tissue, falling by 30-50% at all depths.
    b. Cells in immature articular cartilage are positioned in close proximity to the extracellular matrix (<10 μm), because of a high density and an isotropic, evenly distributed organization.

c. Cells in mature articular cartilage are organized into distinct groups in all zones, leading to regions of tissue relatively far (>20 μm) from a large proportion of the surrounding tissue.

2. The overall density and organization of small groups of closely situated cells in articular cartilage varied significantly with growth, as determined by the novel metric of angle to the nearest neighboring cell (Chapter 3). These changes were especially evident in adult tissue, where cells are arranged into distinct horizontal clusters in the superficial zone, oblique groups in the middle zone, and vertical columns in the deep zone.
    a. The density of cells in cartilage from the surface to 0.8 mm in depth decreased in conjunction with cartilage growth, falling by 30% from 2nd trimester fetal to calf and 60% from the calf to adult stages. The cell density also decreased significantly with depth, in a way that varied between the weight-bearing femoral condyle and the intermittently loaded patellofemoral groove.
    b. Despite large changes in cell density, the distance to the nearest neighboring cell did not vary with either depth or growth. Further, the incidence of mutual neighboring cell pairs was higher than that for randomly arranged cells.
    c. The angle to nearest cells was the same as that for isotropic arrangement, except in superficial and deep zones of the adult, where the angle was ~20° and 60°, respectively.
3. *In vitro* growth of immature articular cartilage is anisotropic, and occurs mostly near the articular surface (Chapter 4). *In vitro* growth of cartilage can

be modulated by altering the extracellular matrix content and organization by applying specific chemical treatments.

   a. Articular cartilage explants grew in axial thickness (perpendicular to the articular surface) by ~20-30% over 6 days of culture. This exceeded growth tangential to the articular surface by a factor of ~20.
   b. Tissue strain in the axial direction due to growth was highest near the articular surface (~50%), and decreased with depth, being only 7% at 0.8 mm in depth. Axial strain also decreased from the center of the disk (r=0, 22%) to the edge (18%), possibly due to cell death occurring at cut tissue surfaces.
   c. Growth was modulated by removal of GAG molecules by chondroitinase ABC prior to culture, and by inhibition of newly formed collagen crosslinks by BAPN. Explants showed near zero growth after depletion of GAG, with only partial recovery of the original distribution of GAG's within the tissue after 14 days in culture. On the other hand, tissue showed accelerated growth without C-ASE digestion in the presence of BAPN, varying from 64% near the surface to 12% at 0.8 mm in depth.

4. Cell proliferation occurs in native immature fetal and calf articular cartilage, and in cultured tissue from both immature and mature animals (Chapter 5).

   a. During *in vitro* culture, cells proliferated through the full thickness of tissue explants, as indicated by BrdU labeling. However, BrdU positive cells were concentrated near the articular surface, suggesting a subpopulation of cells with enhanced proliferative capability here.

b. Cell proliferation events were studied near the articular surface in both cultured and native tissue. These events were much more prevalent in cultured tissue. Although dividing cells were seen in adult tissue after culture, indicating the capacity for these cells to divide, no mitoses were directly observed in the tissue analyzed here.
c. By applying a cellular model of growth, rapid tissue expansion during *in vitro* growth results in a marked decrease in cellularity, which is not significantly attenuated by cell proliferation. In contrast, the slower steady growth that occurs *in vivo* leads to a more subtle alteration in cellularity, while cell proliferation plays a major role in maintaining the density of cells.

6.2 Discussion

Analysis of articular cartilage cell organization and fates, and actual *in vitro* growth, leads to a more complete understanding of the way in which this uniquely functioning tissue grows both normally and in organ culture systems. Such information may guide future tissue engineering efforts, in which a biomimetic approach may be desirable. Also, the observations of cellular properties in adult cartilage may lead to further hypotheses about the limitations of an effective tissue repair response. Thus, it is appropriate to discuss the implications of the results described above as a cohesive whole, such that a more complete picture of cell-guided tissue growth and homeostasis can be formed.

The organization and fates of cells in adult articular cartilage are consistent with the role of the cell population in homeostasis and injury repair. In adult tissue, cells are

sparse and organized into distinct groups with varying orientations (Chapters 2 and 3), possibly comprising individual functional subunits called chondrons [17] with cell-cell interactions that enhance cellular function or phenotype [1]. These chondrons may also aide in shielding chondrocytes from excessive strain and fluid flow during joint loading [2]. This organization may be critical to efficient maintenance of a normal healthy cartilage layer, but unable to mount an effective repair response after injury because of large spaces of tissue devoid of cells (Fig. 2.9). Further, the cells within adult tissue do not show a strong intrinsic nature to proliferate (Chapter 5), although they do have the capacity to do so in tissue explants, in the presence of serum, throughout the tissue, especially near the articular surface (Fig. 4.1, 4.2, 4.3). In light of this observation, repair strategies may include introducing cytokines that stimulate the recruitment of cells from the surrounding tissues, and proliferation of nearby cells to expand their capability to supply and remodel new extracellular matrix molecules into a fully functioning network.

The orientation of small cell groups in adult articular cartilage may be due to a passive response to the surrounding extracellular matrix, or an active role in guiding its continual remodeling. Cell groups are arranged into horizontal clusters in the superficial zone, oblique groups in the middle zone, and vertical columns in the deep zone (Chapters 2 and 3), as quantified by the angle to the nearest neighboring cell (Fig. 3.2), mirroring the orientation of surrounding collagen fibers [16]. Organ cultures of adult osteochondral tissue blocks show a stable phenotype and metabolic activity consistent with turnover of the existing proteoglycans every 50 days [4]. Although remodeling may not occur throughout the tissue, and only in more local regions, it appears that the cells in articular cartilage are arranged ideally to direct such heterogeneous assembly of molecules. On the other hand, these groups may be oriented passively by interdigitating among sheets or columns of collagen fibrils, in the superficial and deep zones, respectively. In this case,

anisotropic self assembly may be directing the organization of the extracellular matrix, in response to local anisotropic deformations or fluid flow. The precise way in which cell organization is related to the arrangement of local extracellular matrix, however, requires further investigation.

Cells in immature articular cartilage are organized to elicit a highly anabolic growth phenotype. In fetal and calf bovine articular cartilage, the cells are dense and isotropically arranged, so that they are closely situated (<10 μm) to the majority of their local extracellular matrix domain (Chapters 2 and 3). From experiments that quantify the transport of newly synthesized matrix molecules, turnover of matrix occurs on the order of a few days within 10 μm from the cell in immature calf tissue [19]. Thus the cells are positioned to allow rapid growth and maturation of the tissue [22, 23], as well as effective repair after experimental wounding [14]. Further, the cells show a strong propensity to proliferate during growth (Chapter 5), both *in vivo* and *in vitro*, so that the cell density remains high while the tissue expands (Figure 5.5D).

Cell groups exist in growing articular cartilage, and the organization of these changes dramatically as the tissue reaches maturation. From 3-D imaging and image processing, the cells in growing articular cartilage maintain a close proximity to their nearest neighboring cell, despite a steady decrease in cell density (Chapter 3). Also, cells were often mutual neighbors to one another at all stages of growth, suggesting that they are physically interacting to maintain a close proximity as the tissue expands. Again, these interactions may enhance cellular metabolism and attenuate the deformation and fluid flow experienced by cells during loading [1, 2]. The formation of larger groups of cells with distinct orientations observed in adult cartilage is not well understood. These may arise from active mechanisms, such as cell death, proliferation, or migration

combined with passive interactions with the extracellular matrix, or responses to convective fluid transport and deformation during joint loading.

Changes in the cell organization during growth of articular cartilage are consistent with combined growth by matrix accretion and cell proliferation. As described in Chapter 1, the density of cells decreases with growth due to expansion of the tissue, although this decrease is ~7 times less than would be expected for a constant size population of cells. The new cells that contribute to increasing the population size may arise from other tissues within the joint, such as synovium, synovial fluid, meniscus, periosteum, or from the underlying bone, or from proliferation of chondrocytes within cartilage. Although some of the tissues of the joint have been found to contain progenitor cells [3, 5, 18], the infiltration of these cells into the cartilage has never been demonstrated. Thus it appears that cell proliferation, in addition to matrix accretion, plays an important role in expanding the cell population during growth.

The intrinsic properties of articular cartilage lead to *in vitro* growth primarily in the axial direction through large expansion of the tissue near the articular surface, and smaller expansion deeper into the tissue (Chapter 4). This heterogeneous and anisotropic growth may be due to a number of factors which may or may not govern normal *in vivo* growth, such as the heterogeneous mechanical properties of the extracellular matrix [9, 15, 20] and organization of cells (Chapters 2 and 3), the metabolic activity of cells [7], and cell proliferation [6, 8, 10-12] (Chapter 5). Most of these vary with depth in a way that is consistent with the profile of growth shown here. The cell density (Chapters 2 and 3), hydraulic permeability [9], and proliferation of cells (Chapter 5) are all highest near the surface, while the resistance to compression [20] and resistance to osmotic swelling [15] are lowest, and these seem to be conducive to higher growth near the surface. On the contrary, deep zone cells seem to show a higher intrinsic rate of synthesis of aggrecan

[7], which may contribute to the (less pronounced) growth of articular cartilage in the deeper regions of tissue, in the absence of extensive cell proliferation.

The role of cell proliferation in maintaining a population of cells during growth was illustrated by simulating tissue expansion and cell proliferation using a cellular model (Chapter 5). Over a short period of *in vitro* growth, the cell density decreased due to tissue expansion, and cell proliferation maintained a high density very near the articular surface due to a high proliferation rate in that region (Figure 5.5A). After carrying simulated growth out to 60 days, the cell density was significantly reduced, and cell proliferation played an insignificant role (Figure 5.5B). This type of expansive growth may not actually be sustainable over long periods, especially with the large reduction in cell density. Certainly, after adjusting growth to a more physiological rate beginning with fetal tissue, cell density remained high, and actually increased with *in vitro* proliferation rates (Figure 5.5C). Again, this high rate of proliferation likely does not occur *in vivo* as evidenced by the smaller incidences of mitotic cells in native relative to cultured tissues. Therefore, after adjusting both the growth and proliferation to more physiological rates, the resulting cell density depth profile resembles that of native calf tissue after 60 days (Figure 5.5D). Application of a cellular model of tissue growth highlights the effects of accelerated growth relative to proliferation on maintenance of a dense population of cells, which may be essential for long-term growth.

The results of this dissertation suggest that articular cartilage is conducive to growth by a combination of interstitial growth by matrix accretion everywhere, and accelerated 'appositional' growth by cell proliferation and matrix accretion near the articular surface. First, the density of cells is highest near the articular surface at all growth stages (Chapter 2 and 3), so that net cellular activity may be much higher here. Next, the capacity for cell proliferation is much higher near the articular surface, as

assessed by organ culture systems, and proliferating cells are present near the articular surface in immature native articular cartilage (Chapter 5). From cellular models of tissue growth (Chapter 5), proliferation and tissue expansion concentrated near the surface during *in vivo* growth leads to a small decrease in cellularity, and maintenance of a distinct depth-dependent profile, consistent with results from 3-D histological studies (Chapters 2 and 3). Finally, culture of articular cartilage *in vitro* results in axial growth concentrated near the articular surface, mediated by matrix metabolism, particularly synthesis of GAG molecules to increase tissue hydration and the swelling pressure relative to the restraining force of the collagen network (Chapter 4). This inhomogeneous mechanism of articular cartilage growth may be essential to allow the articular cartilage to expand in volume, while at the same time achieving structural maturation and acting as a load-bearing and low friction surface for joint articulation in the immature animal.

6.3 Future Work

The findings of this dissertation offer a fuller understanding of the role that cell populations play in guiding growth of articular cartilage, which may be refined with further studies in order to more effectively develop strategies for tissue engineering and repair. Also, the 3-D imaging and image processing methods provide an avenue for studying small incidences of cell fates, such as division and death, which may play major roles in tissue formation and evolution of cell organization.

6.3.1. Cell organization in cartilage degeneration

Cell organization in degenerate human tissue may provide insight into how cell fates, particularly death and proliferation, may be prevalent, and ultimately lead to further tissue degeneration. Cell death may play a detrimental role in articular cartilage during aging and early degeneration, leading to loss of cells [21], and decreased ability to maintain homeostasis. The cell death that occurs in these states may also lead to an altered local cell organization, such as a decrease in the number of cells per cluster, or the decrease in the number of clusters. If the number of cells per cluster is decreasing, then it is possible that individual cells are randomly dying throughout the tissue. On the other hand, if whole cell clusters are dying off, then it may be hypothesized that local factors are causing cell death. Analysis of clusters can be extended to include cell proliferation, which might occur to a large extent in later stages of osteoarthritis as the cells attempt to repair damaged tissue [13]. This leads to pathogenic cell clusters, which may include a large number of cells.

The effects of cell proliferation and death can be simulated by deletion and insertion of cells, to model the local and global changes that may be occurring with aging

and degeneration. Cells can either be deleted randomly from the whole tissue, or whole clusters removed, initially using data from a sample extracted from a young normal patient and progressing towards that of an aged or OA afflicted individual. If the resulting modeled tissue has similar clustering characteristics, including both cluster size and cluster number, as well as the metrics of organization involving the nearest neighbor described in Chapter 3, then the pathway of death may be fairly accurate. These methods could be tested in an *in vitro* setting, where the actual cell death and cell proliferation activity could be assessed using labeling methods described in Chapter 5. Further, cell fate data can be studied more globally in a cellular model, where changes in cellularity are accounted for by the pathogenic processes of cell death and tissue swelling, rather than physiological processes of proliferation and tissue growth analyzed in Chapter 5.

6.4 References

1. Albrecht DR, Underhill GH, Wassermann TB, Sah RL, Bhatia SN: Probing the role of multicellular organization in three-dimensional microenvironments. *Nat Methods* 3:369-75, 2006.

2. Alexopoulos LG, Setton LA, Guilak F: The biomechanical role of the chondrocyte pericellular matrix in articular cartilage. *Acta Biomater* 1:317-25, 2005.

3. De Bari C, Dell'Accio F, Tylzanowski P, Luyten FP: Multipotent mesenchymal stem cells from adult human synovial membrane. *Arthritis Rheum* 44:1928-42, 2001.

4. Dumont J, Ionescu M, Reiner A, Poole AR, Tran-Khanh N, Hoemann CD, McKee MD, Buschmann MD: Mature full-thickness articular cartilage explants attached to bone are physiologically stable over long-term culture in serum-free media. *Connect Tissue Res* 40:259-72, 1999.

5. Fukumoto T, Sperling JW, Sanyal A, Fitzsimmons JS, Reinholz GG, Conover CA, O'Driscoll SW: Combined effects of insulin-like growth factor-1 and transforming growth factor-beta1 on periosteal mesenchymal cells during chondrogenesis in vitro. *Osteoarthritis Cartilage* 11:55-64, 2003.

6. Hayes AJ, MacPherson S, Morrison H, Dowthwaite G, Archer CW: The development of articular cartilage: evidence for an appositional growth mechanism. *Anat Embryol (Berl)* 203:469-79, 2001.

7. Hidaka C: Maturation differences in superficial and deep zone articular chondrocytes. *Cell and Tissue Research* 323:127-35, 2006.

8. Kavanagh E: Division and death of cells in developing synovial joints and long bones. *Cell Biology International* 26:679-88, 2002.

9. Leddy H: Site-specific molecular diffusion in articular cartilage measured using fluorescence recovery after photobleaching. *Annals of Biomedical Engineering* 31:753-60, 2003.

10. Mankin HJ: Localization of tritiated thymidine in articular cartilage of rabbits. I. growth in immature cartilage. *J Bone Joint Surg Am* 44-A:682-98, 1962.

11. Mankin HJ: Localization of tritiated thymidine in articular cartilage of rabbits. II. repair in immature cartilage. *J Bone Joint Surg Am* 44-A:688-98, 1962.

12. Mankin HJ: Mitosis in articular cartilage of immature rabbits. A histologic, stathmokinetic (colchicine) and autoradiographic study. *Clin Orthop Rel Res* 34:170-83, 1964.

13. Meachim G, Collins DH: Cell count of normal and osteoarthritic articular cartilage in relation to the uptake of sulphate (35SO4) in vitro. *Ann Rheum Dis* 21:45, 1962.

14. Namba RS, Meuli M, Sullivan KM, Le A, Adzick NS: Spontaneous repair of superficial defects in articular cartilage in a fetal lamb model. *J Bone Joint Surg Am* 80-A:4-10, 1998.

15. Narmoneva DA, Wang JY, Setton LA: Nonuniform swelling-induced residual strains in articular cartilage. *J Biomech* 32:401-8, 1999.

16. Poole AR, Kojima T, Yasuda T, Mwale F, Kobayashi M, Laverty S: Composition and structure of articular cartilage: a template for tissue repair. *Clin Orthop Rel Res*:S26-33., 2001.

17. Poole CA, Flint MH, Beaumont BW: Chondrons in cartilage: ultrastructural analysis of the pericellular microenvironement in adult human articular cartilages. *J Orthop Res* 5:509-22, 1987.

18. Prockop DJ: Marrow stromal cells as stem cells for nonhematopoietic tissues. *Science* 276:71-4, 1997.

19. Quinn TM, Maung AA, Grodzinsky AJ, Hunziker EB, Sandy JD: Physical and biological regulation of proteoglycan turnover around chondrocytes in cartilage explants. Implications for tissue degradation and repair. *Ann NY Acad Sci* 878:420-41, 1999.

20. Schinagl RM, Ting MK, Price JH, Sah RL: Video microscopy to quantitate the inhomogeneous equilibrium strain within articular cartilage during confined compression. *Ann Biomed Eng* 24:500-12, 1996.

21. Temple M, Bae W, Jadin K, Bissar O, Chen M, Price J, Sah R: Decreased cellularity in the superficial zone of human articular cartilage in early degeneration. *Int Cart Repair Soc* 5:682, 2004.

22. Williamson AK, Chen AC, Masuda K, Thonar EJ-MA, Sah RL: Tensile mechanical properties of bovine articular cartilage: variations with growth and relationships to collagen network components. *J Orthop Res* 21:872-80, 2003.

23. Williamson AK, Chen AC, Sah RL: Compressive properties and function-composition relationships of developing bovine articular cartilage. *J Orthop Res* 19:1113-21, 2001.